Dynamical Properties of Quantum Antiferromagnets in One and Two Dimensions

A Dissertation
Presented to the Faculty of the Graduate School
of
Yale University
in Candidacy for the Degree of
Doctor of Philosophy

by
Chiranjeeb Buragohain

Dissertation Director : Subir Sachdev

December 2001

Abstract

Dynamical Properties of Quantum Antiferromagnets in One and Two Dimensions

Chiranjeeb Buragohain

December 2001

The study of low dimensional antiferromagnetic systems in recent times has led to major advances in our understanding about states of strongly correlated electron systems. The low dimensionality allows one to use a plethora of quantum field theoretical methods in analyzing these systems and it is possible to make detailed comparisons between theory and experiment. In this report we concentrate on the dynamical properties of one and two dimensional antiferromagnets. In one dimension, we show that it is possible to understand the dynamics of both integer and half-integer spin antiferromagnets under a unified formalism. We also study an exactly solvable toy model of spin transport to enhance our understanding of spin transport in finite sized systems. Predictions for various experimentally relevant quantities like neutron scattering cross-section are made. In two dimensions we study the problem of a spin impurity embedded in a two dimensional antiferromagnet. We show that the dynamics of the spin is sensitively coupled to the bulk antiferromagnet and carry out a renormalization group analysis of the system. We also derive various critical exponents for the impurity spin dynamics and magnetization.

Contents

Acknowledgements

Needless to say, that this dissertation would be impossible without the efforts and help of my adviser Subir Sachdev, who with so much patience, diligence and kindness guided me through my years at Yale. I am indebted to my fellow graduate students V. Ashvin, Frederik Bay, Kedar Damle, Michael Ibrahim, Swati Malhotra, Aditi Mitra and Hakan Tureci from whom I learnt a lot of physics. I am also thankful to Matthias Vojta for a very rewarding collaboration. I would like to take this opportunity to thank Simon Mochrie, Erich Poppitz, Charles Sommerfield and A. Douglas Stone for agreeing to serve on my thesis committee. Their numerous suggestions for improvements made a world of difference to the selection and presentation of the material in this report.

On the non-academic aspects, I am grateful to our exemplary physics department registrars Jean Belfonti and Jo-Ann Bonnett who took care of us graduate students and made my life so easy and pleasant.

Last, I would like to thank my professor J. K. Bhattacharjee who was always a great source of encouragement and inspiration.

List of Figures

Chapter 1

Introduction

In the last two decades antiferromagnetic compounds have attracted a lot of attention because of the perceived close connection between antiferromagnetism and high temperature superconductivity. For example, La_2CuO_4 is effectively a two dimensional square lattice antiferromagnet in the pure state and it turns into a superconductor when doped to $La_{2-x}Sr_xCuO_4$. These doped compounds are hard to study because of the complications of doping and proximity to the superconducting state. The interaction between charge, magnetic and superconducting order produces a bewildering array of phases and clear understanding of these materials still elude us. The pure versions of these compounds and other related compounds are no less fascinating and have their own highly interesting phases. Since they are insulators, we can exclusively confine our attention to the magnetic order and make considerable progress in both experimental as well as the theoretical front. It turns out that the low energy properties of these compounds can be described by various quantum field theories. Since the spatial dimensionality is low, these field theories can be analyzed in depth and detailed confrontation between theory and experiment is possible. It is no exaggeration to say in recent times many of our fundamental insights into properties of matter have come from the study of quantum magnetism. With this in mind, in this dissertation we explore dynamic properties of

1. one dimensional antiferromagnets at non-zero temperatures, and

2. non-magnetic impurities in two dimensional antiferromagnets at zero temperature.

As mentioned above, low dimensional quantum field theories play a prominent part in this investigation and we make quantitative predictions verifiable by experiment. In the following sections, we shall provide a brief introduction to the two systems of interest, namely one and two dimensional antiferromagnets. We shall also provide a brief summary of our methodologies and results.

1.1 One dimensional Heisenberg antiferromagnets

1.1.1 Introduction

In one dimension, the simplest model that one could study is a set of spins located along a line in a regular lattice. The spin located at the i-th site is represented by $\boldsymbol{S}_i$. Assuming that the interaction between spins is short-range (i.e. we allow only nearest neighbour spins to interact) and isotropic we arrive at the famous Heisenberg Hamiltonian :

$$H = J \sum_{\langle i,j \rangle} \boldsymbol{S}_i \cdot \boldsymbol{S}_j, \tag{1.1}$$

Here the sum over i, j run over nearest neighbours. J characterizes the strength of interaction between spins and is called the exchange constant. For $J < 0$, this Hamiltonian describes a ferromagnet where all spins are aligned in the same direction in the ground state, while for $J > 0$, this Hamiltonian makes the neighbouring spins point in opposite directions and the Hamiltonian describes an antiferromagnet. If we assume the spins to be classical, then $\boldsymbol{S}_i$ is just a vector of length S. In the quantum case, we must treat $\boldsymbol{S}_i$ to be a quantum operator with $2S + 1$ discrete eigenvalues. Crudely speaking, the spacing between successive quantum states of the Hamiltonian is of the order J/S. When this energy scale is large compared to the energy $k_B T$ of thermal fluctuations the quantum effects become relevant. The classical limit corresponds to $S \to \infty$.

For $J < 0$, the classical and quantum ground states of the Hamiltonian coincide. They both have ferromagnetic order at zero temperature. For $J > 0$, classically the ground state consists of the Néel state where neighbouring spins are anti-aligned. This Néel state is not the quantum ground state though, because it is not an eigenstate of the Hamiltonian. The operator $\boldsymbol{S}_i \cdot \boldsymbol{S}_j = S_i^z S_j^z + \frac{1}{2}(S_i^+ S_j^- + S_i^- S_j^+)$ lowers the spin on one site and raises it on the neighbouring site. So this operator leaves the ferromagnetic ground state invariant, but not the Néel state. This is the reason for our interest in the antiferromagnet where quantum effects lead to very interesting ground state structures. In fact, long time ago Bethe [4] showed that in one dimension the Néel state is completely destroyed by the quantum fluctuations and there is no long range order. In higher dimensions, the effect of quantum fluctuations is not as dramatic, but still very significant.

Although one might feel that this Hamiltonian is too simple to describe any real world material, there are indeed examples of materials to which this is an excellent approximation. A canonical example is $AgVP_2S_6$ [1]. Its structure is shown in Fig 1.1. It consists of layers of V^{3+} ions arranged in a zig-zag pattern which are sandwiched between layers of S atoms. The figure shows one such layer. The V^{3+} ions carry a spin of 1 and they interact strongly only along the zig-zag chain. In fact, the interaction between two spins lying on neighbouring chains is smaller by four orders of magnitude than the interaction between spins lying in the same chain [5]. Also the anisotropic contributions to the Hamiltonian (e.g. $S_{zi}S_{zi}$) are again four orders of magnitude weaker than the rotation invariant part ($\boldsymbol{S}_i \cdot \boldsymbol{S}_j$). So for all intents and purposes this compound is an example of the Heisenberg antiferromagnet in one dimension. These systems have been exhaustively studied both theoretically and experimentally and here I would like to give a brief overview. Experimental information on neutron scattering can be found in the articles by Cowley [6] and Broholm [7]. NMR results are found in references [8, 9].

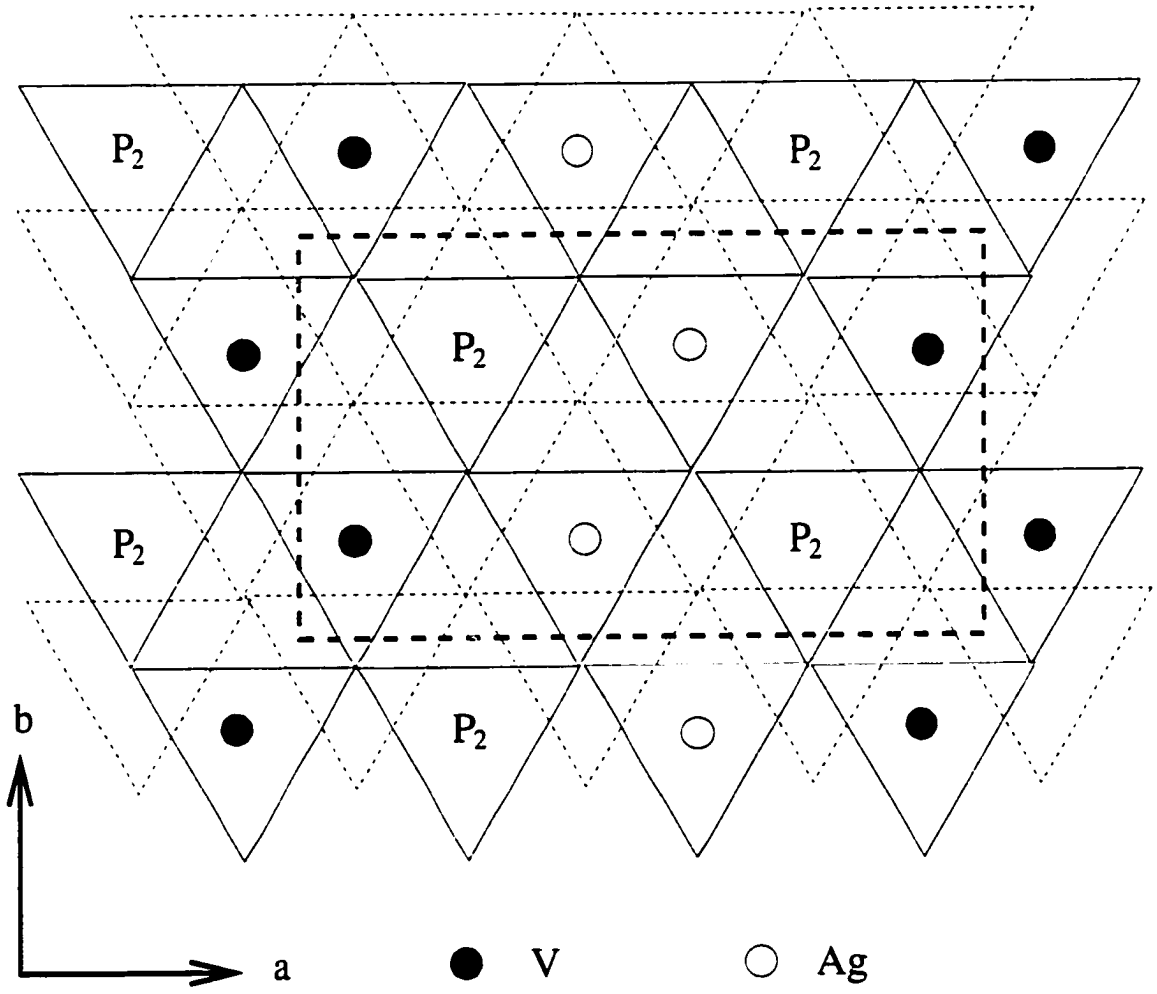

Figure 1.1: The structure of one single layer in the compound $AgVP_2S_6$ [1]. The zig-zag chains of V^{3+} ions constitute a Heisenberg antiferromagnetic chain. The V (solid circle) and Ag (empty circle) ions lie in the same plane. The sulphur network above (below) the plane are shown by the solid (dashed) lines. The bold dashed line indicates a unit cell.

1.1.2 Half-integer Spin Chains

Theoretically the first interesting result about antiferromagnetic spin chains came from a theorem proved by Lieb, Schultz and Mattis [10]. This theorem was afterwards extended to arbitrary half-integer spin chains [11]. Essentially the theorem showed that for a class of Hamiltonians with half-integer spins, either the ground state has no gap to the first excited state, or parity is spontaneously broken and the ground state is two-fold degenerate.

Since the theorem is of great significance it is useful to study it in some detail. This discussion closely follows Affleck's review article [12]. We start with a spin chain of finite length with periodic boundary conditions and. We also assume that the number of sites N is even. Now let us consider the ground state $|0\rangle$ and construct a low energy state $|1\rangle$ orthogonal to the ground state. The meaning of "low energy" is made concrete by demanding that

$$\langle 1|(H - E_0)|1\rangle = \mathcal{O}(1/N) \tag{1.2}$$

where E_0 is the ground state energy. It is not necessary that $|1\rangle$ be an eigenstate of the Hamiltonian. If the expectation value of $H - E_0$ vanishes in the thermodynamic limit, we will have proved the existence of low energy states. To construct $|1\rangle$, we operate on the ground state by a unitary operator $\mathcal{U}$ defined by

$$|1\rangle = \mathcal{U}|0\rangle; \quad \mathcal{U} = \exp\left[\frac{i\pi}{m}\sum_{j=-m}^{+m}(j+m)S^z_m.\right] \tag{1.3}$$

By this operation, we are twisting the j-th spin by an amount $\pi(j+m)/m$ around the z axis. The twist varies from 0 to 2π as we move along the chain from site $-m$ to m. The sites numbered with index $|i| > m$ are untwisted. We choose m to be a number $\mathcal{O}(N)$, e. g. $N/2 - 1$. It is intuitively clear that the state $|1\rangle$ has low energy because the twist between neighbouring spins is $\mathcal{O}(\pi/m) \ll 1$. To see this explicitly we use the following fact:

$$\mathcal{U}^\dagger S^+_i S^-_{i+1}\mathcal{U} = e^{-i\pi/m}S^+_i S^-_{i+1} \tag{1.4}$$

The energy difference between $|0\rangle$ and $|1\rangle$ is

$$\begin{aligned}\Delta E &= \langle 1|(H - E_0)|1\rangle \\ &= \frac{J}{2}\sum_i \left\langle 0 \left| \left(e^{-i\pi/m} - 1\right) S_i^+ S_{i+1}^- + \left(e^{i\pi/m} - 1\right) S_i^- S_{i+1}^+ \right| 0 \right\rangle . \end{aligned} \tag{1.5}$$

If parity is not broken, then the ground state is reflection invariant around any site i and we can interchange the sites i and $i+1$. This simplifies the expectation value:

$$\begin{aligned}\Delta E &= J(\cos(\pi/m) - 1)\sum_i \langle 0 \left| S_i^+ S_{i+1}^- \right| 0\rangle \\ &= J\langle 0|S_0^+ S_1^-|0\rangle(\cos(\pi/m) - 1)(2m+1) = \mathcal{O}(1/m). \end{aligned} \tag{1.6}$$

So here we have shown that $|1\rangle$ is indeed a low energy state, but we haven't established orthogonality. To show orthogonality we carry out a reflection ($S_i \to S_{-i}$) and a rotation around y axis by π ($S_z \to -S_z$). Under this transformation

$$\mathcal{U} \to \mathcal{U} \exp\left[-2i\pi \sum_{j=-m}^{+m} S_j^z\right], \tag{1.7}$$

and

$$|1\rangle \to \mathcal{U} \exp\left[-2i\pi \sum_{j=-m}^{+m} S_j^z\right] |0\rangle. \tag{1.8}$$

The exponential factor will evaluate to +1 or -1 depending on whether S is integer or half-integer (note that the number of sites over which the sum is being carried out is odd). For half integer spins, the parity of $|1\rangle$ is opposite to $|0\rangle$ and hence they are orthogonal to each other. At this point we have two possibilities: either the ground state does not break parity and in that case we have gapless odd parity excitations above the ground state or we have a ground state which spontaneously breaks parity and is two-fold degenerate. An example of the latter type of state is a dimerized state in which every alternate bond along the chain corresponds to a dimer of the two neighbouring spins. This state is also called a spin-Peierls state. The parity invariant state is called the Luttinger liquid and it has critical correlations, i.e. all correlation functions decay as a power law. For spin 1/2 chains the existence of this state can be explicitly demonstrated.

Essentially we first map the Pauli spin operators for $S = 1/2$ to spinless Fermions. Spin up corresponds to a spinless Fermion at the site while spin down corresponds to absence of a Fermion. This mapping is known as the Jordan-Wigner transformations. The Fermionic field theory in one dimension that we arrive at by this method is strongly interacting. The low energy behaviour of this theory can be extracted by considering only the low energy excitations near the Fermi surface. This theory of low energy Fermionic quasiparticles is mapped to a Bosonic theory by a method known as Bosonization [13]. For a discussion see Affleck's elegant review paper [12] or Shankar's review paper on Bosonization [14].

1.1.3 Integer Spin Chains

In this case a crucial contribution was made by Haldane [15, 16] who introduced a coherent state path integral representation for the quantum partition function. For a lucid discussion of coherent state path integrals, one should consult refs [17, 18]. Since coherent states are close approximations to the classical states, this representation works best for large values of spin S. In addition, at large values of S any two neighbouring spins have almost the same orientation. Hence the correlation length is much larger than the lattice spacing and a continuum description of the system becomes possible. It turns out that the coherent state path integral represents the Hamiltonian as a continuum quantum field theory which was studied earlier in particle physics under the name of Non-Linear Sigma Model (NLSM). For half integer spins, there is an additional term in the action which is also called the θ term or the topological term. Although this whole formalism is based on the $S \gg 1$ limit, in practice it turns out that the qualitative results are trustworthy even for spin $S = 1/2$. The field theory is described by the

following partition function [19]:

$$\begin{aligned} \mathcal{Z} &= \int \mathcal{D}n\delta(\boldsymbol{n}^2 - 1)\exp(-S_B - S_n) \\ S_n &= \frac{1}{2cg}\int_0^{1/T} d\tau \int dx \left[c^2(\partial_x \boldsymbol{n})^2 + (\partial_\tau \boldsymbol{n})^2\right] \\ S_B &= i\frac{\theta}{4\pi}\int_0^{1/T} d\tau \int dx\, \boldsymbol{n}\cdot(\partial_x \boldsymbol{n}\times\partial_\tau \boldsymbol{n})\,, \end{aligned} \tag{1.9}$$

$\boldsymbol{n}$ is the antiferromagnetic order parameter unit vector crudely defined as $S\boldsymbol{n}(x_i) \sim (-1)^i\langle \boldsymbol{S}_i\rangle$. $c = 2JSa$ is the spin wave velocity and $g = 2/S$ is the coupling constant. The temperature is denoted by T. We have assumed units of $\hbar \equiv 1 \equiv k_B$. $\theta = 0$ for integer values of S and $\theta = \pi$ for non-integer values of S. S_n is the pure NLSM action, while S_B is the topological term. Notice that although our physical system is one dimensional, the partition function involves integrals over field configurations $\boldsymbol{n}(x,\tau)$ which depend not only on the space, but the time coordinate as well. This is a signature of the fact that we are dealing with the quantum partition function here. In general, a quantum problem in d dimension leads to a partition function in $d+1$ dimensions. The extra dimension of time is finite and the integral over τ extends only up to a time $1/T$. Coming back to the NLSM action, we shall be interested in the case $\theta = 0$ because we are dealing with integer spin chains only.

We can investigate this model in various fashions. A convenient starting point is the large N analysis of the NLSM where N is the number of components of the NLSM field $\boldsymbol{n}$ [20, 21]. At the $N \to \infty$ limit the ground state has a mass gap Δ for all values of g. This result happens to be true for all $N \geq 3$. This action was also analyzed by Polyakov [22] using the renormalization group. Under a rescaling of our cutoff $\Lambda \to \Lambda e^{-l}$, the renormalization group flow of the coupling g is described by

$$\frac{dg}{dl} = \frac{g^2}{2\pi} \tag{1.10}$$

From the flow equation, we note that this is an asymptotically free theory, i.e. the coupling grows as we move into low energy which is characterized by l growing larger, while at higher energies, the coupling approaches zero. For the lattice theory, which is the

high energy limit, the cutoff $\Lambda \sim J$. At the low energy limit when $g \sim \mathcal{O}(1)$, the cutoff corresponds to the energy gap Δ. With these two cutoffs, we can relate the high energy limit to the low energy limit by integrating the differential equation for g as follows:

$$\ln\left(\frac{c\Lambda}{\Delta}\right) = l = \frac{2\pi}{g}. \tag{1.11}$$

Hence the gap is related to the high energy cutoff by

$$\Delta \sim Je^{-2\pi/g}. \tag{1.12}$$

The size of the gap is comparable, but smaller than the exchange constant J. Hence this ground state is radically different from the gapless ground state for half-integer spins. We note that for half integer spins, the effect of the topological term on NLSM is precisely to change the ground state from a spin gap state to Luttinger liquid. This point was explicitly demonstrated by Shankar and Read [23]. To get a feel for the actual numbers for integer spins, we note that for $AgVP_2S_6$, $S = 1, \Delta = 26$ meV and $J = 58$ meV [5].

It is interesting to note that there are related quasi one-dimensional compounds known as ladder compounds which behave in a very similar way. For example a two leg ladder compound consists of two one dimensional spin chains corresponding to the two sides or "legs" of the ladder. Also every spin on one chain is coupled to the corresponding spin on the other chain. These couplings correspond to the "rungs" of the ladder. It is also possible to have more than two legs on the ladder. The qualitative behaviour of a p leg ladder with spin S on each site is equivalent to the behaviour of a single chain with an effective spin of Sp. Hence for half-integer spins (the commonest case), even legged ladders have a spin gap, while the odd legged ladders are gapless. An example two leg ladder compound which has a gapped ground state is $(VO)_2P_2O_7$ which has been shown to have a gap by neutron scattering experiments [24]. An example of a three leg ladder compound is $Sr_2Cu_3O_5$ which has been also experimentally studied [25]. For a discussion, see Dagotto and Rice's review article [26] and references therein.

1.1.4 Intermediate Temperature Regime

From Polyakov's [22] renormalization group analysis, we find that in integer spin chains first excited state is separated from the ground state by a finite gap of size $\Delta \sim Je^{-\pi S}$ ($g = 2/S$ in the mapping from Heisenberg Hamiltonian to the NLSM). At this point it becomes convenient for us to introduce an energy scale which we call $\Lambda_{\overline{MS}}$. To understand the significance of this energy scale, we recall that in renormalization group (RG) analysis we try to find a low energy fixed point for our Hamiltonian. As we explore higher energy scales, $\Lambda_{\overline{MS}}$ is the energy scale at which the our fixed point analysis no longer applies. $\Lambda_{\overline{MS}}$ is a renormalization group invariant, i.e. it does not flow under renormalization group flow and hence can serve as a clear demarcation between high and low energy scales. The interesting point is that since any physical energy scale like Δ is also invariant under RG flow, hence $\Lambda_{\overline{MS}}$ is related to physical length scales by some dimensionless multiplicative constants [27]. Also since there is only one energy scale present in the NLSM, all correlation functions for the NLSM can be uniquely determined once we have the experimental input on Δ or equivalently $\Lambda_{\overline{MS}}$. For a more in depth discussion of $\Lambda_{\overline{MS}}$, see appendix A.

Now we turn to the case of the half integer spin chains. Although there is no gap in the spectrum, we still have a relevant energy scale here which is called T_0 [28]. Recall that the correlation functions for the Luttinger liquid state has power law correlations. At finite temperatures the corrections to the power law behaviour is visible as logarithmic corrections and this introduces a new energy scale to the system. T_0 is precisely this energy scale. We shall argue that T_0 is related to $\Lambda_{\overline{MS}}$ by dimensionless factors [29] as well.

We have already argued that for both half integer as well as integer spin chains, the system is described by the NLSM with or without the topological term. The topological term leads to the radically different ground states—spin gap or Luttinger liquid for the different spins. But at high energies $g \to 0$, we can neglect the topological term S_B compared to the pure NLSM term S_n. So near the high energy fixed point $g = 0$, there

is no difference between the behaviour of integer vs half-integer spin chains. Here high energy refers to energies larger than $\Lambda_{\overline{MS}}$ which itself is of the order $Je^{-\pi S}$. This simplification at high energy is generally not very interesting because for small S, $J \approx \Lambda_{\overline{MS}}$. So in the high energy or temperature ($k_B T \sim J$) regime all the spins are strongly disordered and we recover classical behaviour for the chain. But for large values of spin, there is an intermediate temperature regime

$$J > k_B T > \Lambda_{\overline{MS}} \approx Je^{-\pi S}, \tag{1.13}$$

where we can expect very similar behaviour for both integer and half-integer spins.

In the coming chapters we shall construct a semi-classical formalism to describe this regime of temperature. The core idea behind this is as follows. First we show that the correlation length ξ at high temperature is logarithmically larger than the length scale c/T established by temperature. In fact,

$$\xi \sim c\frac{\ln(T)}{T}. \tag{1.14}$$

Hence at any temperature there will be islands of correlated spins of size up to the correlation length ξ and the lowest energy spin modes inside these islands will have an energy of the order of $T/\ln(T) < T$. Since these Bosonic spin wave modes have energies lower than the thermal energy, their occupation numbers will be high and we can treat them classically. So our effective theory will be a theory of these semi-classical spin-wave modes. The main items of interest will be the time dependent correlation functions which can be related to experimentally measurable quantities like neutron scattering cross section.

As an aside, we note that the spin dynamics for both integer and half-integer spin chains have been studied for asymptotically low temperatures $T \to 0$ previously[30, 8, 31]. Obviously the methodologies used to determine the spin dynamics are very different depending on the values of spin. The significance of our work lies in formulating a unified approach to the dynamics in this temperature range which is independent of spin.

In the first chapter of this report we start with the definition of our model of interest: the NLSM. We study the renormalization group flows for the coupling in the two cases $\theta = 0$ and $\theta = \pi$. From a study of the flow, we show that at the high temperature regime ($J > T > \Lambda_{\overline{MS}}$), the behaviour of both integer as well as half integer spins is identical. Next we turn to the determination of the equal time correlations in this regime. As we have argued above, the spin fluctuations in this temperature are effectively classical. How do we find this classical effective theory describing these fluctuations? Our formalism is derived from a method pioneered by Luscher [32]. Since our dominant fluctuations will have an energy $\omega \sim T/\ln(T) \ll T$, most of the weight in the spectral function $\mathrm{Im}\chi(k,\omega)$ will be concentrated in the low frequency part. In this case we can connect the equal time correlation function to the zero frequency spectral function by a Kramers-Cronig relationship. For a discussion see chapters 4 and 6 of Sachdev's book[19]. So we adopt a multi stage formalism. First we determine the correlation function for the zero frequency fluctuations by integrating out all the non-zero frequency Matsubara modes. The final mode left becomes classical because all frequency dependence has been integrated out. Because of the Kramers-Cronig relation, this correlation function is the same as the equal time correlations in our temperature regime. Thus we get a *classical* theory which describes the *equal-time* correlations. To use this theory to generate unequal time correlation, we simply use the Hamiltonian equations of motion. With the equations of motion in hand we can go on to evaluate actual correlation functions.

The classical theory we arrive at is dimensionless and has no coupling constant in which to carry out a perturbation expansion. So we expand our correlation function

$$C(\bar{x},\bar{t}) = \langle \boldsymbol{n}(\bar{x},\bar{t}) \cdot \boldsymbol{n}(0,0) \rangle \tag{1.15}$$

in powers of $\bar{x}$ and $\bar{t}$. Here $\bar{x},\bar{t}$ are the dimensionless space and time coordinates. Thus our expansion of the correlation function corresponds to a short-distance expansion. Short distance behaviour of the correlation function also provides us with limited information concerning the high frequency limit of the correlation function in Fourier space.

For the long distance, long time limit, we employ numerical techniques to determine the correlation functions. The equations of motion for the continuum fields are discretized in space so that we pass from a continuum Hamiltonian to a discrete lattice Hamiltonian. The thermodynamic properties of the lattice Hamiltonian are studied using conventional Monte-Carlo techniques. The time evolution of any ensemble described by the lattice Hamiltonian is easily carried out by numerically solving the equations of motion. The object of interest is the structure factor $S(k,\omega)$ which is the Fourier transform of the time dependent correlation function $C(x,t)$.

$$S(k,\omega) = \int dx\, dt\, e^{i(kx-\omega t)} C(x,t). \tag{1.16}$$

We numerically determine the structure factor $S(k,\omega)$ in many different limits of k and ω.

Interestingly, the numerical evidence is consistent with the existence of diffusive spin transport at high temperatures. At the low temperature regime ($T \ll \Lambda_{\overline{MS}}$), spin transport in gapped antiferromagnetic chains is known to be diffusive [30]. The case of half-integer chains without a gap is not very clear despite numerous studies [33, 34, 35]. Most of these studies are for the low temperature regime $T < \Lambda_{\overline{MS}} \sim T_0$. Our results are not valid in that regime, but they are still suggestive that diffusion might exist for the lower temperature regime as well. To further study the phenomenon of spin diffusion, we study a toy model of diffusion which is exactly solvable and has many similarities with our classical model of spin transport. In fact, the short time correlations of the toy model coincide with our classical model. At long times, the toy model exhibits diffusion. Since the toy model is exactly solvable even for finite systems, we use it to study the effect of periodic boundary conditions on diffusion and transport.

1.2 Single Impurity in Two Dimensional Heisenberg Antiferromagnet

1.2.1 Introduction

Two dimensional antiferromagnets are considerably more complicated than their one dimensional analogues. To start with, the number of lattices possible in two dimensions is much larger than in one dimension. The square lattice is known as a bipartite lattice because it can be divided into two identical sublattices. The classical ground state in a bipartite lattice is the previously discussed Néel state. In one sublattice we have all spins pointing up, while in the other sublattice all the spins are pointing down.

The ground state in a non-bipartite lattice is much more complicated. An example of a non-bipartite lattice is the triangular lattice. To understand the complications in such a lattice, consider the spins lying on the vertices of one triangle in the lattice. It is clear that no alignment of the three spins can completely satisfy the three antiferromagnetic bonds on the three sides of the triangles. This phenomenon known as frustration, can lead to very rich ground state structures [36]. But we shall not pursue that line of investigation any further here and confine our attention to the square lattice which is also the relevant lattice for cuprate superconductors.

We have argued that the classical ground state for the two dimensional square lattice antiferromagnet is the Néel state. It is expected that quantum fluctuations will considerably modify the ground state for the quantum case. The important question is whether like in one dimension, the Néel state is completely destroyed by quantum fluctuations. There are rigorous proofs [37] that the two dimensional square lattice nearest neighbour Heisenberg antiferromagnet has Néel order for $S \geq 1$. Current theoretical and numerical evidence [38, 39] suggests that the $S = 1/2$ antiferromagnet also has Néel order, but the Néel order is far from complete. To study the properties of the two dimensional antiferromagnet, the obvious way would be to construct a perturbation theory around the Néel ordered classical ground state. This approach suffers from two

problems. The first and most important problem being that most of the real world materials are far from being close to Néel order and the value of results derived from a perturbation expansion will be highly questionable. The second problem is that the results derived in this manner will be dependent on microscopic model parameters like the coupling J and lattice spacing a. So a comparison between theory and experiment will require fitting of various microscopic parameters.

1.2.2 Quantum Phase Transition

To deal with this we approach the problem from a different viewpoint. Consider the model Hamiltonian given below [40, 41]

$$H = J \sum_{i,j \in A} \boldsymbol{S}_i \cdot \boldsymbol{S}_j + \lambda J \sum_{i,j \in B} \boldsymbol{S}_i \cdot \boldsymbol{S}_j. \tag{1.17}$$

The lattice is depicted in Fig 1.2. Here A indicates the bonds in picture denoted by solid lines and B denotes the bonds indicated by dashed lines. $i, j \in A(B)$ means that the site i, j are connected by a $A(B)$ type bond. The $\boldsymbol{S}_i$ are spin $1/2$ operators. The A bonds form a kind of ladder within the square lattice and the B bonds connect ladders to each other. Since this is an antiferromagnet, we concentrate our attention on the regime $J > 0, 0 \leq \lambda \leq 1$. Note that $\lambda = 1$ correspond to the perfect Heisenberg antiferromagnet.

When $\lambda = 0$, the situation is shown in Fig 1.2 (A). The ladders are independent of each other and within the ladder, two neighbouring spins couple together to form a rotationally invariant singlet. There are no long range spin correlations. To create an excitation, we have to break a singlet bond and create a triplet spin 1 excitation that costs energy of the order of J. Hence this is known as the the paramagnetic spin gap phase.

When $\lambda = 1$, we are in the situations shown in Fig 1.2 (B). The ground state has spins are aligned in Néel order. We label the Néel order parameter as ϕ_α. In that case we

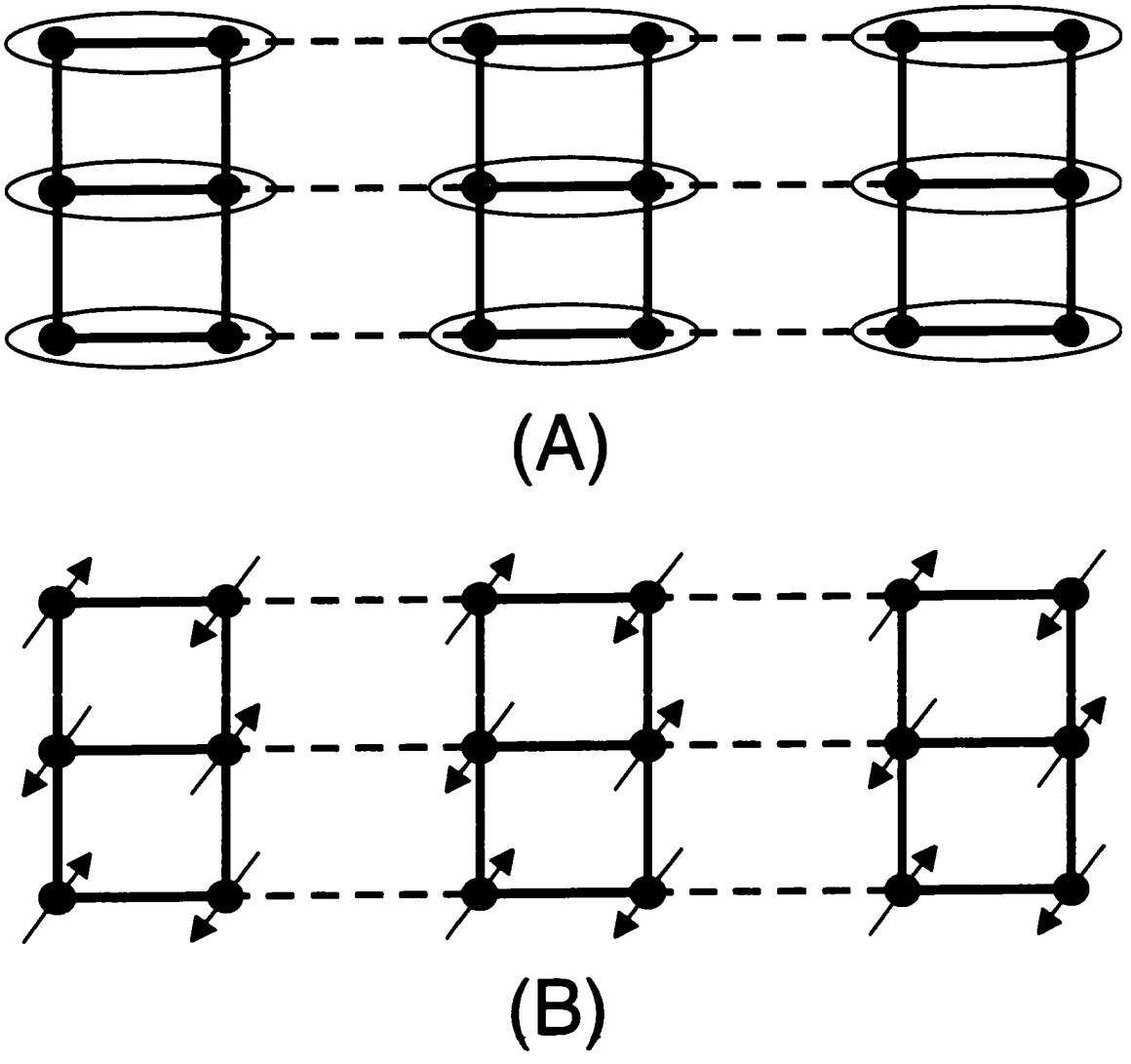

Figure 1.2: The coupled ladder antiferromagnet with the strength J links shown as solid lines while the λJ links shown as dashed lines. (A) The paramagnetic phase ($\lambda < \lambda_c$) with the ellipse around the bond indicating that those two spins have combined to form a local singlet. (B) The Néel phase ($\lambda > \lambda_c$) with alternating spins.

define the Néel order parameter on the site labelled by (i, j) as

$$\langle \phi_a(x = x_i, y = y_j) \rangle = (-1)^{i+j} \langle S_{\alpha i,j} \rangle \neq 0. \tag{1.18}$$

There are gap-less Goldstone excitations above the ground state which correspond to slow twists of the Néel order parameter.

Since for $\lambda = 0$ and $\lambda = 1$ we find two very distinct ground states, they must be connected by a phase transition at some $\lambda = \lambda_c$ as we slowly tune λ from 0 to 1. It turns out that the paramagnetic phase survives to $\lambda > 0$ and the spin gap vanishes at $\lambda_c \approx 0.3$ as $\Delta \sim |\lambda - \lambda_c|^{\nu}$[19]. The corresponding energy scale in the Néel phase ($\lambda > \lambda_c$) is known as the spin stiffness which we denote by ρ_s. Spin stiffness basically characterizes the energy cost to make a slow deformation in the Néel order. As $\lambda \to \lambda_c$, spin stiffness vanishes as $\rho_s \sim |\lambda - \lambda_c|^{\nu}$ with the same exponent ν. Vanishing spin stiffness or gap (Δ) implies that the number of low energy excitations proliferate and we have critical fluctuation on all scales. Note that in this phase transition, temperature has not played any role because we are working at zero temperature at all times. The phase transition happens as we change a parameter λ in the Hamiltonian and the fluctuations that appear in the system at the transition are due to purely quantum effects. This kind of phase transition is called a quantum phase transition [42]. Excellent discussions on quantum phase transitions can be found in the review article by Sondhi et. al. [43] and the book by Sachdev [19]. With phase transitions, comes the ideas of the scaling limit and universality. We'll consider each of them in turn.

There are two relevant length scales in the system: the lattice spacing a and the correlation length ξ. Near the transition, ξ diverges and becomes much larger than a. The scaling limit corresponds to neglecting all corrections to observables which are of the order a/ξ. We essentially take the scaling limit by considering a as fixed and sending ξ to infinity. There is an alternative, but equivalent viewpoint in particle physics where ξ is kept constant because that is the more physical length scale in particle physics and let $a \to 0$. Regardless of the way in which we approach the limit $a/\xi \to 0$, the results that we arrive at are identical. The scaling limit also involves other microscopic quan-

tities such as J. Since in our case $\xi \to \infty$, that means the spins at neighbouring sites are virtually parallel. This can only happen when J becomes very large. So in taking the scaling limit, we keep some quantities like a fixed and let other quantities such as ξ and J go to infinity in such a way that all physical observables like free energy take finite and sensible values.

Universality corresponds to the idea that at the scaling limit, the functional forms of physical observables are not sensitive to the particular details of the microscopic parameters. Heuristically this makes sense. After all, we would expect that a correlation function evaluated at the scale of ξ is not sensitive to the details of the interactions at the scale a. For example we can say that the spin correlation function

$$\langle \boldsymbol{S}(x) \cdot \boldsymbol{S}(0) \rangle = \mathscr{C} \Phi_S \left(\frac{x}{\xi} \right). \tag{1.19}$$

Φ_S is called a universal scaling function and it is dependent only on the ratio x/ξ. All non-universal details of the microscopic constants are hidden away in the prefactor $\mathscr{C}$.

Once we understand the ideas of scaling limit and universality, the next step is the quantum field theory near the critical point. Since at the scaling limit all relevant length scales become infinitely longer than the lattice spacing a, it is possible to pass from a lattice Hamiltonian description of the system to a continuum description which is nothing but a quantum field theory. Universality implies that the form of the field theory is not sensitive to the microscopic details of the model. Hence we can treat a whole class of lattice models by one single theory. The number of parameters that characterize the field theory is typically much smaller than the number of parameters in the lattice theory. For example, in our example of the two dimensional antiferromagnet, the two parameters in the theory are the experimentally measurable quantities Δ and the spin wave velocity c. All correlation functions can be expressed as functions of these two universal quantities and we can directly compare experimental data with theoretical predictions. Also there exists a large class of analytical methods to successfully deal with quantum field theories compared to the lattice models. Last and most important advantage that we gain by this methodology is that our theory is valid far away from the classical Néel

state. To speak loosely, we are expanding not around the Néel state or the dimer state but around a quantum critical point. In the vicinity of the critical point there is already a considerable amount of quantum fluctuations built into the theory and hence it should be a much more realistic description of the properties of the antiferromagnet. Note that it is not necessary that the real experimental material undergoes a quantum phase transition. We only require that the material is in a state not too far from the critical point in the phase diagram.

The quantum field theory that describes this transition is the familiar scalar field theory in d dimensions

$$\mathscr{S}_{\rm bg} = \int d^d x d\tau \left[\frac{1}{2} \left[(\nabla \phi_\alpha)^2 + c^2 (\partial_\tau \phi_\alpha)^2 + m^2 \phi_\alpha^2 \right] + \frac{g_0}{4!} (\phi_\alpha^2)^2 \right], \tag{1.20}$$

where $\phi_\alpha(x_i, y_j) \sim (-1)^{i+j} \langle S(x_i, y_j) \rangle$ is the three component ($\alpha = 1, 2, 3$) Néel order parameter as defined in 1.18. As we tune m^2 from positive to negative values through zero, we pass through the quantum phase transition at $m^2 = 0$. For $m^2 < 0$, the ϕ_α field acquires a non-zero expectation value and that means we are in the Néel phase. There are two massless Goldstone modes above the ground state. For $m^2 > 0$, we are in the dimer state and we have a finite gap $\Delta \equiv m$ to all excitations. Here we are working in d spatial and 1 time dimensions. So this quantum field theory is equivalent to the Wilson-Fisher model [44] in $d + 1$ dimensions. It is well known that the Wilson-Fisher theory possesses a fixed point in $4 - \epsilon$ dimensions with $g_0 \sim \epsilon$. Hence our theory will have a fixed point in $d = 3 - \epsilon$ dimensions. The experimental materials correspond to $\epsilon = 1$ or $d = 2$.

1.2.3 The Impurity Problem

The main topic of interest in this report will be the dynamics of a single non-magnetic impurity such as Zn or Li introduced into the bulk antiferromagnet in the spin gap phase. Such systems have been studied experimentally in both cuprate superconductors [45, 46, 47] as well as ordinary spin gap antiferromagnets like $SrCu_2O_3$ or $CuGeO_3$ [48, 49]. In terms of the lattice model the situation is depicted in Fig 1.3. As is obvious,

the impurity breaks the existing singlet state with its neighbours. So near the impurity there are free spins which can not form a singlet with the impurity. The notable property which emerges from experiments [2] is that such an impurity causes a localized spin moment of spin $1/2$ (the bulk magnetic moments also carry $S = 1/2$) to appear in the vicinity of the impurity [50, 51]. What happens is that there is an excess of one magnetic moment in one sub-lattice compared to the other one. In reality, this magnetic moment is not exactly on the impurity site itself, but is a local deformation of the magnetization vector spread over a few lattice sites. So although we shall treat the impurity spin as localized, this approximation holds only in the long wavelength limit. Experimental evidence for such a localized moment is shown in Fig 1.4.

Now we want to take into account the effect of this impurity on the field theory described above. We model the impurity by adding the following term to our action :

$$\mathscr{S}_{\text{imp}} = \int d\tau \left[iSA_\alpha(\boldsymbol{n}) \frac{dn_\alpha}{d\tau} - \gamma_0 S n_\alpha(\tau) \phi_\alpha(x = 0, \tau) \right]. \tag{1.21}$$

The first term in the action describes the dynamics of the impurity and the second term the coupling of the "impurity spin" to the bulk antiferromagnetic order parameter. Keep in mind that the actual impurity is non-magnetic. The "impurity spin" is the induced moment around the impurity site. Here $A_\alpha(\boldsymbol{n})$ is the vector potential due to a Dirac monopole and it appears as a part of the Berry phase for the spin $\boldsymbol{S}$. See Shankar's book on quantum mechanics [17] for a discussion of the Berry phase term in coherent state path integrals. The spin itself has been represented as its magnitude S times a three component unit vector n_α. It is situated at the origin and is coupled to the antiferromagnetic order parameter locally. Now the question is what is the effect of this impurity term on the original field theory. We show that there are no other relevant couplings (in the renormalization group sense) in this theory and we find a fixed point with $g_0 \sim \epsilon$ and $\gamma \sim \epsilon^{1/2}$ [52]. To one loop

$$g^* = \frac{6\epsilon}{11} \quad \gamma^{*2} = \frac{\epsilon}{2}. \tag{1.22}$$

Near this fixed point we also explore the spin dynamics of the impurity. Since we know

that the impurity spin is coupled to the antiferromagnetic order parameter, the dynamics of the spin will be strongly dependent on what the antiferromagnetic order is. In the disordered spin gap phase, there are no spin excitations in the bulk. In this phase the impurity spin will be confined strongly to the impurity site because of the energy required to create a triplet excitation by breaking the singlets. A way of studying this confinement is to look at the long time limit of the impurity spin autocorrelation. In the long time limit, the autocorrelation function approaches a constant number.

$$\lim_{\tau\to\infty}\langle \boldsymbol{S}_{\rm imp}(\tau)\cdot\boldsymbol{S}_{\rm imp}(0)\rangle = m^2 \neq 0, \tag{1.23}$$

where m is the magnetization at the impurity. As we move closer to the quantum critical point, low energy spin excitations will proliferate and at the critical point there will be excitations at all energies. Hence we expect m to vanish as a power law as we approach the critical point and the impurity spin autocorrelation to follow a power law at long times:

$$\langle \boldsymbol{S}_{\rm imp}(\tau)\cdot\boldsymbol{S}_{\rm imp}(0)\rangle \sim \frac{1}{\tau^{\eta'}}. \tag{1.24}$$

In the ordered regime, the bulk Néel order will force the impurity to align itself with the antiferromagnetic order vector $\boldsymbol{n}$. Again, the impurity magnetization will vanish as a power law we approach the critical point from the ordered side. We shall evaluate all these exponents explicitly in the report by renormalization group methods.

A real world material where our results are relevant is Zn doped $CuGeO_3$ [53]. $CuGeO_3$ by itself consists of chains of Cu^{2+} ions along the c direction coupled antiferromagnetically. The Cu^{2+} ions carry spin 1/2 each. Below 14 K this material dimerizes to a spin gap phase. Zn replaces Cu ions in this material and hence act as a non-magnetic impurity. Note that it is not necessary that the material really undergo a quantum phase transition for our continuum treatment to be valid. Only necessity is that it should be close enough to a quantum critical point such that our assumption $\Delta \ll J$ be satisfied. In this material $J \approx 88$ K and $\Delta \approx 24$ K.

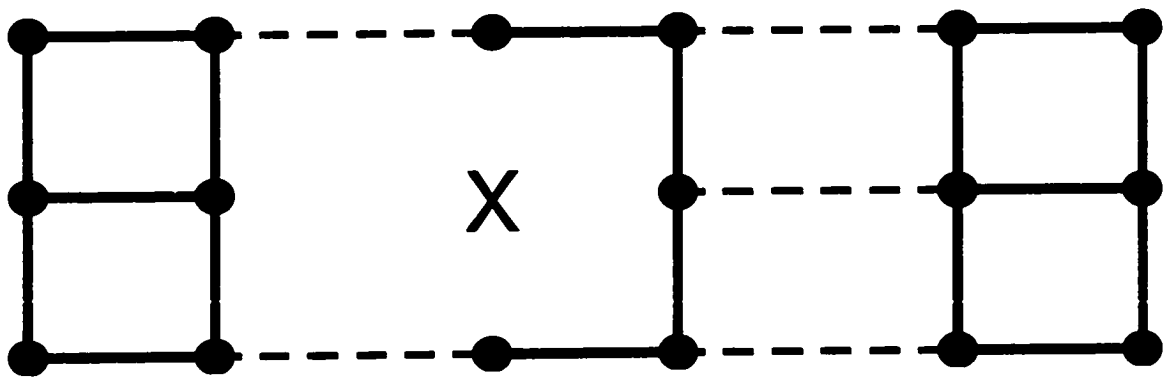

Figure 1.3: The lattice with one impurity. The site from which the spin has been removed is marked by a $\times$.

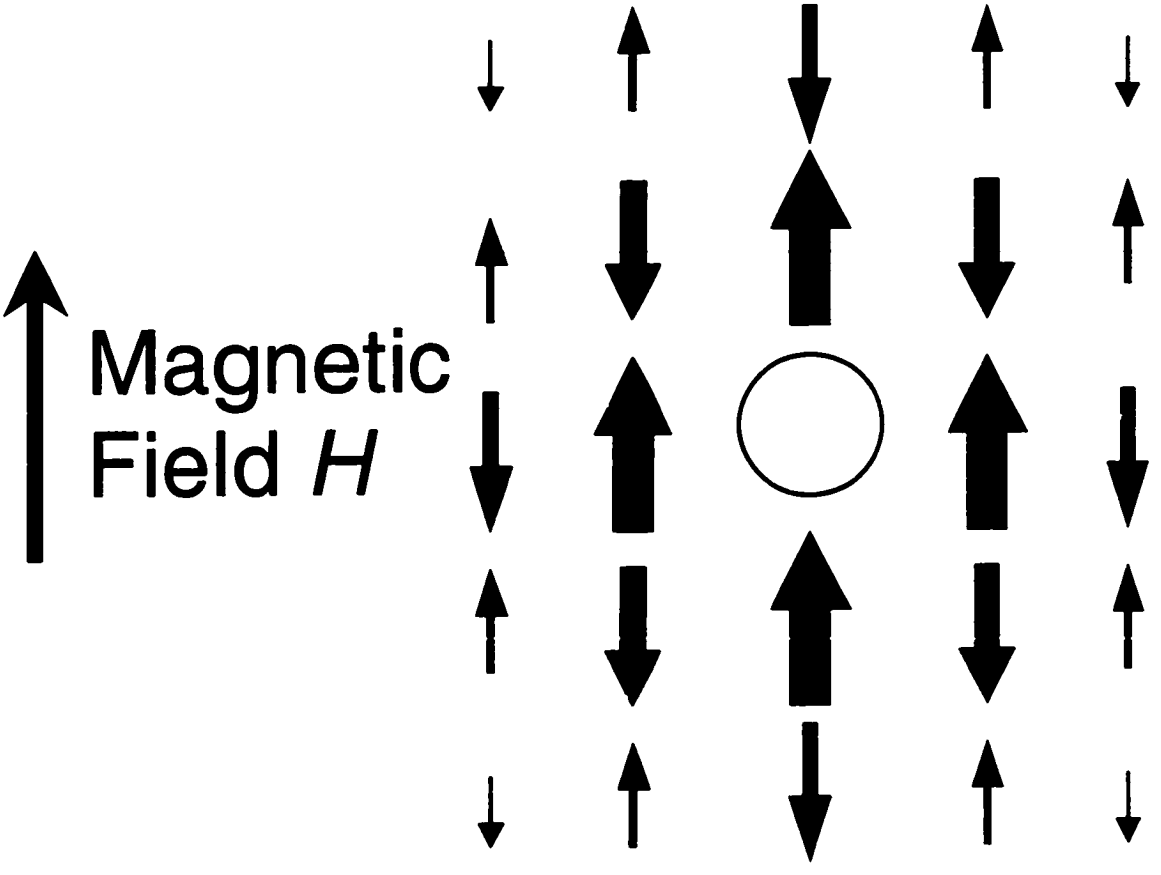

Figure 1.4: From Julien et.al. [2]. The impurity (Zn) site is denoted by an empty circle in the Cu lattice. The arrows show the strength of the magnetization on each Cu atom under an external field. The measurements were done by NMR on $YBa_2Cu_3O_{6.7}$. There is no spin on the Zn atom, but the net magnetic moment around it is centered around it and is expected to have a strength $S = 1/2$.

Chapter 2

One Dimensional Heisenberg Antiferromagnet at Intermediate Temperatures

2.1 The Non-Linear Sigma Model

As we have mentioned before in the introduction, the spin S Heisenberg antiferromagnetic chain is described by the Hamiltonian

$$H = J \sum_i \boldsymbol{S}_i \cdot \boldsymbol{S}_{i+1}, \; J > 0. \tag{2.1}$$

The classical ground state for this Hamiltonian at zero temperature is the Néel state where all the spins are collinear and alternately point up or down. We can construct a coherent state path integral description of this systems by considering fluctuations around this classical state. We define the unit vector field $\boldsymbol{n}(x, \tau)$ which crudely corresponds to the orientation of the spins on the lattice:

$$S\boldsymbol{n}(x_i, \tau) \sim (-1)^i \langle \boldsymbol{S}_i \rangle. \tag{2.2}$$

In terms of this field, the partition function at temperature T corresponding to this Hamiltonian is given by [19]

$$\begin{aligned} \mathcal{Z}_Q &= \int \mathcal{D}n\delta(\boldsymbol{n}^2 - 1)\exp(-S_B - S_n) \\ S_n &= \frac{1}{2cg}\int_0^{1/T} d\tau \int dx \left[c^2(\partial_x \boldsymbol{n})^2 + (\partial_\tau \boldsymbol{n} - i\boldsymbol{H}\times\boldsymbol{n})^2\right] \\ S_B &= i\frac{\theta}{4\pi}\int_0^{1/T} d\tau \int dx\, \boldsymbol{n}\cdot(\partial_x \boldsymbol{n}\times\partial_\tau \boldsymbol{n}), \end{aligned} \tag{2.3}$$

where $\theta = 0$ for integer values of S and $\theta = \pi$ for non-integer values of S. $\boldsymbol{H}$ is a uniform magnetic field. We shall be interested in the linear response to $\boldsymbol{H}$. We have also set $\hbar = k_B = 1$ everywhere. c is a constant with dimensions of velocity and g is the coupling. They are related to microscopic variables by

$$g = \frac{2}{S},\ c = 2JSa, \tag{2.4}$$

where a is the lattice constant. S_n is the ordinary Non-Linear Sigma Model (NLSM) action and S_B is the so called theta term or the Berry phase term. Since $\theta = 0$ for integer spins, the theta term is important only for half-integer spin chains.

Let us now briefly review the properties of this Hamiltonian for both integer and half integer values of spin [19].

2.1.1 Integer Spin

As we have already mentioned, the theta term does not contribute anything to the partition function for integer spin chains. The renormalization group (RG) flow for this Hamiltonian is shown in Fig 2.1. The $g = 0$ point is an unstable ultraviolet fixed point for all values of S. In the long wavelength, low energy limit g flows to the strong coupling limit $g = \infty$. At this limit we are looking at a system with a singlet ground state and a gap Δ to the first excited state.

2.1.2 Half-Integer Spin

Again as in the integer spin case, $g = 0$ is an unstable ultraviolet fixed point. But there is a new fixed point at $g = g_c \sim 1$ which is described by a scale invariant theory. This fixed

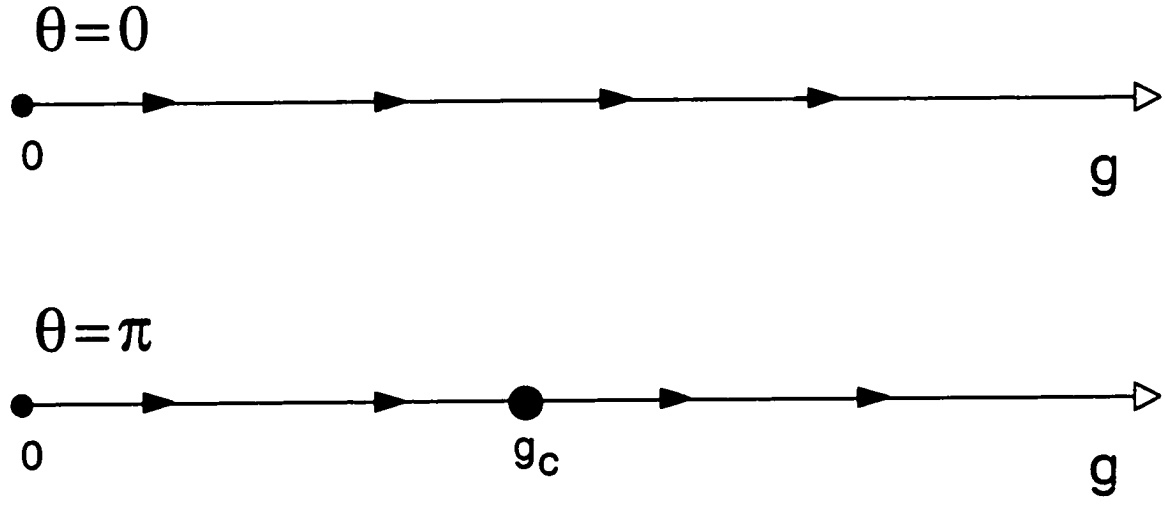

Figure 2.1: Renormalization group flow for the dimensionless coupling g defined in equation 2.3. For $\theta = 0$, there is an unstable fixed point at $g = 0$ and a stable fixed point at $g = \infty$. $g = \infty$ correspond to a gapped state with a gap Δ. For $\theta = \pi$, there is an additional fixed point at $g = g_c \sim 1$. This fixed point correspond to the so called Luttinger liquid gap-less state. In this discussion we shall be mostly interested in the regime $g \ll 1$ where behaviour of both $\theta = 0$ and $\theta = \pi$ chains are identical.

point is a direct consequence of the theta term. At this point the system is gap-less and is known as the Luttinger liquid. The relevant energy scale at this fixed point is denoted by T_0 which denotes the temperature at which logarithmic corrections to the $g = g_c$ fixed point behaviour becomes visible. On the other side of g_c, the coupling flows to the $g = \infty$ strong coupling fixed point.

2.1.3 The Perturbative Regime : $g \ll 1$

As we have seen, both integer and non-integer spins share a common fixed point at $g = 0$. The crucial point to notice is that for small values of the coupling constant $g \ll 1$, the RG flow is independent of theta because the theta term makes only a negligible contribution to the action. The weak coupling behaviour breaks down at an energy scale which we call $\Lambda_{\overline{MS}}$, and the difference between integer and non-integer spins becomes visible. This energy scale is entirely determined by the perturbative beta function for g around the $g = 0$ fixed point. We have provided a discussion on $\Lambda_{\overline{MS}}$ in appendix A. Physically speaking, $\Lambda_{\overline{MS}}$ is same as Δ or T_0 up to constants of order unity. For energies or temperatures smaller than $\Lambda_{\overline{MS}}$, we are in the strong coupling regime and integer and half-integer spin chains behave very differently. But for temperatures larger than $\Lambda_{\overline{MS}}$, the behaviour of the system is controlled by the $g = 0$ fixed point and the difference between integer and half-integers spins is not visible. We can estimate this important energy scale from the one loop beta function for small g and we find that

$$\Lambda_{\overline{MS}} \sim J \exp\left(-\frac{2\pi}{g}\right). \tag{2.5}$$

From equations 2.4 and 2.5 we see that for large values of S, a regime of temperature, $\Lambda_{\overline{MS}} \ll T \ll J$, opens up where we expect both integer and half-integer spin chains behave in a very similar way.

At this point the question naturally arises, whether this regime actually exists in nature. Since $\Lambda_{\overline{MS}}$ is exponentially sensitive to the value of S, we expect that even for small values of S, this regime could exist. We shall discuss evidence for the existence of this regime in section 2.4 after we discuss the expected static properties in the regime.

2.2 Static Properties

At this point let us discuss the temperature below which we expect the quantum action in equation 2.3, to be valid. This argument is due to Elstner et.al. [54]. Our continuum description will be valid as long as the dominant excitations have a wavelength larger than the lattice spacing a. At a temperature T, the dominant spin wave excitation will have a wavelength of the order c/T by equipartition. With the definition of c in 2.4, we can define a temperature $T^{(1)}_{\max}$ given by

$$T^{(1)}_{\max} \sim 2JS. \tag{2.6}$$

We expect our continuum quantum description to be valid below this temperature. Above this temperature, essentially the spins can be treated as classical spins. There is another temperature scale of importance which we denote by $T^{(2)}_{\max}$. Although above a temperature $T^{(1)}_{\max}$, the spin chain becomes essentially classical, a continuum description is still possible. To see this consider the correlation length $\xi_c(T)$ and susceptibility $\chi_u(T)$ for a classical Heisenberg antiferromagnetic chain[55]:

$$\xi_c(T) = \frac{JS^2a}{T}, \tag{2.7}$$

$$\chi_u(T) = \frac{1}{6Ja}. \tag{2.8}$$

At a temperature $T^{(1)}_{\max}$, $\xi_c(T^{(1)}_{\max}) \sim Sa/2$ could be much larger than the lattice spacing a for $S \gg 1$. We define $T^{(2)}_{\max}$ to be the temperature at which the classical correlation length becomes the size of the lattice spacing. Hence

$$T^{(2)}_{\max} \sim JS^2 > T^{(1)}_{\max}. \tag{2.9}$$

In the temperature range $T^{(1)}_{\max} < T < T^{(2)}_{\max}$, we can have a still have a continuum *classical* description of the spin chain. We shall come back to this point later in the chapter. For $T > T^{(2)}_{\max}$, lattice effects come into play and each spin is effectively decoupled from the others.

The important thermodynamic variables that characterize the state of the system as a function of temperature are the correlation length $\xi(T)$ and the uniform magnetic

susceptibility $\chi_u(T)$ defined by

$$\chi_u = \frac{T}{L}\frac{d^2 \ln(\mathcal{Z}_Q)}{dH^2}|_{H=0}, \tag{2.10}$$

where $\boldsymbol{H} = (0, 0, H)$ is an externally applied magnetic field and L is the system size.

Now we turn to a discussion of these static properties as a function of temperature and spin or equivalently θ. We shall distinguish two regimes: the low temperature regime given by $T < \Lambda_{\overline{MS}}$ and the high temperature regime $T > \Lambda_{\overline{MS}}$. This discussion will let us give an operational definition of the so far theoretical quantities like c and $\Lambda_{\overline{MS}}$.

2.2.1 Low Temperature Regime

Integer Spin

As we have noted before, the system has a gap of size Δ. The correlation length is given by [56]

$$\xi = \frac{c}{\Delta}, \ \Delta \ll J. \tag{2.11}$$

The susceptibility is exponentially suppressed by the gap because of a lack of excitations at $T \ll \Delta$ and it has been calculated to be [57, 30]

$$\chi_u(T) = \left[\frac{2\Delta}{\pi T c^2}\right]^{1/2} e^{-\Delta/T}. \tag{2.12}$$

By measuring the susceptibility as a function of temperature, it is clear that we can have a clear experimental determination of c and Δ. To conclude the discussion, we note that Hasenfratz and Niedermeyer [27] has given a relation between Δ and $\Lambda_{\overline{MS}}$ from a full Bethe Ansatz solution of the NLSM.

$$\Lambda_{\overline{MS}} = \frac{e}{8}\Delta. \tag{2.13}$$

Half-Integer Spin

This is the gap-less case and the susceptibility is finite even at $T = 0$ [28].

$$\chi_u(T) = \frac{1}{2\pi c}\left[1 + \frac{1}{2\ln(T_0/T)} + \cdots\right]. \tag{2.14}$$

T_0 is the temperature scale at which the logarithmic corrections to the scale invariant $g = g_c$ critical point appear. As before, knowledge of the susceptibility as a function of temperature gives us the values of c and T_0. Since the system is gap-less, the correlation length $\xi(T)$ diverges as $T \to 0$ and we have [8, 58]

$$\xi(T) = \frac{c}{\pi T}\left[1 + \frac{1}{2\ln(T_0/T)} + \cdots\right]. \tag{2.15}$$

Finally the relationship between T_0 and $\Lambda_{\overline{MS}}$ has been calculated by Sachdev [29]. The discussion is pretty technical and some details are presented in appendix C:

$$\Lambda_{\overline{MS}} = \left[\frac{\pi}{2}\right]^{1/2} e^{3/4-\gamma} T_0, \tag{2.16}$$

where γ is Euler's constant.

2.2.2 High Temperature Regime

From now on, we shall concentrate only on the regime $\Lambda_{\overline{MS}} < T < T^{(1)}_{\max}$ and consider the spin dynamics of the system. In this regime, both integer and half-integer spin chains exhibit the same behaviour. To make connection with experiments, all we need to do is to insert proper values of c and $\Lambda_{\overline{MS}}$ (or Δ, T_0) as found from experiments done in the low temperature regime.

The correlation length $\xi(T)$ and the uniform susceptibility $\chi_u(T)$ of the system has been calculated by Damle and Sachdev [30] and we briefly discuss this in appendix B. Here we just quote the results to the leading order in $T/\Lambda_{\overline{MS}}$:

$$\xi(T) = \frac{c}{2\pi T}\left[\ln\left(\frac{4\pi e^{-\gamma} T}{c\Lambda_{\overline{MS}}}\right)\right] \tag{2.17}$$

$$\chi_u(T) = \frac{1}{3\pi c}\left[\ln\left(\frac{4\pi e^{-\gamma} T}{c\Lambda_{\overline{MS}}}\right)\right]. \tag{2.18}$$

Since the system looks ordered out to a distance $\xi(T)$, the lowest energy spin wave excitations in this regime have a typical energy scale of order $c\xi^{-1}(T)$. If we look at the occupation number of such a mode, we find

$$\frac{1}{e^{c\xi^{-1}/T} - 1} \approx \frac{T}{c\xi^{-1}} \sim \ln\left(\frac{T}{\Lambda_{\overline{MS}}}\right) > 1. \tag{2.19}$$

The occupation number of these lowest energy modes are high and hence they can be treated classically. To describe the dynamics of these modes we shall use a classical model in the following pages. The derivation of this classical model is outlined in appendix B. The idea here is to integrate out all the modes with Matsubara frequency $\omega_n \neq 0$ and derive an effective action in terms of the $\omega_n = 0$ modes only. The classical equations of motion can be derived by replacing all the quantum commutators of the original Hamiltonian by classical Poisson brackets. The effective classical partition function we arrive at is

$$\begin{aligned} \mathcal{Z}_C &= \int \mathcal{D}\boldsymbol{n}\mathcal{D}\boldsymbol{L}\delta(\boldsymbol{n}^2-1)\delta(\boldsymbol{L}\cdot\boldsymbol{n})\exp(-\mathcal{H}/T) \\ \mathcal{H} &= \frac{1}{2}\int dx\left[T\xi(T)\left(\frac{d\boldsymbol{n}}{dx}\right)^2+\frac{1}{\chi_{u\perp}(T)}\boldsymbol{L}^2\right]. \end{aligned} \tag{2.20}$$

Here $\boldsymbol{n}(x)$ is a unit vector field which describes the local orientation of the antiferromagnetic ordering vector and $\boldsymbol{L}(x)$ is the canonically conjugate momentum associated with it. Because $\boldsymbol{n}(x)$ is constrained to be of unit magnitude, the movement of $\boldsymbol{n}$ is always orthogonal to itself. This explains the constraint $\boldsymbol{L}\cdot\boldsymbol{n}=0$ in the partition function. There is no radial component of the momentum and hence the square of the angular momentum $\boldsymbol{L}^2$ accounts for the total kinetic energy of the $\boldsymbol{n}$ field.

The constant $\chi_{u\perp}$ can be determined by demanding that the uniform susceptibility of the classical system coincides with the quantum system and we find

$$\chi_u = \frac{2}{3}\chi_{u\perp}. \tag{2.21}$$

The correlation functions in the classical system are related to the full quantum correlation functions by (see appendix B)

$$\langle\boldsymbol{n}(x,t)\cdot\boldsymbol{n}(0,0)\rangle_Q = \mathscr{A}\mathscr{C}\left[\ln\left(\frac{T}{\Lambda_{\overline{MS}}}\right)\right]^{\frac{N-1}{N-2}}\langle\boldsymbol{n}(x,t)\cdot\boldsymbol{n}(0,0)\rangle_C, \tag{2.22}$$

$$\langle\boldsymbol{L}(x,t)\cdot\boldsymbol{L}(0,0)\rangle_Q = \langle\boldsymbol{L}(x,t)\cdot\boldsymbol{L}(0,0)\rangle_C. \tag{2.23}$$

The subscripts Q, C denote whether the correlation function is evaluated from the quantum or the classical action. The overall scale factor $\mathscr{A}$ is the quasiparticle amplitude

and it depends on the microscopic details of the model. The constant $\mathscr{C}$ is an unknown universal number. The factor of $\ln(T/\Lambda_{\overline{MS}})$ appears from the renormalization group equations for the wave function renormalization of the correlation functions. This factor connects correlations of classical modes which are defined at an energy scale T, to the quantum modes which are defined at the lower energy scale of $\Lambda_{\overline{MS}}$.

2.3 Equation of Motion

As expected of a classical Hamiltonian, our partition function is defined as a functional integral over commuting fields $\boldsymbol{n}(x)$ and $\boldsymbol{L}(x)$ which are independent of time. The classical equations of motion generated by this Hamiltonian will be used to derive the time dependent correlators of these fields. To derive these equations of motion, we need the following Poisson brackets of the fields:

$$\begin{aligned} \{n_\alpha(x), n_\beta(y)\} &= \delta_{\alpha\beta}\delta(x-y) \\ \{L_\alpha(x), L_\beta(y)\} &= \epsilon_{\alpha\beta\gamma}L_\gamma(x)\delta(x-y) \\ \{n_\alpha(x), L_\beta(y)\} &= \epsilon_{\alpha\beta\gamma}n_\gamma(x)\delta(x-y), \end{aligned} \tag{2.24}$$

where the indices α, β and γ run over 1,2 and 3. The real time Hamiltonian equations of motion immediately follow as

$$\begin{aligned} \frac{\partial \boldsymbol{n}}{\partial t} &= \frac{1}{\chi_{u\perp}(T)}\boldsymbol{n}\times\boldsymbol{L} \\ \frac{\partial \boldsymbol{L}}{\partial t} &= T\xi(T)\boldsymbol{n}\times\frac{\partial^2\boldsymbol{n}}{\partial x^2}. \end{aligned} \tag{2.25}$$

These equations of motion constitute a set of non-linear wave equation for the $\boldsymbol{n}(x)$ and $\boldsymbol{L}(x)$ fields. The wave velocity is

$$c(T) = \left(\frac{T\xi(T)}{\chi_{u\perp}(T)}\right)^{1/2} \approx c. \tag{2.26}$$

With these equations of motion we turn to the chief point of interest here which is the determination of the unequal time thermal correlation functions $\langle \boldsymbol{n}(x,t)\cdot\boldsymbol{n}(0,0)\rangle_C$ and

$\langle \boldsymbol{L}(x,t)\cdot\boldsymbol{L}(0,0)\rangle_C$. It is convenient for us to cast all these correlations in terms of dimensionless quantities. By simple dimensional analysis, we arrive at

$$\begin{aligned}\bar{x} &\equiv x/\xi(T)\\ \bar{t} &\equiv t\left[\frac{T}{\xi(T)\chi_{u\perp}(T)}\right]^{1/2},\end{aligned} \tag{2.27}$$

and we define new scaling functions of dimensionless arguments

$$\begin{aligned}\langle \boldsymbol{n}(x,t)\cdot\boldsymbol{n}(0,0)\rangle_C &= \Phi_n(\bar{x},\bar{t})\\ \langle \boldsymbol{L}(x,t)\cdot\boldsymbol{L}(0,0)\rangle_C &= \left[\frac{T\chi_{u\perp}(T)}{\xi(T)}\right]\Phi_L(\bar{x},\bar{t}).\end{aligned} \tag{2.28}$$

In the rest of the chapter our goal will be to estimate these two scaling functions analytically as well as numerically.

At this point we come back to the question of effective temperature range over which we can apply the classical model described above. We have already argued that in the temperature range $\Lambda_{\overline{MS}} < T < T^{(1)}_{\max}$, our effective classical model is applicable. But we know from the discussion succeeding equation 2.9, that the temperature range $T^{(1)}_{\max} < T < T^{(2)}_{\max}$ is also described by a classical model. So we expect that our model has in fact, a greater range of validity stretching from $\Lambda_{\overline{MS}}$ to $T^{(2)}_{\max}$.

In the regime $T^{(1)}_{\max} < T < T^{(2)}_{\max}$, the values of the susceptibility and correlation length are no longer universal (independent of microscopic variable like J and a). For a nearest neighbour exchange Heisenberg chain we have the result [55]

$$\chi_u(T) = \frac{1}{6Ja},\ \xi(T) = \frac{JS^2a}{T}. \tag{2.29}$$

We note that these expressions match with the expressions for $\chi_u(T)$ and $\xi(T)$ in equations 2.18 and 2.17 at the common temperature $T^{(1)}_{\max}$. For example

$$\xi(T^{(1)}_{\max}) \sim \frac{c}{2\pi T^{(1)}_{\max}} \ln\left(\frac{T^{(1)}_{\max}}{\Lambda_{\overline{MS}}}\right) \sim \frac{JS^2a}{T^{(1)}_{\max}}. \tag{2.30}$$

Here we have used the fact that $\ln(T^{(1)}_{\max}/\Lambda_{\overline{MS}}) \approx 2\pi/g$ and used the definitions of $T^{(1)}_{\max}$, g and c from equations 2.6 and 2.4.

2.4 Evidence for the Existence for the Intermediate Temperature Regime

Before we plunge into an analysis of this model, we would like to pause for a moment and investigate the question whether there is any evidence for the existence of the temperature regime $T > \Lambda_{\overline{MS}}$. We shall show that Monte Carlo simulations have shown definite indications that for values of S as small as 2, this regime might be accessible to experiments.

Let us first turn to the Monte Carlo study of Kim et. al. [59] on $S = 2$ spin chains. Their results are displayed on Fig. 2.2. On the upper graph, they plot $T\xi(T)/c$ while on the lower graph they plot $c\chi_u(T)$ as a function of temperatures. The interesting regime is the temperature regime between $\Lambda_{\overline{MS}} \sim \Delta < T < J$ which they plot with solid lines. The dashed line plots are not germane to the discussion and they are explained in the caption. Note that the fits are *without* any adjustable parameters. c and Δ have been determined by measuring the small temperature susceptibility defined in equation 2.12. The good match reinforces our confidence in these results.

Next is the quantum Monte Carlo study of 5 leg spin 1/2 ladders by Frischmuth et. al. [3]. p leg ladders with each spin of magnitude S behave essentially like a single chain of spin Sp. So the discussion for half-integer spin chains is applicable in this case. The result for the uniform susceptibility is displayed in Fig. 2.3. The fitting parameters are c and T_0. There is some arbitrariness here in choosing the temperature regime over which to fit the data and depending on that the values of c and T_0 can vary quite a bit. Unlike the integer spin case, the data at low temperatures are not very reliable and this leads to the problem of estimating c and T_0 properly. This fit yields $c = 2.06Ja$ and $T_0 = 0.0058J$.

2.5 Short Time Expansion

In this section we will determine the small $\bar{t}, \bar{x}$ expansion of the scaling functions $\Phi_n(\bar{x}, \bar{t})$ and $\Phi_L(\bar{x}, \bar{t})$. Also in this section, and in appendix D, we will use units in which $T =$

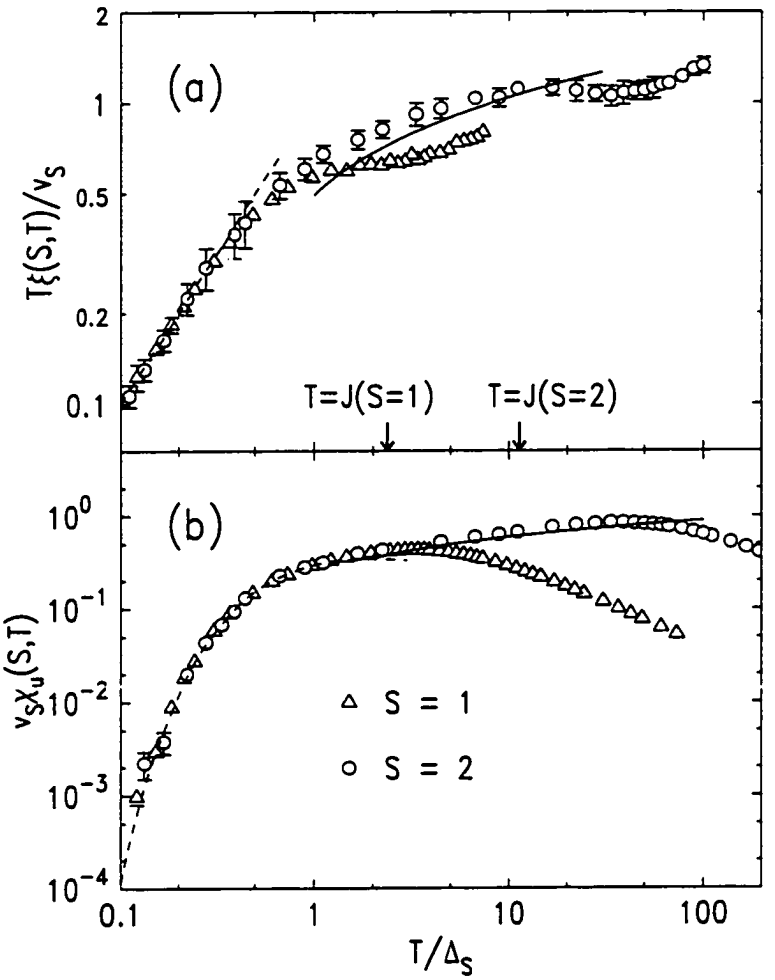

Figure 2.2: (a) Correlation length and (b) uniform susceptibility plotted as a function of temperature for $S = 1$ and $S = 2$. Here the notation $v_s \equiv c$ and $\Delta_s \equiv \Delta$. The solid lines are fits from equations 2.17 and 2.18 respectively without any free parameters. In (a), the dashed line is the fit from $\xi = \frac{\Delta}{c}$, and in (b) the dashed line is the fit of the low temperature susceptibility given in equation 2.12.

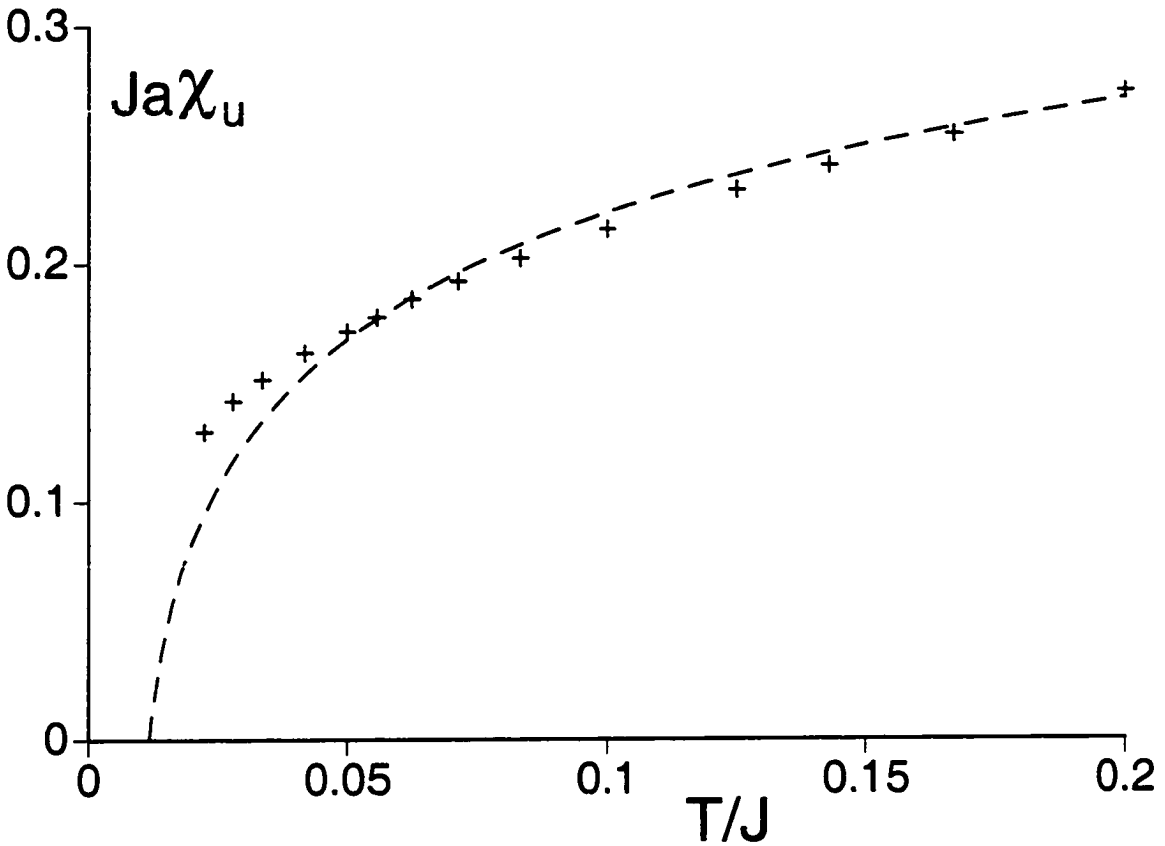

Figure 2.3: Comparison of numerical results of Frischmuth et. al. [3] with the uniform susceptibility of a 5 leg ladder with $S = 1/2$ from the equation 2.18. The value of $\chi_u(T)$ is susceptibility per rung.

$\chi_{u\perp}(T) = 1$. However, we will retain explicit dependence on $\xi \equiv \xi(T)$. It turns out to be quite useful to keep track of powers of ξ. Indeed, our computations will be designed to generate an expansion of the correlators in powers of $\bar{t}/\xi$. We will return to physical units in stating our final results.

We therefore consider the problem of unequal time correlation functions of the $\boldsymbol{n}(x,t)$ and $\boldsymbol{L}(x,t)$ fields. The fields evolve according to the non-linear partial differential equations

$$\begin{aligned} \frac{\partial \boldsymbol{n}(x,t)}{\partial t} &= \boldsymbol{L}(x,t) \times \boldsymbol{n}(x,t), \\ \frac{\partial \boldsymbol{L}(x,t)}{\partial t} &= \xi \boldsymbol{n}(x,t) \times \frac{\partial^2 \mathbf{n}(x,t)}{\partial x^2}, \end{aligned} \tag{2.31}$$

and the average is over the ensemble of initial conditions defined by the partition function

$$\mathscr{Z}_C = \int \mathscr{D}\boldsymbol{n}(x)\mathscr{D}\boldsymbol{L}(x)\delta(\boldsymbol{n}^2 - 1)\delta(\boldsymbol{L}\cdot\boldsymbol{n}) \exp\left(-\frac{1}{2}\int dx \left[\xi\left(\frac{d\boldsymbol{n}}{dx}\right)^2 + \mathbf{L}^2 - 2\xi m^2 n_z\right]\right). \tag{2.32}$$

The last term in the action represents a field of strength ξm^2 turned on in the z direction and serves as an infrared regularization parameter for our perturbation expansion. At the end of our calculations we shall let $m \to 0$. What we shall be doing here is to assume that the field n is ordered along the z direction and then carry out a harmonic expansion of small fluctuations around this ordered state. The field in z direction ensures that this ordering is true. From this partition function, one can immediately find the equal time correlation functions to be (in the limit $m \to 0$)

$$\begin{aligned} \langle \boldsymbol{L}(x,0)\cdot\boldsymbol{L}(0,0)\rangle_C &= 2\delta(x) \\ \langle \boldsymbol{n}(x,0)\cdot\boldsymbol{n}(0,0)\rangle_C &= e^{-|x|/\xi}; \end{aligned} \tag{2.33}$$

the subscript C is implied on all averages in this section, unless stated otherwise.

We first construct our perturbation expansion in powers of $1/\xi$ for the equal time problem specified by (2.32), and check that we do arrive at the correct correlation functions as specified in (2.33). The extension to the unequal time problem will then be

straightforward. First, the constraints on the fields $\boldsymbol{n}$ and $\boldsymbol{L}$ are solved by introducing two complex scalar fields ϕ and ψ.

$$\begin{aligned} n_x &= \frac{1}{\sqrt{2\xi}}(\phi + \phi^*) \\ n_y &= \frac{1}{i\sqrt{2\xi}}(\phi - \phi^*) \\ n_z &= \sqrt{1 - 2\phi\phi^*/\xi} \\ L_x &= \frac{1}{\sqrt{2}}(\psi + \psi^*) \\ L_y &= \frac{1}{i\sqrt{2}}(\psi - \psi^*) \\ L_z &= -\frac{\phi\psi^* + \phi^*\psi}{\sqrt{\xi}\sqrt{1 - 2\phi\phi^*/\xi}} \end{aligned} \tag{2.34}$$

We introduce this decomposition to the functional integral (2.32) and expand the square roots in power series of $1/\xi$. In this manner, we arrive at an interacting field theory with an infinite number of interactions, with $1/\xi, 1/\xi^2, 1/\xi^3 \ldots$ as the small coupling constants. However, to any particular order in perturbation theory in $1/\xi$, we only need to keep a finite set of interaction terms. We evaluate the correlation functions in real space using the ordinary machinery of diagrammatic perturbation theory. It is well known that such a perturbation expansion is plagued by infrared divergences. The decomposition (2.34) takes it for granted that the $\boldsymbol{n}$ field is ordered in the z direction and ϕ represents small spin wave fluctuations around the ordered state. The infrared divergences are a signature of the fact that this assumption is wrong in one dimension. By introducing the external field ξm^2, we introduce long range order into the system and thus regularize the divergences. The divergences show up as poles in $1/m$. But if we calculate the O(3) invariant correlation functions as in (2.33), we find that all poles cancel. Keeping this in mind, it is not difficult to show that the results of perturbation theory agree with (2.33) at every order. The details are to be found in Appendix D.

Once we have the correlation functions in the equal time ensemble, we proceed to evaluate the unequal time correlation functions. To do that we again insert (2.34) into

the equations of motion (2.31) and expand in powers of $1/\xi$ to get

$$\begin{aligned}\frac{\partial\psi}{\partial t} &= i\xi^{1/2}\left[\frac{\partial^2\phi}{\partial x^2}+\frac{1}{\xi}\frac{\partial}{\partial x}\left(\phi^2\frac{\partial\phi^*}{\partial x}\right)+\cdots\right]\\ \frac{\partial\phi}{\partial t} &= -i\xi^{1/2}\left[\psi+\frac{1}{\xi}\left(\phi^2\psi^*\right)+\cdots\right].\end{aligned} \tag{2.35}$$

Higher order terms add further nonlinear interactions. We solve the initial value problem for each of the fields by an iterative strategy. First the free wave equation is solved and the solution is plugged back into the lowest order nonlinear term to solve the problem to the first order. To evaluate the correlation functions, we just multiply the fields and carry out the average over initial conditions. The initial condition averages are, of course, known from the calculations described above. The technical details are relegated to Appendix D and here we only quote the results to one loop order:

$$\begin{aligned}\left(\frac{\xi(T)}{T\chi_{u\perp}(T)}\right)\langle \boldsymbol{L}(x,t)\cdot\boldsymbol{L}(0,0)\rangle_C &= \left(\delta(\bar{x}-\bar{t})+\delta(\bar{x}+\bar{t})\right)\left(1-\frac{|\bar{t}|}{2}\right)\\ &\quad+\frac{1}{2}\left(\theta(\bar{x}+\bar{t})-\theta(\bar{x}-\bar{t})\right)\\ &\quad+\mathcal{O}(\bar{x},\bar{t})\end{aligned} \tag{2.36}$$

$$\begin{aligned}\langle \boldsymbol{n}(x,t)\cdot\boldsymbol{n}(0,0)\rangle_C &= 1-\frac{1}{2}(|\bar{x}+\bar{t}|+|\bar{x}-\bar{t}|)\\ &\quad+\frac{1}{16}\left(3(\bar{x}+\bar{t})^2+3(\bar{x}-\bar{t})^2+2|\bar{x}+\bar{t}||\bar{x}-\bar{t}|\right)\\ &\quad+\mathcal{O}(\bar{x},\bar{t})^3,\end{aligned} \tag{2.37}$$

where $\bar{x}$ and $\bar{t}$ are defined in (2.27), and the delta function in (2.36) is interpreted as $\mathcal{O}(\bar{x}^{-1},\bar{t}^{-1})$.

In these results if we set $t=0$, we immediately recover the equal time results (2.33) to the corresponding order in $1/\xi$. The structure of the correlation function (2.36) reflects the causal propagation of the conserved angular momentum $\boldsymbol{L}$. The first term simply represents the free propagation of the angular momentum density which is completely concentrated on the "light cone" ($\bar{x}^2-\bar{t}^2=0$). However, interactions to order $1/\xi$ do modify the free propagation and transfer the angular momentum density from the surface of the light cone to its interior. This is represented by the second term which is

non-vanishing only inside the light cone ($|\overline{x}| < |\overline{t}|$). It can be checked that the spatial integral of (2.36) remains independent of t, as must be the case due to conservation of total angular momentum.

2.6 Spin Wave Damping At Large Momentum

The short time expansion derived above can provide us with information concerning the large momentum behaviour of the spin-spin correlation function. The relevant dynamic structure factor is

$$S(k,\omega) = \int dx\, dt\, \langle \boldsymbol{n}(x,t) \cdot \boldsymbol{n}(0,0) \rangle_Q e^{-i(kx-\omega t)}. \tag{2.38}$$

Using the scaling property we write the dynamic structure factor as

$$S(k,\omega) = \left[\frac{\xi(T)\chi_{u\perp}(T)}{T}\right]^{1/2} S(k)\Phi_S(\overline{k},\overline{\omega}), \tag{2.39}$$

where $S(k)$ is the equal time structure factor and Φ_S is a universal scaling function of the dimensionless variables

$$\begin{aligned} \overline{k} &= k\xi(T) \\ \overline{\omega} &= \omega\left[\frac{\xi(T)\chi_{u\perp}(T)}{T}\right]^{1/2}. \end{aligned} \tag{2.40}$$

Since $S(k)$ is the equal time structure factor, it is known exactly up to a normalization constant:

$$S(k) = \int \frac{d\omega}{2\pi} S(k,\omega) = \mathscr{A}\left[\ln\left(\frac{T}{\Lambda_{\overline{MS}}}\right)\right]^2 \frac{2\xi}{1+\overline{k}^2} \tag{2.41}$$

The RHS is just the Fourier transform of the equal time correlation function in equation 2.33. With this definition of $S(k)$, Φ_S satisfies the normalization condition

$$\int \frac{d\overline{\omega}}{2\pi} \Phi_S(\overline{k},\overline{\omega}) = 1. \tag{2.42}$$

In the short distance regime ($\overline{k} \gg 1$, $\overline{\omega} \gg 1$), we are exploring distances much shorter than the correlation length and the system should look ordered. We expect the

dominant excitations at this length scale will be spin waves with linear dispersion and some damping given by $\gamma(\bar{k})$. Hence we postulate the following form for $\Phi_S(\bar{k},\bar{\omega})$ consistent with the normalization given above:

$$\Phi_S(\bar{k},\bar{\omega}) = \frac{\gamma(\bar{k})}{(\bar{\omega}-\bar{k})^2+\gamma(\bar{k})^2} + \frac{\gamma(\bar{k})}{(\bar{\omega}+\bar{k})^2+\gamma(\bar{k})^2}. \tag{2.43}$$

Our goal will be to determine the large $\bar{k}$ limit of $\gamma(\bar{k})$.

We shall now take the Fourier transform of $S(k,\omega)$ from 2.39 and compare it with 2.37. The frequency integral in the Fourier transform can be performed easily to get

$$\langle \boldsymbol{n}(x,t)\cdot\boldsymbol{n}(0,0)\rangle = \int \frac{d\bar{k}}{2\pi}\frac{e^{i\bar{k}\bar{x}-\gamma(\bar{k})|\bar{t}|}\cos(\bar{k}\bar{t})}{2(1+\bar{k}^2)}. \tag{2.44}$$

In the large momentum limit we can safely ignore 1 compared to $\bar{k}^2$ in the denominator. We now impose a low momentum cutoff on this integral and expand the exponential in powers of $|\bar{t}|$.

$$\begin{aligned}\langle \boldsymbol{n}(x,t)\cdot\boldsymbol{n}(0,0)\rangle &= \frac{2}{\pi}\int_{\bar{k}_1}^{\infty} d\bar{k}\frac{\cos(\bar{k}\bar{x})\cos(\bar{k}\bar{t})}{\bar{k}^2} \\ &\quad -\frac{2|\bar{t}|}{\pi}\int_{\bar{k}_2}^{\infty} d\bar{k}\frac{\gamma(\bar{k})\cos(\bar{k}\bar{x})\cos(\bar{k}\bar{t})}{\bar{k}^2}+\cdots,\end{aligned} \tag{2.45}$$

where $\bar{k}_{1,2}$ are arbitrary large positive cutoffs. Also we have assumed that $\gamma(\bar{k})$ is an even function of $\bar{k}$. The important point here is that the leading non-analytic terms in $\bar{x},\bar{t}$ are independent of the precise values of the cutoffs $\bar{k}_{1,2}$. Asymptotically

$$\int_{\bar{k}_1}^{\infty}\frac{d\bar{k}}{\bar{k}^{\nu}}\cos(\bar{k}\bar{x}) = \frac{\pi|\bar{x}|^{\nu-1}}{2\Gamma(\nu)\cos(\pi\nu/2)}+\cdots. \tag{2.46}$$

All the omitted terms contain only even non-negative integer powers of $\bar{x}$ (including a constant term). We now assume that

$$\lim_{\bar{k}\to\infty}\gamma(\bar{k}) \sim \bar{k}^{\alpha}, \tag{2.47}$$

and demand that the forms 2.37 and 2.45 be consistent with each other. We immediately conclude that $\alpha = 0$ and hence $\gamma(\infty)$ is a constant. Applying the expansion 2.46 to 2.45, we find

$$\langle \boldsymbol{n}(x,t)\cdot\boldsymbol{n}(0,0)\rangle = \cdots -\frac{1}{2}(|\bar{x}+\bar{t}|+|\bar{x}-\bar{t}|)(1-\gamma(\infty)|\bar{t}|)+\cdots. \tag{2.48}$$

We need to compare 2.48 to 2.37 in the vicinity of the light cone $\bar{x} = \pm\bar{t}$. In this vicinity

$$|\bar{x} + \bar{t}||\bar{x} - \bar{t}| \approx 2|\bar{t}||\bar{x} \mp \bar{t}|. \tag{2.49}$$

Now comparing 2.48 and 2.37, we immediately arrive at the exact result that

$$\gamma(\infty) = \frac{1}{2}. \tag{2.50}$$

Restoring the dimensions to $\gamma(\bar{k})$, we find the spin wave damping rate to be

$$\Gamma(T) = \frac{1}{2}\left[\frac{T\chi_{u\perp(T)}}{\xi(T)}\right]^{1/2}. \tag{2.51}$$

Similar results for spin-wave damping in the classical antiferromagnets have been obtained by Reiter and Sjölander [60]. If we use the classical values of the susceptibility (eq. 2.8) and correlation length (eq. 2.7) in eq. 2.51, we obtain

$$\Gamma(T) = \frac{T}{S} \tag{2.52}$$

which agrees with their results.

2.7 Numerical Results

Since the large $\bar{t}$ regime of this model is not accessible analytically, we use numerical methods to solve the equations 2.25. First we construct a non-dimensional version of the Hamiltonian in 2.20. We set

$$\begin{aligned}
\bar{x} &\equiv x/\xi \\
\bar{t} &\equiv t/\tau_\phi \\
\overline{L} &\equiv L\left(\frac{\xi}{T\chi_{u\perp}}\right)^{1/2} \\
\tau_\phi &\equiv \left(\frac{\xi\chi_{u\perp}}{T}\right)^{1/2}.
\end{aligned} \tag{2.53}$$

With these definitions, all reference to the dimensionful parameters $(T, \xi, \chi_{u\perp})$ in the Hamiltonian and the partition function disappear and we are left with the equations of

motion

$$\begin{aligned}\frac{\partial n_\alpha}{\partial \bar{t}} &= \epsilon_{\alpha\beta\gamma}\bar{L}_\beta n_\gamma \\ \frac{\partial \bar{L}_\alpha}{\partial \bar{t}} &= \epsilon_{\alpha\beta\gamma} n_\beta \frac{\partial^2 n_\gamma}{\partial \bar{x}^2},\end{aligned} \tag{2.54}$$

where the index $\alpha = 1, 2, 3$.

2.7.1 The Lattice Model

The non-linear partial differential equation 2.54 is handled in two steps. First we shall replace the continuous space variable x with a lattice indexed by i and then on this lattice each variable will be evolved in time. For notational simplicity, for the rest of this section we shall drop the bar from $\bar{x}$ etc, i.e. write x, t, L, when we mean $\bar{x}, \bar{t}, \bar{L}$. We choose a lattice spacing a, and replace

$$\begin{aligned} n_\alpha(x,t) &\rightarrow n_{\alpha i}(t), \\ L_\alpha(x,t) &\rightarrow \frac{1}{a} L_{\alpha i}(t), \\ \frac{\partial n_\alpha(x,t)}{\partial x} &\rightarrow \frac{n_{\alpha i+1}(t) - n_{\alpha i-1}(t)}{2a}. \end{aligned} \tag{2.55}$$

With these definitions, our partition function and the equations of motion take the form

$$\begin{aligned} \mathscr{Z}_c &= \int \prod_i \mathscr{D}\boldsymbol{n}_i(t)\mathscr{D}\boldsymbol{L}_i(t)\delta(\boldsymbol{n}_i^2 - 1)\delta(\boldsymbol{n}_i \cdot \boldsymbol{L}_i)\exp(-\mathscr{H}_c) \\ \mathscr{H}_c &= \frac{1}{2a}\sum_i \left[-\frac{1}{2}\boldsymbol{n}_{i+1}\cdot\boldsymbol{n}_{i-1} + \boldsymbol{L}_i \cdot \boldsymbol{L}_i\right] \\ \frac{\partial n_{\alpha i}}{\partial t} &= \frac{1}{a}\epsilon_{\alpha\beta\gamma} L_{\beta i} n_{\gamma i} \\ \frac{\partial L_{\alpha i}}{\partial t} &= \frac{1}{a}\epsilon_{\alpha\beta\gamma} n_{\beta i}\frac{n_{\gamma i+2} - 2n_{\gamma i} + n_{\gamma i-2}}{4} \end{aligned} \tag{2.56}$$

It is easy to verify that this lattice discretization scheme conserves angular momentum exactly, i.e.

$$\frac{\partial}{\partial t}\sum_i L_{\alpha i} = 0.$$

For computing correlation functions, we need to average over all initial conditions which are generated by thermalizing an ensemble governed by the discrete Hamiltonian

2.56. The thermalization algorithm used was the Wolff algorithm [61]. This algorithm has the advantage that it avoids critical slowing down for small temperatures. The time evolution was carried out by a fourth order predictor-corrector method. The predictor-corrector method is significantly faster than Runge-Kutta algorithms and it also conserves angular momentum exactly. The accuracy of the time evolution was tested by keeping track of the total energy and the norm of individual $\boldsymbol{n}_i$ vectors. For the total duration of the time evolution, energy was conserved to 4 significant digits. The $\boldsymbol{L}$ autocorrelation was calculated with a lattice of 800 sites and averaged over 9600 initial conditions.

2.7.2 Dynamics of n Field

We obtained results for the dynamic structure factor $S(k,\omega)$ beyond the regime covered by the short time expansion where $\overline{k},\overline{\omega} \gg 1$. The specific correlation functions that we studied are the autocorrelation function, and $S(k=0,\omega)$.

The autocorrelation function allows us to compute the local dynamic structure factor $S_l(\omega)$ defined by

$$S_l(\omega) = \int \frac{dk}{2\pi} S(k,\omega) = \int dt e^{i\omega t} \langle \boldsymbol{n}(0,t)\cdot\boldsymbol{n}(0,0)\rangle_Q \tag{2.57}$$

By equations 2.39 and 2.41 $S_l(\omega)$ satisfies the scaling relation

$$\begin{aligned} S_l(\omega) &= \mathscr{A}\left[\ln\left(\frac{T}{\Lambda_{\overline{MS}}}\right)\right]^2 \left[\frac{\xi(T)\chi_{u\perp}}{T}\right]^{1/2} \Phi_l(\overline{\omega}), \\ \int \frac{d\overline{\omega}}{2\pi}\Phi_l(\overline{\omega}) &= 1. \end{aligned} \tag{2.58}$$

Here $\Phi_l(\overline{\omega})$ is a universal function of its dimensionless argument.

The autocorrelation function $\langle \boldsymbol{n}(0,t)\cdot\boldsymbol{n}(0,0)\rangle_C$ and the universal function $\Phi_l(\overline{\omega})$ obtained by the Fourier transform of the autocorrelation are shown in Figs. 2.4 and 2.5. Two different lattice spacings were used to compute the autocorrelation and since both data sets match almost exactly, we are confident that we are in the continuum limit and no finite lattice spacing artifacts exist.

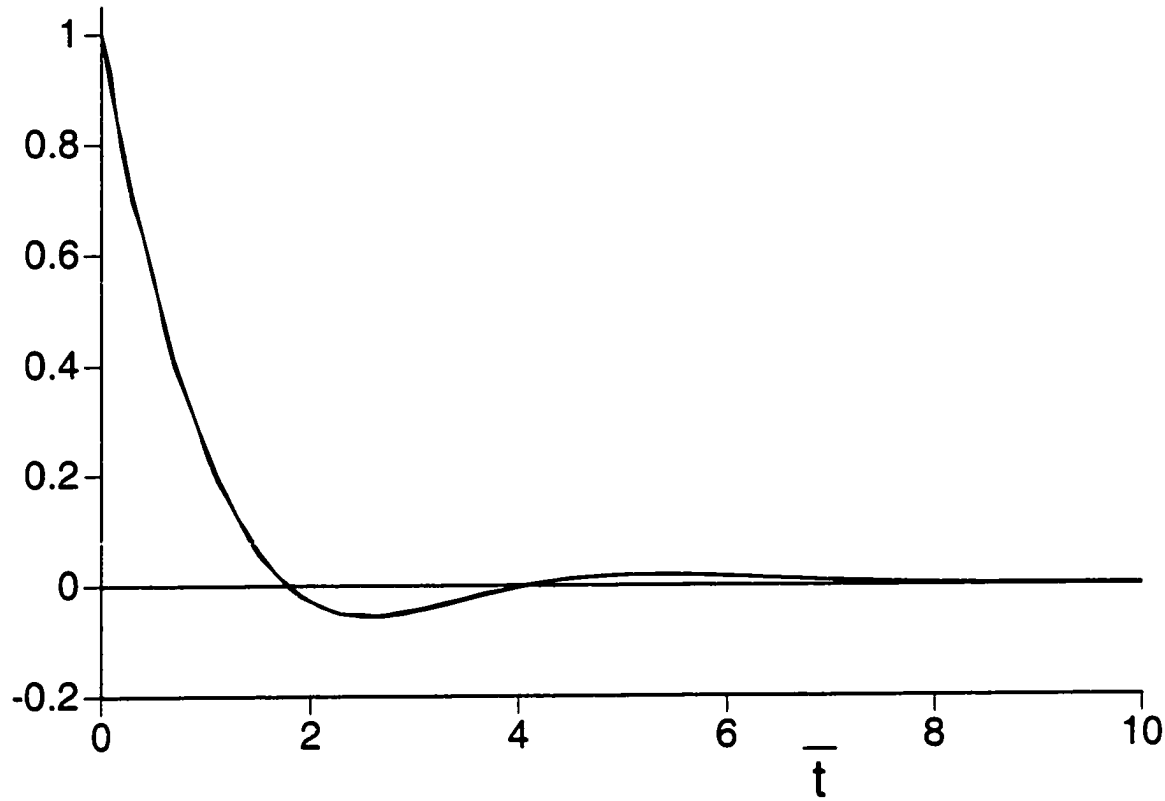

Figure 2.4: The correlator $\langle \boldsymbol{n}(0,\bar{t}) \cdot \boldsymbol{n}(0,0) \rangle_C$ as a function of $\bar{t}$. Results for lattice spacings $\xi/16$ and $\xi/8$ are shown together and the perfect overlap of the two data sets show that we are effectively in the continuum limit.

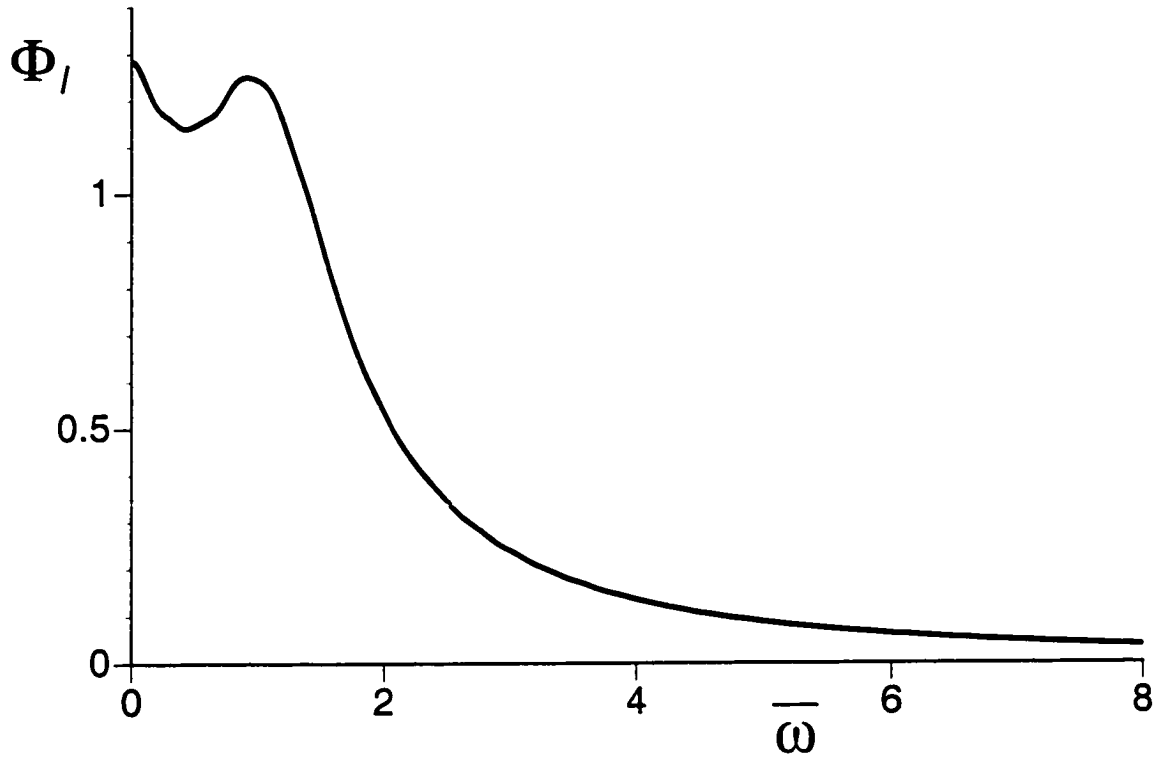

Figure 2.5: The Fourier transform of the autocorrelation function shown in Fig.2.4 normalized to unity. This is the universal scaling function $\Phi_l\bar{\omega}$.

Next we compute the zero momentum correlation function $\int d\bar{x}\langle \boldsymbol{n}(\bar{x},\bar{t}) \cdot \boldsymbol{n}(0,0)\rangle$. The Fourier transform into the frequency domain gives us the universal scaling function $\Phi_S(0,\bar{\omega})$ defined in equation 2.39. Since we are not in the limit $\bar{k},\bar{\omega} \gg 1$, the ansatz 2.43 is no longer correct. We show the correlation function in real time and in frequency space in Figs. 2.6 and 2.7 respectively.

We note that both the autocorrelation function ($x = 0$), as well as the $\bar{k} = 0$ correlation functions show brief oscillations in the time domain and this leads to peaks at finite $\bar{\omega}$ in their respective Fourier transforms $\Phi_l(\bar{\omega})$ and $\Phi_S(0,\bar{\omega})$. In the latter case, the peak is broadened into a sort of broad shoulder. There is a heuristic way to understand these important features in the scaling functions.

The model with an N component field $\boldsymbol{n}$ is exactly soluble in the limit $N \to \infty$ [62], [63]. In this limit $S(0,\omega)$ has a delta function contribution at a frequency

$$\omega \sim \frac{T}{\ln(T/\Lambda_{\overline{MS}})}. \tag{2.59}$$

We can interpret our finite frequency peak as a remnant of this $N = \infty$ delta function at $N = 3$.

A more physical way of thinking about this is as follows. The fundamental degrees of freedom in our model are the $\boldsymbol{n}$ vectors with a fixed norm $|\boldsymbol{n}| = 1$. But the correlation functions for these modes decay exponentially over a length scale of $\xi(T)$. So if we coarse grain to a scale of $\xi(T)$ and call this coarse grained field ϕ_α, we expect that the coarse grained field will show large amplitude fluctuations. In that sense the theory of the ϕ_α field will look like perhaps the ordinary ϕ^4 theory. Most importantly there will be harmonic oscillation of this field about its effective potential. These harmonic oscillations correspond to the amplitude fluctuations about a nonzero value of $|\phi_\alpha|$, and give rise to the finite frequency peak. Also there will be angular fluctuations of the field which are responsible for the zero frequency peak seen in $S(0,\omega)$.

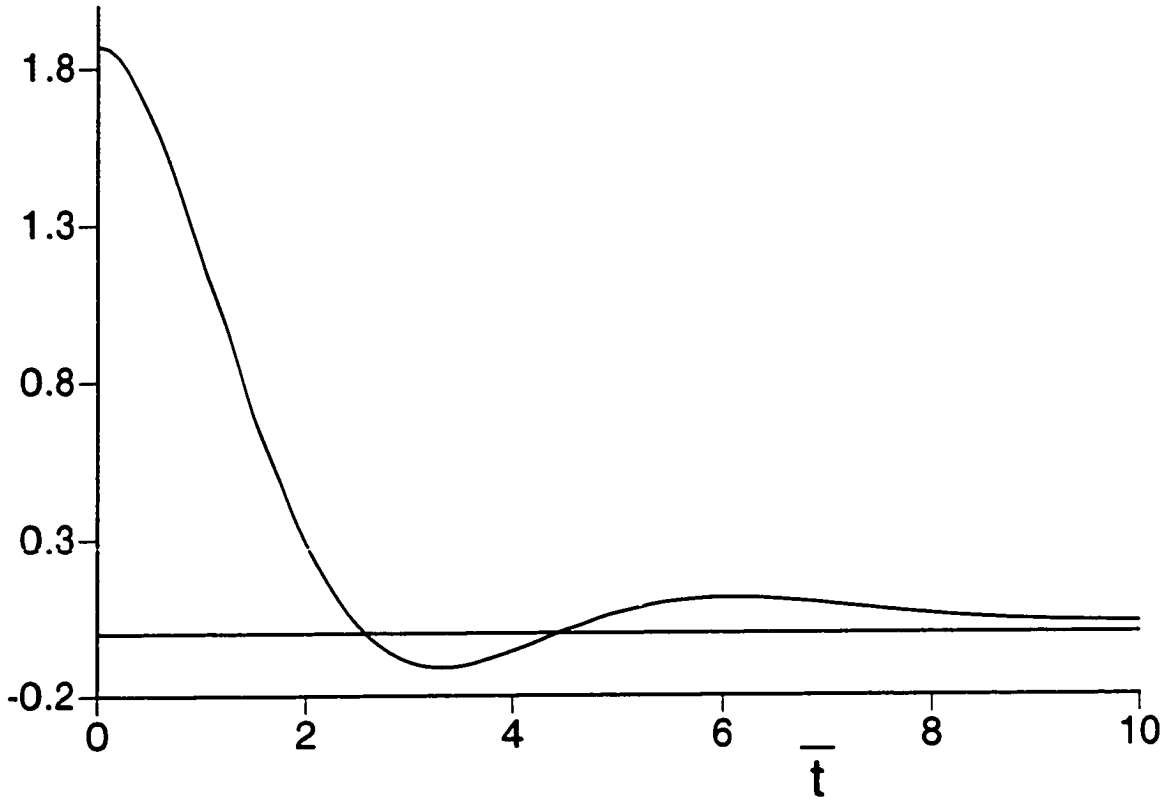

Figure 2.6: The correlation function $\int d\bar{x}\langle \boldsymbol{n}(0,\bar{t}) \cdot \boldsymbol{n}(0,0)\rangle_C$ as a function of $\bar{t}$. Results for lattice spacings $\xi/8$ are shown. By equation 2.41, at $\bar{t} = 0$, the function should have a value of 2. The discrepancy is an artifact of finite lattice spacing.

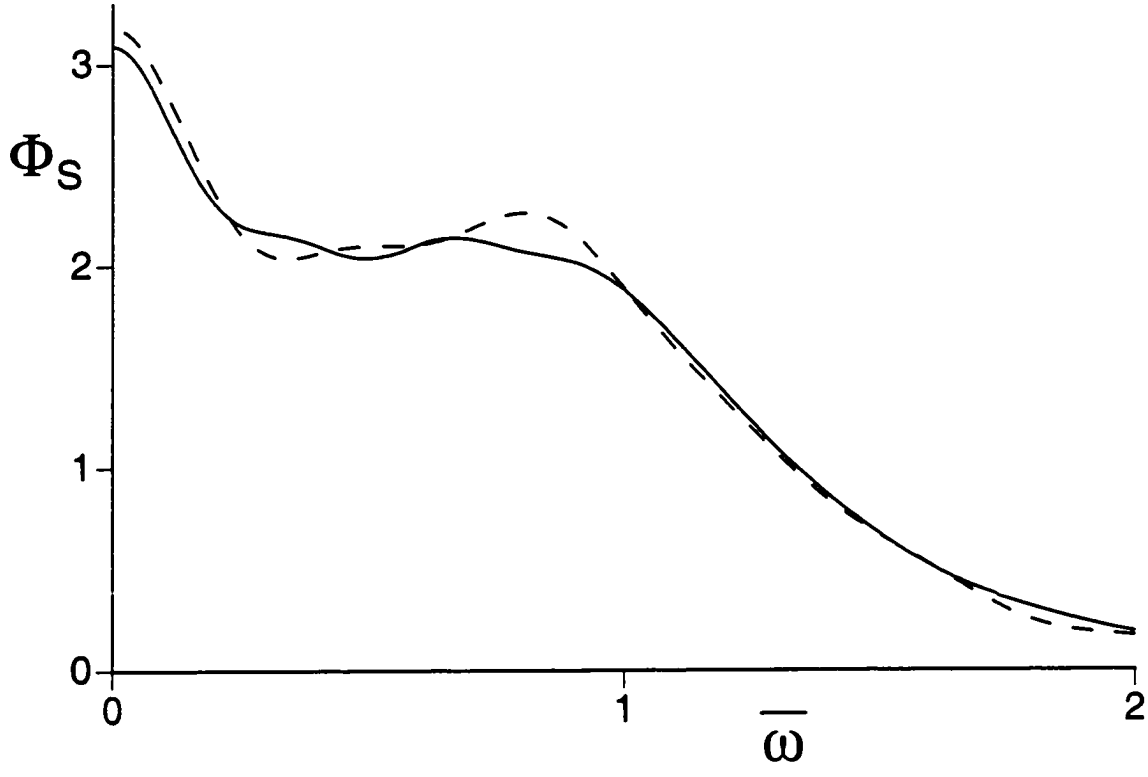

Figure 2.7: The Fourier transform of the data in Fig. 2.6, which leads to the scaling function $\Phi_S(0,\omega)$. Results for lattice spacings $\xi/16$ (dashed line) and $\xi/8$ (solid line) are shown together. The data for lattice spacing $\xi/16$ is noisier because of insufficient averaging. The overlap between the two sets of data are quite satisfactory within the limits of the noise.

2.7.3 Dynamics of L Field and Evidence for Spin Diffusion

Our numerical results for the L field is confined to the autocorrelation function of L which is the most interesting quantity in determining the presence of spin diffusion. L is a conserved quantity and hence the conservation law should be crucial in determining how the autocorrelation of L decays. A natural assumption is that at long times the autocorrelation exhibits a diffusive form:

$$\langle \boldsymbol{L}(0,t) \cdot \boldsymbol{L}(0,0) \rangle = \frac{3T\chi_u}{(4\pi Dt)^{1/2}}, \tag{2.60}$$

where D is the diffusion constant. Consistency with the scaling form 2.28 implies that the diffusion constant obeys

$$D = \mathscr{B}\left[\frac{T\xi^3(T)}{\chi_{u\perp}(T)}\right]^{1/2}, \tag{2.61}$$

where $\mathscr{B}$ is a universal dimensionless number.

As a check on our numerical calculations, we tested our results against the short time expansion as exhibited in Fig 2.8. First we carried out a short time expansion (an analogue of the results shown in equation 2.36) for the lattice model in equation 2.56 with a lattice spacing of $a\xi$. The result is

$$\begin{aligned}\langle \boldsymbol{L}(\bar{x},\bar{t}) \cdot \boldsymbol{L}(0,0) \rangle &= 2\int_{-\pi/a}^{\pi/a} \frac{dk}{2\pi} e^{ik\bar{x}} \cos(\omega_k \bar{t}) \left[1 + \int_{-\pi/a}^{\pi/a} \frac{dp}{2\pi} \frac{\cos(\omega_p t) e^{ip\bar{x}} - 1}{\omega_p^2}\right] \\ &+ 2\left[\int_{-\pi/a}^{\pi/a} \frac{dk}{2\pi} e^{ik\bar{x}} \sin(\omega_k \bar{t})\right]^2, \end{aligned} \tag{2.62}$$

where $\omega_k = [2(1-\cos(ka))/a^2]^{1/2}$. It can be verified that in the limit $a \to 0$, equation 2.62 reduces to the equation 2.36. As we see from Fig. 2.8, the agreement between numerical and analytical computation is very satisfactory.

The results for large $\bar{t}$ are shown in Fig. 2.9. Fitting a power law decay $\bar{t}^{-\alpha}$ gave a value of $\alpha = 0.61$. An equally good fit can be obtained by fitting the form $a_1 \frac{1}{\sqrt{\bar{t}}} + a_2 \frac{1}{\bar{t}}$ which is consistent with diffusion. With this fit we find that $a_2/a_1 = 0.65$ and the second term contributes only about a 10% correction to the first term for the largest values of $\bar{t}$.

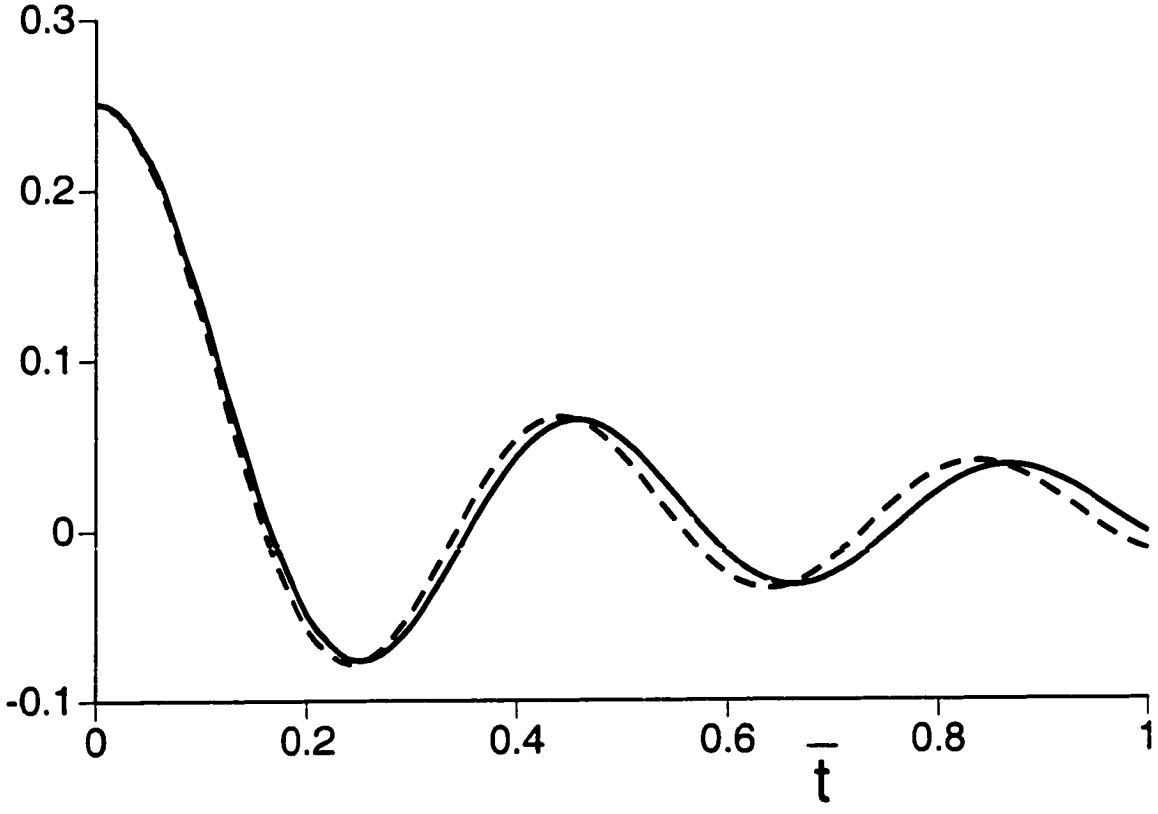

Figure 2.8: The analytical results for the correlation function $\langle \boldsymbol{L}(0,\bar{t}) \cdot \boldsymbol{L}(0,0) \rangle$ (dashed line) compared with the numerical results (solid line) for $\bar{t} < 1$. Results are for a lattice spacing of $\xi/8$. The analytical results are valid for $\bar{t} \ll 1$.

With this form of fit, we obtain an estimate for $\mathscr{B}$ to be

$$\mathscr{B} \approx 3.32. \tag{2.63}$$

2.8 Experimental Consequences

We have already seen from the Monte Carlo results [59, 3] that the temperature range over which our results hold should exist for $S \geq 2$. There has been studies on the classical properties of such magnetic materials. For example $(CD_3)_4NMnCl_3$ (TMMC) has $S = 5/2$ and $(C_{10}H_8N_2)MnCl_3$ has $S = 2$. We believe that careful experiments on these compounds from the perspective of this report should prove fruitful.

The static properties such as the behaviour of $\xi(T)$ at intermediate temperatures where it shows logarithmic temperature dependence as in equations 2.17 should be also accessible by neutron scattering experiments. Amongst the dynamic properties, the qualitative features of the line shapes that we have shown in Figs 2.5 and 2.7 should be verifiable directly by neutron scattering.

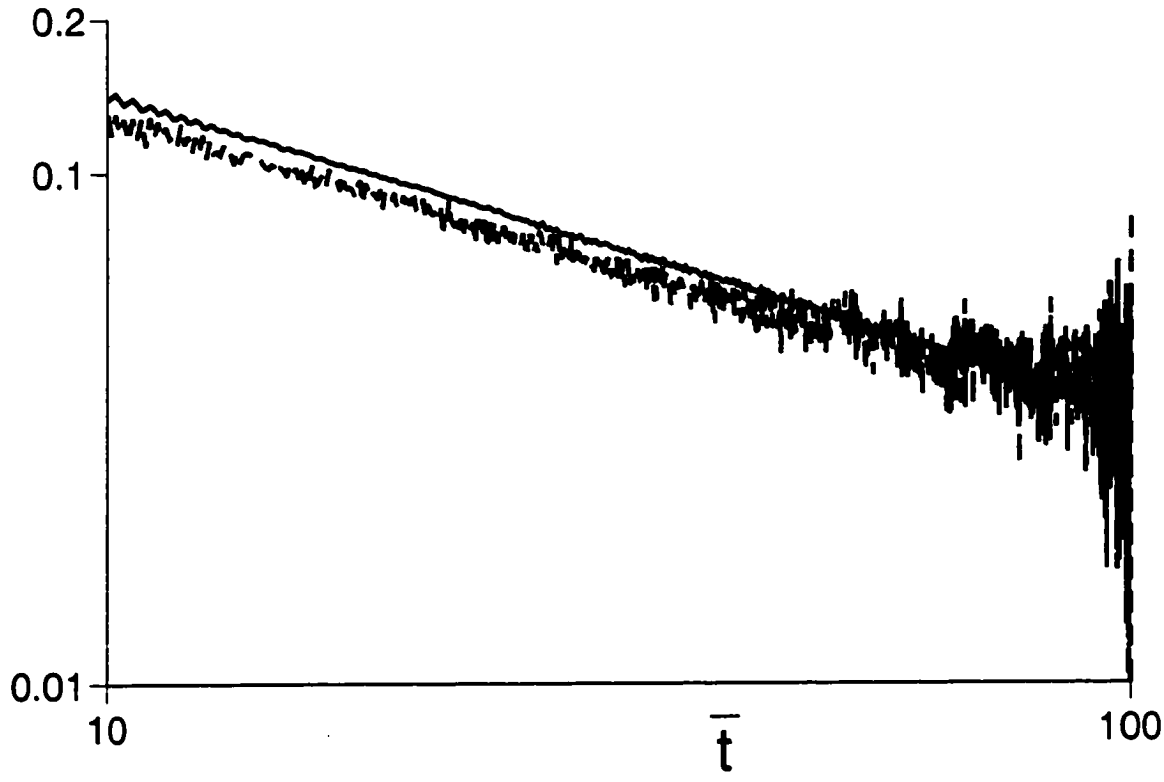

Figure 2.9: Numerical results for $(\xi(T)/T\chi_{u\perp}(T))\langle \mathbf{L}(0,t)\cdot\mathbf{L}(0,0)\rangle$ as a function of $\bar{t}$ in a log-log plot. The smoother line is for lattice spacing $\xi/8$, while the noisier line is for lattice spacing $\xi/16$. The agreement of the two results is evidence that this decay is a property of the continuum limit. A straight line fit (not shown) to the $\xi/8$ data is almost perfect, and its slope indicates that the correlator decays as $\bar{t}^{-0.61}$. An equally good fit to the data was obtained by the function $a_1/\sqrt{\bar{t}} + a_2/\bar{t}$, with the second sub-leading term contributing only about a 10% correction at the largest $\bar{t}$.

Chapter 3

Spin Diffusion in a Toy Model

In this chapter we shall investigate a toy model of spin transport which is exactly solvable. There have been conjectures [33] that integrable models of spin transport do not exhibit diffusion and we believe that this model is a clear counter example to that. The properties of interest of this model are as follows:

1. The spin correlation function can be evaluated in closed form, and in the long time limit it reduces to the diffusive form.

2. The short time behaviour of the spin correlation function in the toy model is very similar to the classical model of intermediate temperature spin dynamics that we studied in the last chapter.

3. It is possible to study the toy model in a finite system of size L, and hence investigate spin transport in two different limits. We show that the behaviour of spin correlations while letting $t \to \infty$ and then taking the thermodynamic limit $L \to \infty$ is very different from taking the limits in the opposite order. The diffusive form of the correlation function is recovered only when the thermodynamic limit is taken *before* letting $t \to \infty$. In the opposite order of limits, a great deal of interesting dynamics including recurrence is seen.

3.1 The Toy Model

The toy model consists of a set of N hard core particles of equal mass moving in a one dimensional line of length L with periodic boundary conditions. We label the particles by the index i, $i = 0, 1, \ldots, N-1$. The initial positions of the particle at time $t = 0$ are given by x_i where the x_i are chosen from a uniform random distribution lying between 0 and L. Each particle has the initial velocity v_i, chosen randomly from a prespecified velocity distribution $g(v)$. Each particle also carries a 'spin' m_i again chosen from a distribution $h(m)$. As the system evolves, each particle moves in a straight line until it hits its neighbour and bounces off. Since we have chosen the particles to be hard core, so each particle simply exchanges velocity with its neighbour as shown in the Fig. 3.1. The spin remains unaltered. Note that the hard core condition implies that the ith particle is always to be found between $i-1$ and the $i+1$th particle. We could have chosen the particles to be non-hardcore with a non-zero probability of both transmission and reflection. In that case the exact solution is not known to us.

Our interest here is the correlation of the spin density function $L(x,t)$ defined by

$$L(x,t) = \sum_{i=0}^{N-1} m_i \delta(x - x_i(t)), \tag{3.1}$$

where $x_i(t)$ is the position of the ith particle at time t. Our spin correlator will be the two point correlator of $L(x,t)$ averaged over all initial conditions given by x_i, $g(v)$ and $h(m)$. To ensure that the average spin and average velocity is zero, we shall choose $h(m)$ and $g(v)$ to be even functions of their arguments. Then the correlation function takes the form

$$\begin{aligned} \langle L(x,t)L(0,0)\rangle &= \sum_{i,i'} \langle m_i m_{i'}\rangle \langle \delta(x - x_i(t))\delta(x_{i'}(0))\rangle \\ &= \langle m^2\rangle \sum_{i} \langle \delta(x - x_i(t))\delta(x_i(0))\rangle \\ &= \langle m^2\rangle \rho P(x,t). \end{aligned} \tag{3.2}$$

The second line above follows because the values of m_i and $m_{i'}$ are entirely uncorrelated. In the last line $\rho \equiv N/L$ is the density of particles and $P(x,t)$ is the probability

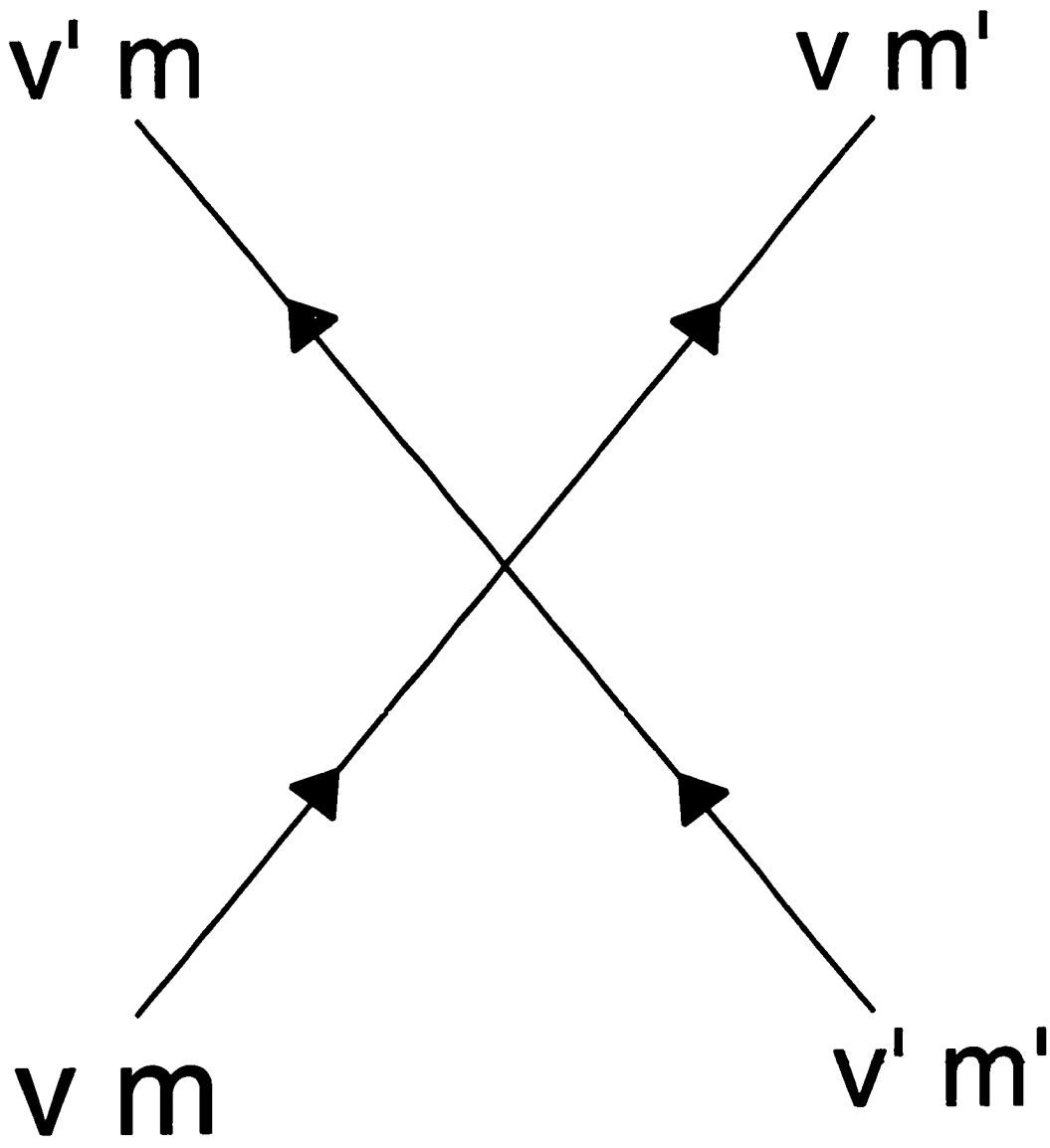

Figure 3.1: A two particle collision. The particles come in with velocity and spin (v, m) and (v', m') respectively and they exchange velocities, but the spin remains with them.

that a particle at $x = 0$ at time $t = 0$ will be found at time t at the point x. Also

$$\langle m^2 \rangle = \sum_m m^2 h(m). \tag{3.3}$$

Most of our results will be on a particular, simple, velocity distribution, which is designed to mimic the properties of the continuum model defined by equations 2.20,2.25:

$$g(v) = \frac{1}{2}\left[\delta(v - c) + \delta(v + c)\right]. \tag{3.4}$$

So each particle is allowed to have only one of two velocities, $\pm c$. This is similar to the fact that linear spin-waves in the continuum model also have velocities $\pm c$.

The remainder of this section will describe the computation of the function $P(x, t)$ using the method of Jepsen [64]. Although later more elegant solutions were put forward by Lebowitz and Percus [65] for solving the model in the thermodynamic limit, we shall use the relatively cumbersome machinery of Jepsen because it allows us to consider finite systems.

At time $t = 0$ the N particles are at random positions on the ring. We shall put the origin of the coordinate system at the location of particle 0. The rest of the particles from $0, 1, 2, \cdots N - 1$ are numbered such that the $(i+1)$-th particle is immediately to the right of the i-th one. As a particle moves with uniform velocity, in a "space-time" diagram we can represent its motion as a straight line which we'll call a trajectory. When two trajectories cross, there is a collision. The particles bounce off each other, and in effect the particles exchange trajectories. So at the beginning the zeroth particle starts on the zeroth trajectory and as this trajectory crosses others, the zeroth particle moves onto a different trajectory.

Now define $A_{jk}(t)$ to be one if the particle j is on the trajectory k at time t and zero otherwise. If we form an ensemble of systems, the the average $\langle A_{jk}(t) \rangle$ is the probability that the particle j is on the trajectory k at time t. A knowledge of $A_{jk}(t)$ for all values of j, k, t constitute a full solution to the dynamics of the system. These points are discussed

in more detail in appendix E. The solution is given by [64]

$$\begin{aligned} A_{jk}(t) &= \frac{1}{N}\sum_u e^{-iju}\prod_{h=0}^{N-1} S[u, w_{kh}] \\ u &= \frac{2\pi l}{N},\ \ l = 0, 1, 2, \ldots, N-1;\ \ \sum_u \equiv \sum_{l=0}^{N-1} \\ S[u, w] &= e^{inu} \text{ when } (n-1)L < w \leq nL \text{ for each } n \\ w_{kh} &= x_k - x_h + (v_k - v_h)t. \end{aligned} \tag{3.5}$$

We shall note some periodicity properties of $S[u, w]$ and $A_{jk}(t)$ here. By the above definition

$$S[u, w + L] = e^{iu}S[u, w], \text{ hence } S[u, w + NL] = S[u, w]. \tag{3.6}$$

Also, for the distribution (3.4), noting the fact that $|v_k - v_h| = 0, 2c$, we arrive at

$$A_{jk}\left(t + \frac{NL}{2c}\right) = \frac{1}{N}\sum_u e^{-iju}\prod_{h=0}^{N-1} S\left[u, w_{kh} + NL\frac{v_k - v_h}{2c}\right] = A_{jk}(t). \tag{3.7}$$

Let us define a time $\mathscr{T} \equiv L/c$ which is the time required by a free particle to go once around the system. Every trajectory returns exactly to its starting point after this interval of time. It is now obvious that in a period of time $NL/c = N\mathscr{T}$, each particle will return to its initial positions and velocities. Thus the Poincare recurrence time of the system, with the velocities chosen under (3.4), is of order N, rather than being of the order of e^N or larger.

3.2 Diffusion in the Thermodynamic Limit

Now we go to the thermodynamic limit and address the question of diffusion. The limit is defined such that N and L approach infinity while the density $N/L = \rho$ being held finite. The zeroth particle starts out at the origin and we ask what is the probability, $P(y, t)$, that it is at position y at time t (both y and t are held finite as the limit $L \to \infty$ is taken). This can be written as

$$P(y, t) = \langle\delta(y - x_0(t))\rangle = \sum_k \langle\delta(y - x_k - v_k t)A_{0k}(t)\rangle, \tag{3.8}$$

where the angular brackets an average over all possible initial ensembles of velocity and positions of particles, while keeping the zeroth particle at the origin. The average can be evaluated exactly (see appendix E), and there is a simple, closed form result:

$$\begin{aligned} P(y,t) &= \frac{1}{2}\left[\delta(y+ct)+\delta(y-ct)\right]e^{-\rho c|t|}+\frac{\rho}{2}\left[\theta(y+ct)-\theta(y-ct)\right] \\ &\times\ e^{-\rho c|t|}\left[\frac{c|t|}{\sqrt{c^2t^2-y^2}}I_1(\rho\sqrt{c^2t^2-y^2})+I_0(\rho\sqrt{c^2t^2-y^2})\right]. \end{aligned} \tag{3.9}$$

I_0 and I_1 are the modified Bessel functions of order zero and one respectively. The resemblance to the correlation function of the non-linear wave model given in (2.36) is clear. The first term in (3.9) is a delta function along the light cone, but its contribution decreases exponentially with time. The second term lies within the light cone, and becomes increasingly important for large time. Also, if we take the short time limit of (3.9), we get

$$P(y,t)=\frac{1}{2}\left[\delta(y+ct)+\delta(y-ct)\right](1-\rho c|t|+\dots)+\frac{\rho}{2}\left[\theta(y+ct)-\theta(y-ct)\right], \tag{3.10}$$

which is precisely of the form (2.36). However, unlike (2.36), we can now also study the long time limit analytically. We take this limit within the light cone with $y \sim \sqrt{t}$, and then the asymptotic expansions of the modified Bessel functions yields

$$P(y) \approx \frac{1}{(4\pi Dt)^{1/2}}\exp\left(-\frac{y^2}{4Dt}\right) \tag{3.11}$$

$$D = \frac{c}{2\rho}, \tag{3.12}$$

which is the diffusive form assumed for the classical wave model in (2.60). As shown by Jepsen, this calculation can also be done for a general velocity distribution $g(v)$, and provided the distribution is symmetric in v, we obtain (3.12) but with

$$D=\frac{1}{\rho}\int_0^\infty vg(v)dv. \tag{3.13}$$

3.3 Effect of Periodic Boundary Conditions in a Finite Geometry

Here we go back to the finite system and think more about it. The Poincare recurrence time is only linear in N, is because the phase space available to the system becomes very restricted once we allow only two possible velocities. An interesting effect is that the recurrence time can be very different depending upon whether there are even or odd number of particles in the system. The recurrence time is the lowest common multiple of $\mathscr{T}$ (the time required for trajectories to return to their initial position) and $NL/2c = N\mathscr{T}/2$ (the time required for particles to come back to their initial trajectory). With an odd number of particles, $N = 2p - 1$, the recurrence time is $N\mathscr{T} = (2p-1)\mathscr{T}$ as mentioned above. But if we add one single extra particle to the system, the recurrence time almost becomes half because $NL/2c = N\mathscr{T}/2 = p\mathscr{T}$ is an exact multiple of $\mathscr{T}$.

In fact, the recurrence time could be even smaller. If we take an even number N of particles and choose their velocities as $\pm c$ randomly, the most likely scenario is one where half of them have velocity $+c$, and the rest have velocities $-c$. In that case

$$A_{jk}(t+\mathscr{T}) = \frac{1}{N}\sum_{u} e^{-iju} \prod_{h=0}^{N-1} S\left[u, w_{kh} + \mathscr{T}(v_k - v_h)\right] \tag{3.14}$$

Amongst all the factors that we have in the product on RHS, half of them will not contribute any phase to the product because for them $v_k - v_h = 0$. The other half will contribute a phase of exactly $\exp(\pm 2iu)$ each by equation 3.6. So the total phase contribution will be $\exp(\pm 2iuN/2) \equiv 1$! Hence the most probable recurrence time for a random ensemble of even number of particles is $\mathscr{T}$. It turns out that with reflecting hard wall boundary conditions, the recurrence time is $2\mathscr{T}$ regardless of the initial conditions.

Now let us see how the effect of the recurrence time might show up in the probability distribution of a diffusing particle. We shall essentially try to find the autocorrelation function for a single specific particle moving around in a ring for all times $t < \mathscr{T} = L/c$ and $t > \mathscr{T} = L/c$. We shall again choose this particle to be the zeroth particle and at time $t = 0$, its position and velocity are $x_0 \equiv 0$, v_0 respectively. The probability

distribution is defined as before in (3.8). Since $A_{jk}(t)$ is periodic with a period of $N\mathscr{T}/2$, all distribution functions will also be periodic with the same period. Moreover

$$\begin{aligned} A_{jk}(N\mathscr{T}/2-t) &= \frac{1}{N}\sum_u e^{-iju}\prod_{h=0}^{N-1} S\left[u, w_{kh}+(v_k-v_h)(N\mathscr{T}/2-t)\right] \\ &= \frac{1}{N}\sum_u e^{-iju}\prod_{h=0}^{N-1} S\left[u, w_{kh}-(v_k-v_h)t\right]. \end{aligned} \tag{3.15}$$

When we carry out the average over the initial conditions, the particles k and h will have the velocities $+v_k, +v_h$ and $-v_k, -v_h$ with equal probability. So the probability distribution function will satisfy

$$P(y, N\mathscr{T}/2-t) = P(y,t). \tag{3.16}$$

Thus we need to evaluate this function only for $0 \le t \le N\mathscr{T}/4$.

The details of the evaluation of $P(y,t)$ are again relegated to the appendix E. Let us represent the distribution function as

$$P(y,t) = [\delta(y+ct)+\delta(y-ct)]P^{(1)}(t) + [\theta(y+ct)-\theta(y-ct)]P^{(2)}(y,t). \tag{3.17}$$

We write down explicit series solutions for $P^{(1)}(t)$ and $P^{(2)}(0,t)$. These sums could not be evaluated in a closed analytic form. So we carried out the sums numerically for specific values of N and L. $P^{(1)}(t)$ and $P^{(2)}(0,t)$ are plotted in Figs 3.2 and 3.3 respectively.

For times $t \ll \mathscr{T}$ and $N \gg 1$ with N/L fixed, these results reduce to the results (3.9) derived in the thermodynamic limit. For $t > \mathscr{T}$, we see lots of complicated structures. Not all of them are well understood. But some of the prominent ones are easy to understand. For example at times $t = n\mathscr{T}$, $n = 1, 2, 3, \ldots$ we see peaks in $P^{(1)}$, each of whose height turns out to be $1/\sqrt{2\pi N}$. The origin of this is very easy to understand. Out of the whole ensemble of initial conditions, a fraction of them will have exactly half of the particles with velocity $+c$ and the others with velocity $-c$ (with the assumption that N is even). Since these set of initial conditions have a recurrence time of only $\mathscr{T}$, so they come back to the original distribution after a time $\mathscr{T}$ and hence contribute to this peak. Using the binomial distribution, it is easy to prove that the fraction of ensembles which

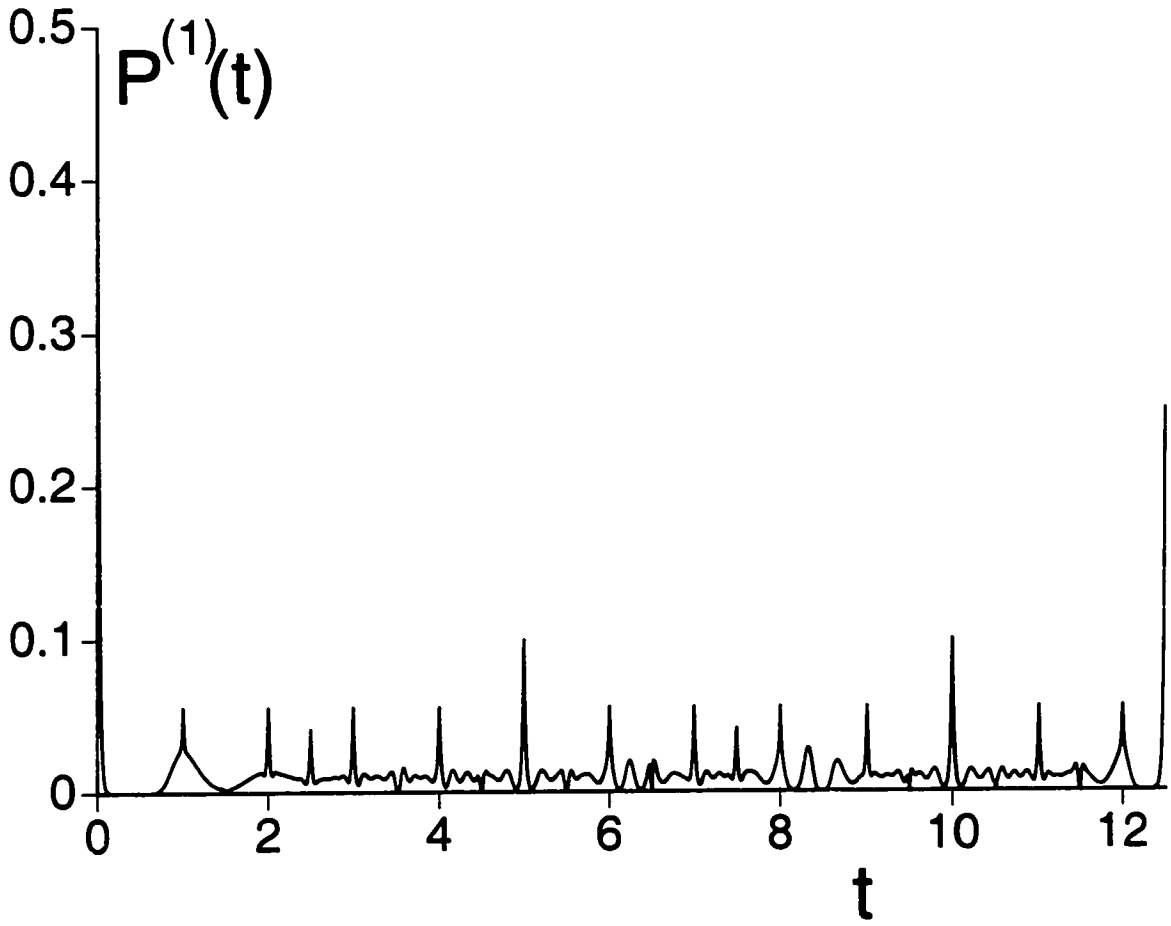

Figure 3.2: The probability distribution function $P^{(1)}(t)$ plotted as a function of time $0 \leq t \leq N\mathscr{T}/4$ for $N = 50$. The unit of time is $\mathscr{T}$. The stronger peaks at multiples of 5 is due to the fact that 5 is a prime factor of N

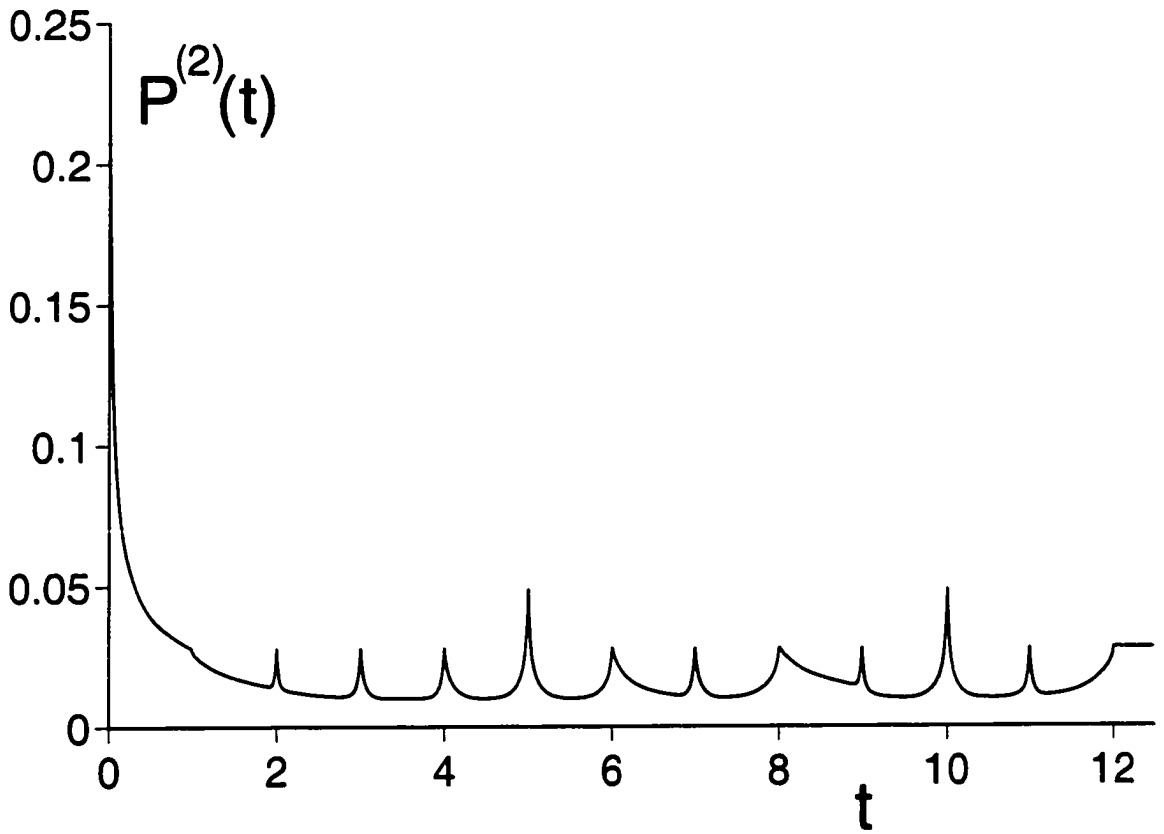

Figure 3.3: The probability distribution function $P^{(2)}(t)$ plotted as a function of time for $N = 50$ for $0 < t < N\mathscr{T}/4$. The unit of time is $\mathscr{T}$.

have exactly half the particles with one velocity and the other half with the opposite velocity is exactly $\sqrt{2/\pi N}$. The extra factor of $1/2$ comes from the fact that we have both left and right going initial conditions for our test particle. If we change the number of particles by one, N becomes odd. So no set of initial conditions will have a recurrence time $\mathscr{T}$, and these peaks will disappear as shown in Fig 3.4.

3.4 Conclusion

We have seen that this toy model exhibits diffusion provided we take the thermodynamic limit $L \to \infty$ before we take the $t \to \infty$ limit. This has important bearings on the question of existence of diffusion in spin chains. There have been several studies [33] where the authors compute a frequency dependent conductivity in a *finite* system and then evaluate the conductivity in the zero frequency limit. Such studies have shown spin transport in Heisenberg chains to be ballistic. In our opinion such studies might not be conclusive precisely because taking $\omega \to 0$ limit in a finite system corresponds to taking the $t \to \infty$ limit before the thermodynamic limit.

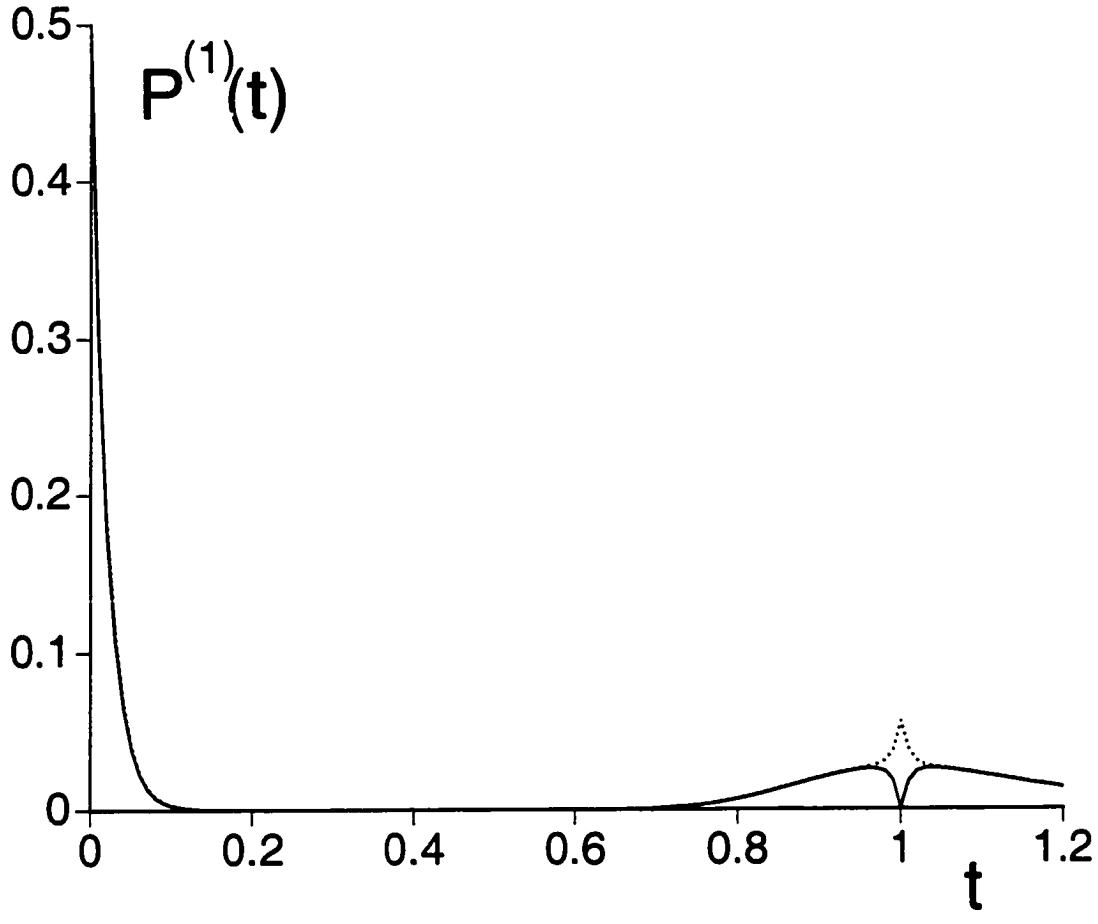

Figure 3.4: The probability distribution function $P^{(1)}(t)$ plotted as a function of time for $N = 50$ (dashed line) and $N = 51$ (full line). The unit of time is $\mathscr{T}$. Notice the disappearance of the peak at $t = 1$ for $N = 51$.

Chapter 4

Impurity in Two Dimensional Critical Antiferromagnet

4.1 Introduction

As we discussed in the introduction, we shall be considering a two dimensional antiferromagnet near its transition from the Néel phase to the paramagnetic phase. In the Néel phase, we have a non-zero expectation value of the antiferromagnetic order parameter and gap-less Goldstone modes above the ground state. In the paramagnetic spin gap regime, we have no Néel order and the excitations above the ground state are triplet in nature. We can think of this triplet excitation as a broken singlet which creates a spin 1 excitation. To describe this transition the action for the antiferromagnetic order parameter that we shall be considering is [19]

$$\mathcal{S}_{bg} = \int d^d x d\tau \left[\frac{1}{2} \left[(\nabla \phi_\alpha)^2 + c^2 (\partial_\tau \phi_\alpha)^2 + m^2 \phi_\alpha^2 \right] + \frac{g_0}{4!} (\phi_\alpha^2)^2 \right] \tag{4.1}$$

$\phi_\alpha(x_i, y_j) \sim (-1)^{i+j} \langle S_\alpha(x_i, y_j) \rangle$ is the three component ($\alpha = 1, 2, 3$) Néel order parameter. As we tune m^2 from positive to negative values through zero, we pass through the quantum phase transition at $m^2 = 0$. For $m^2 < 0$, the ϕ_α field acquires a non-zero expectation value and we have two massless Goldstone modes above the ground state. For $m^2 > 0$, the ground state is rotation invariant and we have a finite gap $\Delta \equiv m$ to all

excitations.

Now we couple a single impurity spin S situated at the origin to the antiferromagnetic order parameter. Using the coherent state path integral for spins [17, 19], we can write the partition function as an integral over the unit vector field $n_\alpha(\tau)$ which represents the instantaneous orientation of this spin.

$$\begin{aligned} \mathscr{Z} &= \int \mathscr{D}\phi_\alpha \mathscr{D}n_\alpha \delta(n_\alpha^2 - 1) \exp(-\mathscr{S}_{\rm bg} + \mathscr{S}_{\rm imp}) \\ \mathscr{S}_{\rm imp} &= \int d\tau \left[iSA_\alpha(\boldsymbol{n}) \frac{dn_\alpha}{d\tau} - \gamma_0 S n_\alpha(\tau) \phi_\alpha(x=0,\tau) \right]. \end{aligned} \tag{4.2}$$

Here $A_\alpha(\boldsymbol{n})$ is the vector potential due to a Dirac monopole and it appears as a part of the Berry phase for the spin $\boldsymbol{S}$. $A_\alpha(\boldsymbol{n})$ satisfies

$$\epsilon_{\alpha\beta\gamma} \frac{\partial A_\beta(\boldsymbol{n})}{\partial n_\gamma} = n_\alpha. \tag{4.3}$$

4.2 One Loop Renormalization Group Analysis

At first we carry out a simple power counting analysis of the action in 4.2. Demanding that the time derivative part of the action remain invariant under a scale transformation, we immediately find that

$$\dim[\phi_\alpha] = \frac{d-1}{2}, \quad \dim[n_\alpha] = 0. \tag{4.4}$$

Hence the dimension of the coupling constant γ_0 is

$$\dim[\gamma_0] = \frac{3-d}{2}, \quad \dim[g_0] = 3 - d. \tag{4.5}$$

Since we are interested in two dimensional antiferromagnets, γ_0 is a relevant perturbation. Our strategy will be to work in $d = 3 - \epsilon$ dimensions and determine a fixed point value of γ_0 within this epsilon expansion.

There are other possible couplings such as

$$\lambda_1 \int d\tau \phi_\alpha(x=0,\tau)^2.$$

By dimensional analysis we see that this coupling is irrelevant for small ϵ because

$$\dim[\lambda_1] = 2 - d. \tag{4.6}$$

Similarly we could have the spin couple to the angular momentum of the background field.

$$\lambda_2 \int d\tau L_\alpha(x = 0, \tau) S n_\alpha(\tau).$$

where

$$L_\alpha = i\epsilon_{\alpha\beta\gamma}\phi_\beta \partial_\tau \phi_\gamma. \tag{4.7}$$

Again by dimensional analysis

$$\dim[\lambda_2] = 1 - d, \tag{4.8}$$

which is strongly irrelevant.

Now we turn to an actual momentum shell RG calculation. The action in its present form is not convenient for such a calculation. So we write our partition function as follows:

$$\mathcal{Z} = \int \mathcal{D}\phi \langle 0 | T_\tau \exp\left(-\mathcal{S}_{\rm bg} - \gamma_0 \int d\tau S_\alpha(\tau)\phi_\alpha(0,\tau)\right)|0\rangle, \tag{4.9}$$

$S_\alpha(\tau)$ is the quantum mechanical spin operator obeying the usual commutation rules:

$$[S_\alpha, S_\beta] = i\epsilon_{\alpha\beta\gamma} S_\gamma. \tag{4.10}$$

The label τ in $S_\alpha(\tau)$ is purely for time ordering purposes. The state $|0\rangle$ is the spin ground state and the T_τ is the time ordering symbol of the $S_\alpha(\tau)$ operators. For example

$$T_\tau\left[S_\alpha(\tau_1) S_\beta(\tau_2)\right] = \theta(\tau_1 - \tau_2) S_\alpha S_\beta + \theta(\tau_2 - \tau_1) S_\beta S_\alpha. \tag{4.11}$$

To carry out the momentum shell RG analysis, we shall impose an arbitrary high frequency cutoff Ω on our frequency integrals. We define

$$\phi_\alpha(\omega) = \int \frac{d^d k}{(2\pi)^d} \phi_\alpha(k, \omega), \tag{4.12}$$

and write $\phi(\omega) = \phi_<(\omega) + \phi_>(\omega)$. Here $\phi_<$ has support only in frequencies between 0 and Ωe^{-l} and $\phi_>$ has support in the shell $\Omega e^{-l} < |\omega| < \Omega$. l is an infinitesimal parameter.

It will turn out that to one loop order in the epsilon expansion, we can treat the field $\phi_\alpha(x,t)$ as a free field and forget about the quartic coupling g_0. So we can rewrite our whole partition function in terms of only the local field field $\phi_\alpha(t) \equiv \phi_\alpha(x=0,t)$ as

$$\mathcal{Z} = \int \mathcal{D}\phi(t) \langle 0|T_\tau \exp\Bigg(- \int d\tau_1 d\tau_2 \phi_\alpha(\tau_1) D_0^{-1}(\tau_1 - \tau_2)\phi_\alpha(\tau_2) - \gamma_0 \int d\tau S_\alpha(\tau)\phi_\alpha(\tau)\Bigg)|0\rangle, \tag{4.13}$$

where the propagator $D_0(\tau)$ is defined by

$$D_0(\tau) \equiv \int \frac{d^dk}{(2\pi)^d}\frac{d\omega}{2\pi}\frac{e^{-i\omega\tau}}{k^2+\omega^2} = \frac{\tilde{S}_{d+1}}{\tau^{d-1}}. \tag{4.14}$$

$\tilde{S}_d$ is a phase space factor defined by

$$\tilde{S}_d = \frac{\Gamma(d/2-1)}{4\pi^{d/2}}. \tag{4.15}$$

Note that we are defining the propagator D_0 at the critical point $m = 0$ of the background field ϕ_α.

As usual with the momentum shell RG formulation, we carry out the integration over the $\phi_>$ modes in the partition function and calculate the correction to γ_0. We find that the interaction term gets a correction as follows:

$$\begin{aligned} \gamma_0 \int d\tau S_\alpha(\tau)\phi_\alpha(\tau) \quad &\rightarrow \\ \gamma_0 \int d\tau S_\alpha(\tau)\phi_\alpha(\tau) \quad &- \frac{\gamma_0^3}{2}\int d\tau_1 d\tau_2 d\tau_3 \phi_\alpha(\tau_1)\delta_{\beta\gamma} D_{0>}(\tau_2-\tau_3) \\ &\times \; T_\tau\left[S_\alpha(\tau_1)S_\beta(\tau_2)S_\gamma(\tau_3)\right]. \end{aligned} \tag{4.16}$$

Here the notation $D_{0>}$ means that the propagator has support for only high frequency modes. The time ordered product can be easily evaluated as

$$\begin{aligned} \delta_{\beta\gamma} T_\tau\left[S_\alpha(\tau_1)S_\beta(\tau_2)S_\gamma(\tau_3)\right] &= S(S+1)S_\alpha \\ &- S_\alpha[\theta(\tau_2-\tau_1)\theta(\tau_1-\tau_3) + \theta(\tau_3-\tau_1)\theta(\tau_1-\tau_2)]. \end{aligned} \tag{4.17}$$

Now we can write the second term of the RHS in equation 4.16 as

$$\frac{\gamma_0^3}{2}\int d\tau_1 d\tau_2 d\tau_3 \phi_\alpha(\tau_1) D_{0>}(\tau_2-\tau_3) S_\alpha[\theta(\tau_2-\tau_1)\theta(\tau_1-\tau_3)+\theta(\tau_3-\tau_1)\theta(\tau_1-\tau_2)] \quad (4.18)$$

The contribution from the term proportional to $S(S+1)$ vanishes because the propagator has support only for high frequency modes. The integral shall be evaluated in Fourier space using the following representations for the relevant quantities:

$$\theta(\tau) = \int \frac{d\omega}{2\pi i}\frac{e^{i\omega\tau}}{\omega - 0^+} \quad (4.19)$$

$$D_0(\omega) \equiv \int \frac{d^dk}{(2\pi)^d}\frac{1}{k^2+\omega^2} = \frac{\Gamma(1-d/2)}{(4\pi)^{d/2}}|\omega|^{d-2}. \quad (4.20)$$

With these definitions and some tedious manipulations, we write the correction in equation 4.18 as

$$-\gamma_0^3\int d\tau \phi_\alpha(\tau) S_\alpha \frac{\Gamma(1-d/2)}{(4\pi)^{d/2}}\int_{\Omega>|\omega|>\Omega e^{-l}}\frac{d\omega}{2\pi}\frac{|\omega|^{d-2}}{\omega^2} \quad (4.21)$$

Evaluating all integrals in $d=3$, we find that

$$\gamma_0|_{\Omega e^{-l}} = \gamma_0|_\Omega - \frac{\gamma_0^3}{4\pi^2}l, \quad (4.22)$$

or

$$\Omega\frac{d\gamma_0}{d\Omega} = -\frac{\gamma_0^3}{4\pi^2}. \quad (4.23)$$

At this point we find it convenient to define a rescaled dimensionless coupling γ defined by

$$\gamma_0 = \frac{\mu^{\epsilon/2}}{(\tilde{S}_{d+1})^{1/2}}\gamma. \quad (4.24)$$

The mass scale μ is introduced such that γ is dimensionless in all dimensions $d=3-\epsilon$. With this definition we find that in $d=3-\epsilon$ dimensions we have

$$\Omega\frac{d\gamma}{d\Omega} = \frac{\epsilon\gamma}{2} - \gamma^3. \quad (4.25)$$

The leads to a fixed point for γ at one loop at

$$\gamma^{*2} = \frac{\epsilon}{2}. \quad (4.26)$$

To show that we can reach a true fixed point when both γ_0 and g_0 are non-zero, we need to carry out this analysis to two loops. The present formalism is very cumbersome for such an analysis. It suffices to say that such an analysis has been carried out to two loops using the field theoretic RG formulation [66, 67] and we shall be content to quote the results for the beta functions here. First we need to define renormalizations for various fields and couplings as follows:

$$\begin{aligned}
\phi_\alpha &= Z^{1/2}\phi_{R\alpha}, \\
n_\alpha &= Z'^{1/2} n_{R\alpha}, \\
g_0 &= \frac{\mu^\epsilon Z_4}{Z^2 S_{d+1}} g, \\
\gamma_0 &= \frac{\mu^{\epsilon/2} Z_\gamma}{(ZZ'\tilde{S}_{d+1})^{1/2}} \gamma.
\end{aligned} \tag{4.27}$$

S_d is a phase space factor defined to be

$$S_d = \frac{2}{\Gamma(d/2)(4\pi)^{d/2}} \tag{4.28}$$

We shall not quote the expressions for various values of the renormalization functions here. The renormalizations Z, Z_4 and the beta function for g have been already determined by Brezin *et. al.*[68]. The beta functions are

$$\begin{aligned}
\beta(g) &\equiv \mu\frac{dg}{d\mu} = -\epsilon g + \frac{11g^2}{6} - \frac{23g^3}{12}, \\
\beta(\gamma) &\equiv \mu\frac{d\gamma}{d\mu} = -\frac{\epsilon\gamma}{2} + \gamma^3 - \gamma^5 + \frac{5g^2\gamma}{144} + \frac{g\gamma^3\pi^2}{3}\left[S(S+1) - \frac{1}{3}\right].
\end{aligned} \tag{4.29}$$

We immediately find the infra-red fixed points to be

$$\begin{aligned}
g^* &= \frac{6\epsilon}{11} + \frac{414\epsilon^2}{1331}, \\
\gamma^{*2} &= \frac{\epsilon}{2} + \epsilon^2\left(\frac{29}{121} - \frac{\pi^2}{11}[S(S+1) - 1/3]\right).
\end{aligned} \tag{4.30}$$

For the purposes in this report we shall not need to use these results. They have been quoted here for the sake of completeness.

4.3 Impurity Spin Correlations

4.3.1 Spin Gap Regime

In this regime, there is a finite gap $\Delta = m$ to any spin excitation. So our partition function is still given by equation 4.13, but $D_0(\tau)$ is replaced by $D(\tau)$ where

$$D(\tau) \equiv \int \frac{d^d k}{(2\pi)^d} \frac{d\omega}{2\pi} \frac{e^{-i\omega\tau}}{k^2 + \omega^2 + m^2} = \pi \frac{2^{(3-d)/2} \tilde{S}_{d+1}}{\Gamma((d-1)/2)} K_{(d-1)/2}(m|\tau|) \frac{m^{d-1}}{(m|\tau|)^{d-1}}. \quad (4.31)$$

Here $K_{(d-1)/2}(m|\tau|)$ is a modified Bessel function. The $m \to 0$ limit of this equation gives us equation 4.14. We have as usual, ignored the coupling g_0 to this order. Since our system has a finite gap to any excitation, we expect that our impurity spin will not be able to leak away through excitations in the bulk and hence will be confined. In other words, we expect the autocorrelation of the impurity spin to be non-zero at the limit $\tau \to \infty$. Our calculations below will bear out this expectation.

A one loop calculation (see details in appendix F), leads us to

$$\langle S_\alpha(\tau) S_\alpha(0) \rangle = S(S+1) \left[1 - \gamma_0^2 \int_0^\tau d\tau_1 \int_{-\infty}^0 d\tau_2 D(\tau_1 - \tau_2) \right] \quad (4.32)$$

We have assumed that $\tau > 0$. The integral on the RHS is ultraviolet divergent and we shall need to dimensionally regulate it. Even then the integral is non-trivial and we evaluate it approximately in the limit $\tau \to \infty$. The details are left to the appendix F and we find that

$$\lim_{\tau\to\infty} \langle S_\alpha(\tau) S_\alpha(0) \rangle = S(S+1) \left[1 - 2\gamma^2 \left(\frac{1}{\epsilon} \left(\frac{\mu}{m} \right)^\epsilon + \left(\frac{\pi}{2} \right)^{1/2} \Gamma(1/2, 1) \right) \right]. \quad (4.33)$$

The function $\Gamma(1/2, 1)$ is the incomplete gamma function. The pole in ϵ can be removed by defining a suitably renormalized spin field $S_\alpha(\tau)$. From the definitions in equation 4.27 we write:

$$\langle S_\alpha(\tau) S_\alpha(0) \rangle = Z' \langle S_\alpha(\tau) S_\alpha(0) \rangle_R, \quad Z' = 1 - \frac{2\gamma^2}{\epsilon}. \quad (4.34)$$

This makes all the correlation functions to come out finite to this order and we arrive at the final result

$$\lim_{\tau\to\infty} \langle S_\alpha(\tau) S_\alpha(0) \rangle_R = S(S+1) \left[1 - 2\gamma^2 \left(\ln \left(\frac{\mu}{m} \right) + \left(\frac{\pi}{2} \right)^{1/2} \Gamma(1/2, 1) \right) \right]. \quad (4.35)$$

Near the fixed point $\gamma^{*2} = \epsilon/2$, we can exponentiate the $\ln(\mu/m)$ term to find that

$$m_{\text{imp}} \equiv (\lim_{\tau\to\infty} \langle S_\alpha(\tau) S_\alpha(0)\rangle_R)^{1/2} \sim \left(\frac{m}{\mu}\right)^{\epsilon/2} \sim \Delta^{\epsilon/2}. \tag{4.36}$$

So we see that as we approach the critical point by tuning $m \to 0$, the magnetization of the impurity vanishes. This is easily understandable because near the critical point, low energy spin fluctuations in the background proliferate and the spin is no longer confined. In the next section, we shall indeed show that the spin correlations in the critical regime, in fact, decay as a power law.

4.3.2 Critical Regime

In the critical regime, the algebra simplifies considerably because we can replace $D(\tau)$ by $D_0(\tau)$. After carrying out the integral in equation 4.32, we find that

$$\langle S_\alpha(\tau) S_\alpha(0)\rangle = S(S+1)\left[1 - \gamma^2 \frac{(\mu\tau)^\epsilon}{\epsilon}.\right] \tag{4.37}$$

Using the definition of Z' from equation 4.34, we find that

$$\langle S_\alpha(\tau) S_\alpha(0)\rangle_R = S(S+1)(1 - 2\gamma^2 \ln(\mu\tau)) = S(S+1)\frac{1}{(\mu\tau)^\epsilon}. \tag{4.38}$$

The last equation follows by using the fixed point value γ^* from equation 4.26 and exponentiating the $\ln(\mu\tau)$ term.

This result can be also obtained straightforwardly from the anomalous dimension of the n_α field. The anomalous dimension is given by

$$\eta' = \mu\frac{dZ'}{d\mu} = \beta(\gamma)\frac{\partial \ln Z'}{\partial\gamma} = \epsilon \tag{4.39}$$

4.3.3 Ordered Regime

In the ordered regime, the expectation value of the background field ϕ_α is non-zero and we have two massless Goldstone modes. To calculate the impurity spin correlations, we shall first expand our background field action around the ordered phase. The action that we start out with is

$$\mathcal{S}_{\text{bg}} = \int d^d x d\tau \left[\frac{1}{2}\left((\partial_\tau\phi_\alpha)^2 + (\nabla\phi_\alpha)^2 - m^2\phi_\alpha^2\right) + \frac{g_0}{4!}(\phi_\alpha\phi_\alpha)^2\right]. \tag{4.40}$$

Since the "mass" term in this action is negative, this leads to non-zero expectation value of one of the ϕ_α fields and by convention we take this direction to be the ϕ_z field, i.e.

$$\langle \phi_z \rangle \equiv v = \left(\frac{6m^2}{g_0} \right)^{1/2} . \tag{4.41}$$

Now we make the replacement $\phi_z \to \tilde{\phi}_z + v$, so that $\langle \tilde{\phi}_z \rangle \equiv 0$. With this when we expand the action in equation 4.40, we get

$$\begin{aligned} \mathscr{S}_{\text{bg}} &= \int d^d x d\tau \left[\sum_{\alpha=x,y} \frac{1}{2} \left((\partial_\tau \phi_\alpha)^2 + (\nabla \phi_\alpha)^2 \right) + \frac{1}{2} \left((\partial_\tau \tilde{\phi}_z)^2 + (\nabla \tilde{\phi}_z)^2 + 2m^2 \tilde{\phi}_z^{\,2} \right) \right] \\ &+ \int d^d x d\tau \left[\left(\frac{g_0 m^2}{6} \right)^{1/2} \tilde{\phi}_z (\phi_x^2 + \phi_y^2) + \frac{g_0}{4!} (\tilde{\phi}_z^{\,2} + \sum_{\alpha=x,y} \phi_\alpha \phi_\alpha)^2 \right] . \end{aligned} \tag{4.42}$$

We note the appearance of two massless Goldstone modes characterized by ϕ_x and ϕ_y. The impurity part of the action is also modified to

$$\mathscr{S}_{\text{imp}} = \int d\tau \left[v S_z(\tau) + \tilde{\phi}_z(x=0,\tau) S_z(\tau) + \sum_{\alpha=x,y} \phi_\alpha(x=0,\tau) S_\alpha(\tau) \right] . \tag{4.43}$$

The first term in the impurity action is equivalent to having a magnetic field of strength v, turned on in the z direction. So essentially, the impurity spin will be kept aligned in the z direction by this field and the expectation value $\langle S_z \rangle$ will be non-zero. We shall be interested in finding the value of this magnetization near the critical point when $m \to 0$. A calculation whose details we again leave to the appendix shows that

$$\langle S_z \rangle_R = -S \left[1 + \gamma^2 \left(\ln(m/\mu) + \text{constants} \right) \right] . \tag{4.44}$$

Again near the fixed point, we can exponentiate the $\ln(m/\mu)$ and we find that the impurity spin magnetization is

$$m_{\text{imp}} \equiv \langle S_z \rangle_R \sim \left(\frac{m}{\mu} \right)^{\epsilon/2} . \tag{4.45}$$

4.4 Conclusion

We have shown that the theory of a single impurity in a host antiferromagnet near the host transition is described by a new fixed point. Within the epsilon expansion, the

new fixed point is completely determined by the parameters in the old theory—we do not need to input any external parameters. We have also evaluated the impurity spin correlations in both the ordered and disordered regimes as well as the critical regime.

Appendix A

A Technical Note on $\Lambda_{\overline{MS}}$

Whenever we carry out a field-theoretic renormalization group analysis, an arbitrary mass scale is introduced by dimensional regularization. $\Lambda_{\overline{MS}}$ is a way of relating this arbitrary mass scale to actual physical quantities in the system. To use the most relevant example, let us look at the definition of the renormalized coupling g_R in $d = 1 - \epsilon$ space dimensions for the $O(3)$ NLSM.

$$g = g_R(\mu)\mu^{-\epsilon} Z_g(g_R). \tag{A.1}$$

$Z_g(g_R)$ is a renormalization factor and μ is the mass scale introduced. In ordinary momentum shell renormalization group we introduce an explicit cutoff Λ and we study the flow of the coupling under a rescaling of this cutoff. In field-theoretic formalism, we send the cutoff Λ to infinity and instead study the flow of couplings under rescaling of the renormalization scale μ. Under a rescaling $\mu \to \mu e^l$, we obtain the one loop renormalization group beta function for the N component NLSM.

$$\mu \frac{dg_R}{d\mu} = \frac{dg_R}{dl} = \frac{N-2}{2\pi} g_R(\mu)^2. \tag{A.2}$$

Using this formalism when we calculate any physical quantity, the physical quantity will be dependent on μ and $g_R(\mu)$. To take a concrete example, let us think of any physical length scale (such as Δ/c) for a spin-1 Heisenberg chain. By dimensional analysis

this length scale, which we christen $\Lambda_{\overline{MS}}^{-1}$, must satisfy

$$\Lambda_{\overline{MS}} = \mu F(g_R(\mu)), \tag{A.3}$$

where $F(g_R(\mu))$ is some function to be determined. Since $\Lambda_{\overline{MS}}$ is a physical length scale, it must be independent of μ, or in other words must be invariant under the RG flow A.2, i.e.

$$\mu \frac{d}{d\mu} \Lambda_{\overline{MS}} = \left(\mu \frac{\partial}{\partial \mu} + \beta(g_R) \frac{\partial}{\partial g_R} \right) \Lambda_{\overline{MS}} = 0. \tag{A.4}$$

This constraint fixes this length scale up to a multiplicative constant and we find using A.2 that

$$\Lambda_{\overline{MS}} = \mu (4\pi e^{-\gamma})^{1/2} \exp\left(-\frac{2\pi}{g_R(N-2)} \right). \tag{A.5}$$

The prefactor is chosen for convenience. Higher loop results for the beta function will lead to corrections in the prefactor of the exponential.

This reasoning immediately leads to the conclusion that all physical $T = 0$ length scales must be universal constants times $\Lambda_{\overline{MS}}^{-1}$. But we have not yet related an experimentally measurable length scale to this length scale defined by convention within the RG formalism. This was done for the integer spin Heisenberg chain by Hasenfratz and Niedermeyer through an exact solution. Their simple result is as follows:

$$\Lambda_{\overline{MS}} = \frac{e}{8} \Delta. \tag{A.6}$$

A similar result by Sachdev [29] exists for the half-integer spin chains and is given in equation 2.16.

Appendix B

Derivation of Effective Classical Model

This discussion is adopted from [30]. We start with deriving the equal time correlations for the action in equation 2.3 ignoring the theta term. The idea here is to write down an effective Hamiltonian for only the zero frequency Matsubara modes after carrying out the sum over all the non-zero frequency modes in the partition function. This procedure is identical to integrating out high frequency modes in the momentum shell RG formulation and deriving a new effective Hamiltonian for the low energy modes. In this case the only mode that is left is a time independent unit vector field $n_\alpha(x)$, $(\alpha = 1 \cdots n)$. We have generalized here to an N component field for the sake of generality. The physical case is $N = 3$, as usual. This leads to an effective Hamiltonian of the form

$$\mathscr{Z} = \int \mathscr{D}\boldsymbol{n}(x)\delta(\boldsymbol{n}^2 - 1) \exp\left[\frac{(N-1)\xi}{4}\int dx \left(\frac{\partial n_\alpha(x)}{\partial x}\right)^2\right]. \tag{B.1}$$

A point to note is that this is the Feynman path integral in imaginary time for a particle whose coordinate at time x is given by $n_\alpha(x)$ and moreover the particle is constrained to be on the unit sphere. So this is nothing but the partition function for a quantum rotor. From this analogy we can immediately find the gap for the quantum system or equivalently the correlation length for the $n_\alpha(x)$ field. The constants up front in the exponential has been chosen such that the correlation length of the model is exactly ξ.

Now coming back to the RG analogy, the procedure for integrating out $\omega_n \neq 0$ modes is beautifully described by Polyakov [22]. We start out with the action in equation 2.3 at temperature T. We find that after a one loop calculation, our correlation length (equivalent to renormalized coupling constant in RG language) is given by

$$\frac{(N-1)T}{2}\xi = \frac{c}{g} - c^2(N-2)\int \frac{dk}{2\pi} T \sum_{\omega_n \neq 0} \frac{1}{c^2k^2 + \omega_n^2}, \quad \omega_n \equiv 2\pi n T. \tag{B.2}$$

The integral on the right hand side is not ultraviolet convergent and hence we regulate it by dimensional regularization in $d = 1 - \epsilon$. Also we introduce a renormalization of the coupling constant by

$$g_R(\mu) = \mu^\epsilon Z_g g. \tag{B.3}$$

This procedure has been discussed by Brezin and Zinn-Justin [69] and they calculate Z_g in the minimal subtraction scheme to be

$$Z_g = 1 - \frac{(N-2)g_R(\mu)}{2\pi\epsilon} + \cdots. \tag{B.4}$$

After defining Z_g and $g_R(\mu)$, what we need to do is to substitute for g in B.2 from B.3 and B.4, and evaluate all integrals in $d = 1 - \epsilon$ dimensions. After this procedure, all poles in ϵ will cancel and the limit $\epsilon \to 0$ can be safely taken. Some details of the evaluation of the integrals are shown below.

$$\begin{aligned}
\int \frac{d^dk}{(2\pi)^d} T \sum_{\omega_n \neq 0} \frac{1}{c^2k^2 + \omega_n^2} &= \int \frac{d^dk}{(2\pi)^d} \left[T \sum_{\omega_n \neq 0} \frac{1}{c^2k^2 + \omega_n^2} - \int \frac{d\omega}{2\pi} \frac{1}{c^2k^2 + \omega^2 + T^2} \right] \\
&+ \int \frac{d^{d+1}k}{(2\pi)^{d+1}} \frac{1}{c^2k^2 + T^2} \\
&= \frac{1}{c}\left[\frac{T}{c}\right]^{-\epsilon} \int \frac{d^{1-\epsilon}k}{(2\pi)^{1-\epsilon}} \left[\frac{1}{2k} \coth\frac{k}{2} - \frac{1}{k^2} - \frac{1}{2(1+k^2)^{1/2}} \right] \\
&+ \frac{1}{c}\left[\frac{T}{c}\right]^{-\epsilon} \frac{\Gamma(\epsilon/2)}{(4\pi)^{1-\epsilon/2}}
\end{aligned} \tag{B.5}$$

On the RHS of the first line, we added and subtracted an integral to isolate the divergence. In the second line, the first integral is both UV and IR convergent and as long as we are interested in only poles in ϵ and constant terms, we can evaluate it directly at

$\epsilon = 0$. The poles in ϵ will come from the Gamma function in ϵ and will be canceled by the poles in the definition of Z_g. After all is said and done, we find that

$$\frac{(N-1)T}{2c}\xi = \frac{1}{g_R(\mu)} - \frac{N-2}{2\pi}\ln\left(\frac{c\mu}{T(4\pi e^{-\gamma})^{1/2}}\right) \tag{B.6}$$

This form is not convenient to deal with because it contains the arbitrary renormalization scale μ. At this point our acquaintance with the renormalization group invariant $\Lambda_{\overline{MS}}$ pays off. Recalling the definition of $\Lambda_{\overline{MS}}$ from A.5, we arrive at the one loop result

$$\xi = \frac{(N-2)c}{\pi(N-1)}\frac{1}{T}\ln\left(\frac{4\pi e^{-\gamma}T}{c\Lambda_{\overline{MS}}}\right). \tag{B.7}$$

Note that all dependence on μ or $g_R(\mu)$ has been eliminated from ξ, and this is as it should be because ξ is a physically measurable length scale independent of any regularization scheme. Physical prediction for ξ can be now made by using the result A.6.

Next we proceed to find the dynamics of this model Hamiltonian. Since this is a classical Hamiltonian, the dynamics is described by the Hamiltonian equations of motion. But we do not have the kinetic energy term in the Hamiltonian yet. Since our canonical coordinate is a unit vector, it is describable as a rotor. The canonical momentum will be an angular momentum. The moment of inertia of the rotor will be related to the susceptibility χ_u of the system to an external magnetic field H. We couple the field $n_\alpha(x)$ to an external field H and then expand the free energy to order H^2. The calculations are very similar to the calculation of ξ and so we will only quote the end result here:

$$\chi_u(T) = \frac{N-2}{N\pi c}\ln\left(\frac{4\pi e^{-\gamma}T}{c\Lambda_{\overline{MS}}}\right). \tag{B.8}$$

The last important point we need to address is the relation of the correlation functions defined in the full quantum theory to the correlation function of the corresponding fields in the effective classical theory. The case of $\boldsymbol{L}$ is straightforward because $\boldsymbol{L}$ is a conserved quantity and

$$\langle \boldsymbol{L}(x,t)\cdot\boldsymbol{L}(0,0)\rangle_Q = \langle \boldsymbol{L}(x,t)\cdot\boldsymbol{L}(0,0)\rangle_C. \tag{B.9}$$

The case of the $\boldsymbol{n}$ field is more subtle. What we need in this case is the anomalous

dimension of the $\boldsymbol{n}$ field in the NLSM. The anomalous dimension $\gamma(g(\mu))$ has been calculated by Brezin and Zinn-Justin [69] and we have

$$\gamma(g(\mu)) \equiv \mu \frac{d\ln(Z)}{d\mu} = \frac{(N-1)g(\mu)}{2\pi}, \tag{B.10}$$

where Z is the field renormalization for the $\boldsymbol{n}$ field. With this in hand and using the of the beta function A.2, we can show that

$$Z^{-1}(g(\mu_1))C(x,t;g(\mu_1),\mu_1) = \left[\ln\left(\frac{\mu_1}{\mu_2}\right)\right]^{\frac{N-1}{N-2}} Z^{-1}(g(\mu_2))C(x,t;g(\mu_2),\mu_2), \tag{B.11}$$

where $C(x,t;g(\mu_1),\mu_1)$ is the correlation function $\langle \boldsymbol{n}(x,t)\cdot\boldsymbol{n}(0,0)\rangle$ evaluated at the particular mass scale μ_1. The physical energy scale at which our correlation function is defined is at low energies at $\mu \sim \Lambda_{\overline{MS}}$, while our classical effective Hamiltonian was derived for the energy scale $\mu \sim T \gg \Lambda_{\overline{MS}}$. Using these two facts, we can relate our quantum and classical correlation functions as

$$\langle \boldsymbol{n}(x,t)\cdot\boldsymbol{n}(0,0)\rangle_Q = \mathscr{A}\mathscr{C}\left[\ln\left(\frac{T}{\Lambda_{\overline{MS}}}\right)\right]^{\frac{N-1}{N-2}} \langle \boldsymbol{n}(x,t)\cdot\boldsymbol{n}(0,0)\rangle_C, \tag{B.12}$$

where $\mathscr{A}$ is a non-universal quasi-particle residue and $\mathscr{C}$ is an unknown universal constant.

Appendix C

Relation Between T_0 and $\Lambda_{\overline{MS}}$

In this appendix we briefly outline the reasoning which led to equation 2.16. Recall that the NLSM with $\theta = \pi$ has two fixed points: $g = 0$ and $g = g_c$. The energy scale $\Lambda_{\overline{MS}}$ characterizes the flow of g away from $g = 0$ fixed point, while T_0 characterizes the flow of g into the $g = g_c$ fixed point. Hence $\Lambda_{\overline{MS}}$ shows up in a high temperature expansion around $g = 0$ (eqn. 2.18), while T_0 appears in the low temperature expansion (eqn. 2.15). If we can connect these two temperature scales through a Bethe ansatz solution, we can arrive at the desired relation between $\Lambda_{\overline{MS}}$ and T_0. Actually this analysis has already been done [70, 71] and we shall simply use their publsihed results to match the expressions for the NLSM free energy $\mathscr{F}_Q$ various regimes of T and H (magnetic field).

First we consider the $O(3)$ NLSM at $\theta = \pi$ for $H \neq 0$. The $T = 0$ properties for this model were worked out by Fateev et. al. [70]. For the two limits $H \gg \Lambda_{\overline{MS}}$ and $H \ll \Lambda_{\overline{MS}}$ they respectively obtained

$$\mathscr{F}_Q = -\frac{H^2}{4\pi c} \ln\left[\frac{H}{e^{1/2}\Lambda_{\overline{MS}}}\right] + \cdots, \quad H \gg \Lambda_{\overline{MS}}, T = 0 \tag{C.1}$$

$$\mathscr{F}_Q = -\frac{H^2}{4\pi c}\left[1 + \frac{1}{2\ln\left(2(2\pi)^{1/2}e^{-3/4}\Lambda_{\overline{MS}}/H\right)}\right] + \cdots; \quad H \ll \Lambda_{\overline{MS}}, T = 0 \tag{C.2}$$

The first equation can also be obtained by doing a renormalized perturbation expansion around $g = 0$ and was obtained earlier by Hasenfratz et. al [72].

Now we approach the problem from the other end, i.e. try to find the free energy

as a function of T_0. Recently Lukyanov [71] has computed the H and T dependence of the free energy for the $S = 1/2$ Heisenberg antiferromagnetic chain with nearest neighbour interactions. Because of universality, this model maps onto the $O(3)$ NLSM in the vicinity of the $g = g_c$ fixed point. So we can freely use results by Lukyanov to derive the free energy as a function of T_0. From his eqns (3.18) and (3.20) [71], we find that

$$T_0 = \left(\frac{\pi}{2}\right)^{1/2} e^{\gamma+1/4} J. \tag{C.3}$$

This result is not universal, but we find a universal expression for the free energy

$$\mathscr{F}_Q = -\frac{H^2}{4\pi c}\left(1 + \frac{1}{2\ln(2\pi e^{-\gamma} T_0/H)}\right) + \cdots; \quad H \ll T_0, T = 0. \tag{C.4}$$

Since $\Lambda_{\overline{MS}} \sim T_0$, we can immediately make a comparison between equations C.2 and C.4 and see that

$$\Lambda_{\overline{MS}} = \left(\frac{\pi}{2}\right)^{1/2} e^{3/4-\gamma} T_0 \tag{C.5}$$

which is the result quoted in eq. 2.16.

Appendix D

Details of Short Time Expansion

We start with the expression (2.32) and insert (2.34) into it and the expand to first order to find

$$\mathcal{Z}_c = \int \mathcal{D}\psi\mathcal{D}\psi^*\mathcal{D}\phi\mathcal{D}\phi^* \exp(-\int d\tau\, \mathcal{L}), \tag{D.1}$$

where

$$\begin{aligned}
\mathcal{L} &= \psi\psi^* + \frac{1}{2\xi}(\phi\psi^* + \phi^*\psi)^2 \\
&+ \left|\frac{\partial\phi}{\partial x}\right|^2 + \frac{1}{2\xi}\left(\phi\frac{\partial\phi^*}{\partial x} + \phi^*\frac{\partial\phi}{\partial x}\right)^2 \\
&+ m^2\phi\phi^* + \frac{m^2}{2\xi}\phi^2\phi^{*2} \\
&- \frac{1}{2a\xi}\phi\phi^*.
\end{aligned} \tag{D.2}$$

Here we have dropped some additive constants and integrated by parts in places. As advertised before, the magnetic field in the z direction parametrized by m^2 adds a mass term to the action and makes the $\langle\phi\phi^*\rangle$ propagator infrared finite. The last term in the action arises from the Jacobian of the delta functionals $\delta(\boldsymbol{n}\cdot\boldsymbol{L})\delta(\boldsymbol{n}^2-1)$ in the measure. This Jacobian is infinite for a continuum system. To regularize it, we can introduce a discrete lattice in space. In that case the parameter a is the lattice constant, or equivalently

the volume of the Brillouin zone.

$$\frac{1}{a} \equiv \frac{1}{L} \sum_{k \in \mathrm{BZ}} 1 \tag{D.3}$$

This can be finite only in a finite volume system, but we shall carry it through and ultimately it will cancel all ultraviolet divergences arising from unrestricted momentum sums over the $\langle \psi \psi^* \rangle$ propagator. In terms of ψ and ϕ, the $\langle \boldsymbol{L}(x,t) \cdot \boldsymbol{L}(0,0) \rangle$ is written as

$$\begin{aligned} \langle \boldsymbol{L}(x,t) \cdot \boldsymbol{L}(0,0) \rangle &= \langle \psi(x,t) \psi^*(0,0) \rangle + \text{c.c.} \\ &+ \frac{1}{\xi} \langle \phi(x,t) \psi^*(x,t) \phi(0,0) \psi^*(0,0) \rangle + \text{c.c.} \\ &+ \frac{1}{\xi} \langle \psi(x,t) \phi^*(x,t) \psi^*(0,0) \phi(0,0) \rangle + \text{c.c.} \end{aligned} \tag{D.4}$$

Using (2.34) in the dynamical equations (2.31), we find the following equations of motion:

$$\begin{aligned} \frac{\partial \psi}{\partial t} &= i \left[\frac{\partial^2 \phi}{\partial x^2} + \frac{1}{\xi} \frac{\partial}{\partial x} \left(\phi^2 \frac{\partial \phi^*}{\partial x} \right) \right] \\ \frac{\partial \phi}{\partial t} &= -i \left[\psi + \frac{1}{\xi} \left(\phi^2 \psi^* \right) \right]. \end{aligned} \tag{D.5}$$

These equations differ from (2.35) in that we have absorbed a factor of $c = \xi^{1/2}$ into the definition of time so that time and distance have the same units.

To solve for $\psi(x,t)$, we make a Fourier transform in space of (D.5) and convert it to an initial value problem given by

$$\frac{\partial}{\partial t} \begin{bmatrix} \psi(k,t) \\ \phi(k,t) \end{bmatrix} = \begin{bmatrix} -ik^2 \phi(k,t) \\ -i\psi(k,t) \end{bmatrix} + \begin{bmatrix} A(k,t) \\ B(k,t) \end{bmatrix}. \tag{D.6}$$

We have here written the nonlinearities as the inhomogeneous part of a set of first order equations. The solution to the initial value problem is given by

$$\begin{bmatrix} \psi(k,t) \\ \phi(k,t) \end{bmatrix} = \mathscr{K}(t) \mathscr{K}^{-1}(0) \begin{bmatrix} \phi(k,0) \\ \psi(k,0) \end{bmatrix} + \mathscr{K}(t) \int_0^t d\tau \, \mathscr{K}^{-1}(\tau) \begin{bmatrix} A(k,\tau) \\ B(k,\tau) \end{bmatrix}. \tag{D.7}$$

The columns of the 2×2 matrix $\mathscr{K}(t)$ is made up of the two linearly independent solution vectors of the homogeneous problem.

$$\mathscr{K}(t) = \begin{bmatrix} ke^{-ikt} & -ke^{ikt} \\ e^{-ikt} & e^{ikt} \end{bmatrix} \tag{D.8}$$

Armed with this, we can solve for the fields in terms of the initial conditions and iterate the solution to go to higher orders by plugging the solution back in A and B. Also calculations simplify very much if we work out everything back in real space. So at last we write down the final iterative form from which the entire perturbation series can be generated.

$$\begin{aligned}\psi(x,t) &= \frac{1}{2}\left[\psi(x+t,0)+\psi(x-t,0)\right]+\frac{i}{2}\frac{\partial}{\partial x}\left[\phi(x+t,0)-\phi(x-t,0)\right] \\ &+ \frac{1}{2}\int_0^t d\tau\int dx'\left[\delta(x-x'+t-\tau)+\delta(x-x'-t+\tau)\right]A(x',\tau) \\ &+ \frac{i}{2}\int_0^t d\tau\int dx'\left[\delta(x-x'+t-\tau)-\delta(x-x'-t+\tau)\right]\frac{\partial}{\partial x'}B(x',\tau) \qquad \text{(D.9)}\end{aligned}$$

$$\begin{aligned}\phi(x,t) &= \frac{1}{2}\left[\phi(x+t,0)+\phi(x-t,0)\right]-\frac{i}{2}\int dx'\left[\theta(x-x'+t)-\theta(x-x'-t)\right]\psi(x',0) \\ &+ \frac{1}{2}\int_0^t d\tau\int dx'\left[\delta(x-x'+t-\tau)+\delta(x-x'-t+\tau)\right]B(x',\tau) \\ &- \frac{i}{2}\int_0^t d\tau\int dx'\left[\theta(x-x'+t-\tau)-\theta(x-x'-t+\tau)\right]A(x',\tau) \qquad \text{(D.10)}\end{aligned}$$

To simplify notation let us denote the zeroth order solutions for the fields as $\psi^{(0)}(x,t)$ and $\phi^{(0)}(x,t)$.

$$\begin{aligned}\psi^{(0)}(x,t) = &\quad \frac{1}{2}\left[\psi(x+t,0)+\psi(x-t,0)\right]+\frac{i}{2}\frac{\partial}{\partial x}\left[\phi(x+t,0)-\phi(x-t,0)\right] \\ \phi^{(0)}(x,t) = &\quad \frac{1}{2}\left[\phi(x+t,0)+\phi(x-t,0)\right] \\ &\quad -\frac{i}{2}\int dx'\left[\theta(x-x'+t)-\theta(x-x'-t)\right]\psi(x',0) \qquad \text{(D.11)}\end{aligned}$$

Now we can proceed to evaluate each of the correlation functions in (D.4). As an example let us look at $\langle\psi(x,t)\psi^*(0,0)\rangle$. The correlations to zeroth order are

$$\begin{aligned}\langle\psi^{(0)}(x,t)\psi^{(0)*}(0,0)\rangle &= \frac{1}{2}\left[\delta(x+t)+\delta(x-t)\right] \\ \langle\phi^{(0)}(x,t)\phi^{(0)*}(0,0)\rangle &= \frac{1}{4m}\left[e^{-m|x+t|}+e^{-m|x-t|}\right] \\ \langle\phi^{(0)}(x,t)\psi^{(0)*}(0,0)\rangle &= \frac{i}{2}\left[\theta(x+t)-\theta(x-t)\right] \qquad \text{(D.12)}\end{aligned}$$

To compute the one loop correlation $\langle\psi(x,t)\psi^*(0,0)\rangle$, we write down

$$\begin{aligned}\langle\psi(x,t)\psi^*(0,0)\rangle &= \langle\psi^{(0)}(x,t)\psi^{(0)^*}(0,0)\rangle \\ &+ \frac{1}{2}\int_0^t d\tau\int dx'\left[\delta(x-x'+t-\tau)+\delta(x-x'-t+\tau)\right]\times \\ &\quad \frac{1}{\xi}\frac{\partial}{\partial x'}\left\langle\phi^2(x',\tau)\frac{\partial\phi^*(x',\tau)}{\partial x'}\psi^{(0)^*}(0,0)\right\rangle \\ &+ \frac{i}{2}\int_0^t d\tau\int dx'\left[\delta(x-x'+t-\tau)-\delta(x-x'-t+\tau)\right]\times \\ &\quad \frac{\partial}{\partial x'}\left\langle-\frac{i}{\xi}\phi^2(x',\tau)\psi^*(x',\tau)\psi^{(0)^*}(0,0)\right\rangle \end{aligned} \tag{D.13}$$

On the second and third terms of the RHS, we can replace $\phi(\psi)$ by $\phi^{(0)}(\psi^{(0)})$ since it is already first order in $1/\xi$. Now all the correlation functions on the RHS are expressed in terms of correlation functions at time $t = 0$. So we evaluate them using the partition function (D.1). Other correlations can be evaluated in the same manner. So we shall only write down the final answers here.

$$\langle\psi(x,t)\psi^*(0,0)\rangle = \frac{1}{2}\left[\delta(x+t)+\delta(x-t)\right]\left(1-\frac{1}{2m\xi}\right) \tag{D.14}$$

$$\langle\phi(x,t)\psi^*(x,t)\phi(0,0)\psi^*(0,0)\rangle = \frac{1}{4\xi}\left[\theta(x+t)-\theta(x-t)\right] \tag{D.15}$$

$$\langle\psi(x,t)\phi^*(x,t)\psi^*(0,0)\phi(0,0)\rangle = \frac{1}{8m\xi}\left[\delta(x+t)+\delta(x-t)\right]\left(1+e^{-2mt}\right). \tag{D.16}$$

Adding them all and taking the limit $m \to 0$ leads to the expression quoted in (2.36). Note that all terms which diverge as $m \to 0$, cancel each other only when we evaluate the O(3) invariant correlation $\langle \boldsymbol{L}(x,t)\cdot\boldsymbol{L}(0,0)\rangle$.

Appendix E

Various Distribution Functions in the Toy Model

In this appendix we shall try to give a self contained description of the solution to the toy model described in section 3.1. This solution was described by Jepsen [64] and we shall adhere to his notations and conventions.

Section 3.1 already gives a description of the model and we shall not repeat that here. The quantity that we wish to calculate is $B(x,t) \equiv \sum_i \langle \delta(x - x_i(t))\delta(x_i(0))\rangle$. The angular brackets imply an average over all initial positions and initial velocities. The initial positions are distributed uniformly over the whole length L of the system (we use periodic boundary conditions) and the velocities are chosen from an initial velocity distribution $g(v)$. For example the classical Maxwell-Boltzmann thermal ensemble is given by $g(v) = (m/2\pi T)^{1/2} \exp(-mv^2/(2T))$. In our case, only two possible velocities $\pm c$ exists and we have

$$g(v) = \frac{1}{2}(\delta(v + c) + \delta(v - c)). \tag{E.1}$$

Our solution will be in terms of a function $A_{jk}(t)$ which is equal to one if the particle j is on trajectory k at time t and zero otherwise. Recall that particles are labelled from 0 to $N - 1$ with the assumption that the initial position of the ith particle is $x_i(0)$ and $x_i(0) < x_j(0)$ if and only if $i < j$. The trajectory of the particles are labelled by the

number of the particle which occupied it at time $t = 0$. If we consider the ensemble average $\langle A_{jk}(t) \rangle$, then this is the probability that the particle j is on trajectory k at time t. The key point to note in the solution of this model is that the particles maintain their initial order at all times, i.e. if $i < j$, then $x_i(t) < x_j(t)$ for all t. So we can find out which particle is on a given trajectory simply by counting the number of times this trajectory has been crossed by other trajectories from each side. For example, in Fig E consider the trajectory 2. Whenever the trajectory is crossed from the right by another trajectory, the number of the particle on that trajectory increases by 1. Similarly a crossing from the left decreases the number of the particle by 1. We define a collision from the left as a "negative" collision and a collision from the right as a "positive" collision. With this convention, if a trajectory k has suffered a total of n collisions since time $t = 0$, the particle on that trajectory is numbered $k + n$. Because of the periodic boundary conditions, particle numbers are always counted modulo N.

Because the dynamics of the system is so simple, it exhibits some pathological behaviour. For example, the particles never change their order and since in every collision, two particles merely exchange their velocities, the velocity distribution never changes. Hence if we treat the particles as indistinguishable, the system will be equivalent to a trivial non-interacting system. The only interesting properties arise, when we treat the particles as distinguishable.

To make progress towards the solution we define $r_n(h, k, t)$ to be equal to 1 if trajectory h crosses trajectory k, n times in time t and zero otherwise. Averaged over an ensemble, r_n is the probability that trajectory h crosses k a total of n times. We now define the characteristic function for the probability distribution as

$$s(u; h, k, t) \equiv \sum_{n=-\infty}^{\infty} r_n(h, k, t) e^{inu}. \tag{E.2}$$

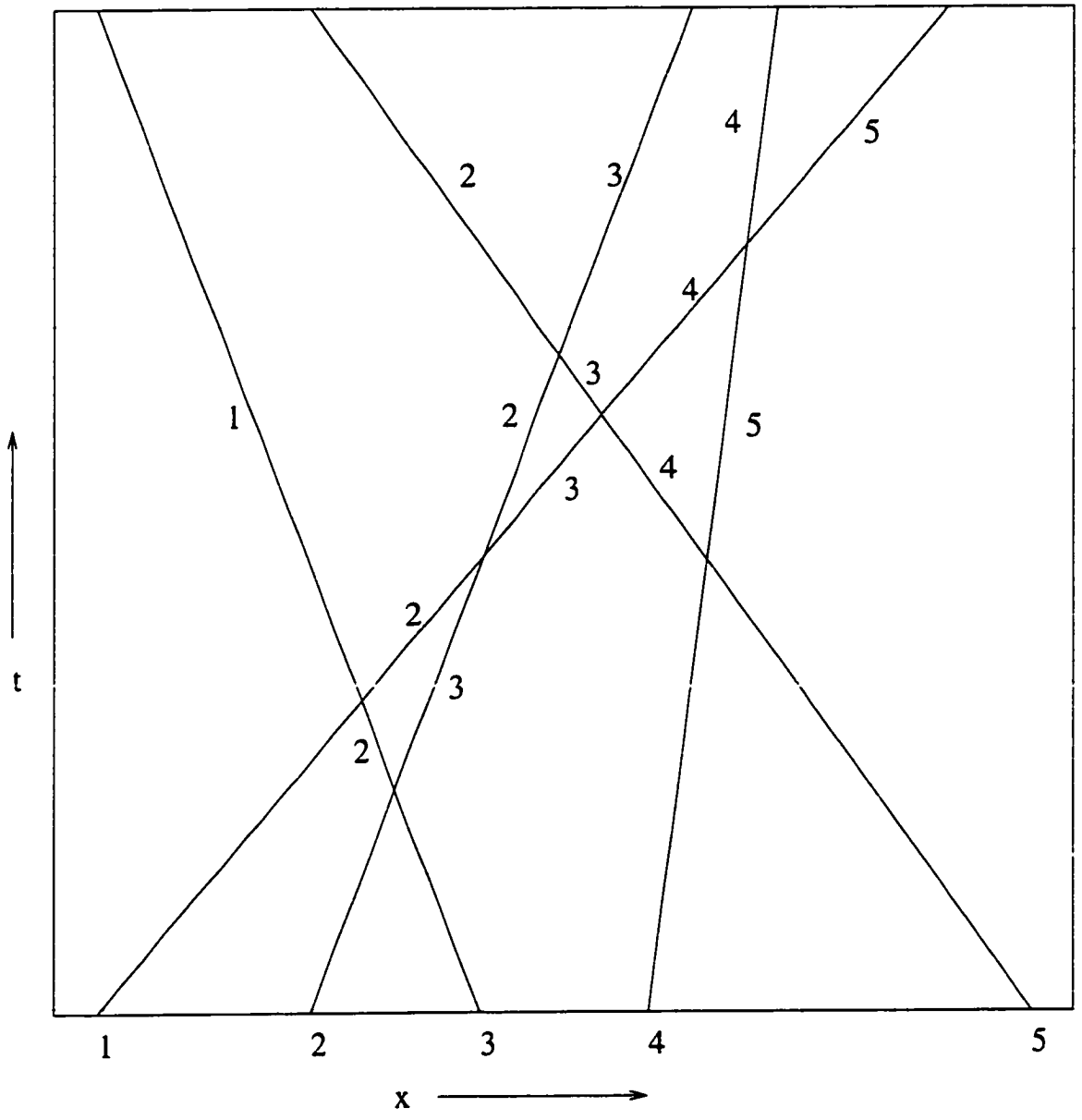

Figure E.1: Nature of dynamics in our toy model. If a trajectory is crossed from the left by another trajectory, the number of the particle on the trajectory decreases by one. A crossing from the right has the opposite effect.

In terms of s, now we write down the solution

$$\begin{aligned} A_{jk}(t) &= \frac{1}{N}\sum_{l=0}^{N-1}\exp\left[-\frac{2\pi i}{N}(j-k)l\right]\prod_{h=0}^{N-1}s(2\pi l/N;h,k,t), \\ &= \sum_{n_0,n_1,\cdots,n_{N-1}=-\infty}^{\infty}\left[\frac{1}{N}\sum_{l=0}^{N-1}\exp\left(\frac{2\pi i l}{N}(n_0+n_1+\cdots n_{N-1}-j+k)\right)\right] \\ &\times\ r_{n_0}r_{n_1}\cdots r_{n_{N-1}}, \end{aligned} \tag{E.3}$$

with the understanding that $s(u;k,k,t)\equiv 1$. To see that this is the solution, we note that if we ignore the exponential factor in the second line above, the rest of the sum just describes the probability of all possible collisions which trajectory k can undergo. The exponential factor simply ensures that the unrestricted sum is restricted to only those combinations which can put the particle j on trajectory k.

We can write down a simple expression for $s(u;h,k,t)$ as follows:

$$\begin{aligned} s(u;h,k,t) &= S(u,w_{kh}),\ h>k, \\ &= e^{-iu}S(u,w_{kh}),\ h<k. \end{aligned} \tag{E.4}$$

Here

$$S(u,w)=e^{inu}\text{ when }(n-1)L<w\leq nL, \tag{E.5}$$

and

$$w_{kh}=x_k-x_h+(v_k-v_h)t. \tag{E.6}$$

Here x_k, v_k are the initial positions and velocities of the kth particle. Note that

$$S[u,w+L]=e^{iu}S[u,w]. \tag{E.7}$$

In terms of S, we rewrite E.3 as

$$A_{jk} = \frac{1}{N}\sum_u e^{-iju}\prod_{h=0}^{N-1}S[u,w_{kh}] \tag{E.8}$$

$$u = \frac{2\pi l}{N}$$

$$\sum_u \equiv \sum_{l=0}^{N-1}.$$

Now we are ready to take on the problem of calculating relevant correlations.

E.1 Evaluation of the Diffusive form in the Thermodynamic Limit

Let us start with equation 3.8. Following Jepsen's notation we write

$$\begin{aligned} P(y,t) &= \sum_{k\neq 0}\langle\delta(y-x_k-v_kt)A_{0k}(t)\rangle + \langle\delta(y-v_0t)A_{00}(t)\rangle = \\ &\frac{1}{N}\sum_u \frac{N-1}{L}\int_0^L dx_k \int_{-\infty}^{\infty} dv_k g(v_k) Q(u, x_k+v_kt, v_k) \\ \times &\left[\frac{1}{L}\int_0^L dx_h R[u, x_k+v_kt-x_h]\right]^{N-2} \\ + &\frac{1}{N}\int_{-\infty}^{\infty} dv_0 g(v_0)\delta(y-v_0t)\left[\frac{1}{L}\int_0^L dx_h R[u, x_0+v_0t-x_h]\right]^{N-1}, \end{aligned} \tag{E.9}$$

with the definitions that

$$\begin{aligned} g(v_k) &= \frac{1}{2}(\delta(v_k-c)+\delta(v_k+c)), \\ Q((u, x_k+v_kt, v_k) &= \int_{-\infty}^{+\infty} dv_0 g(v_0)\delta(y-x_k-v_kt)S[u, x_k+v_kt-v_0t] \\ &= \frac{1}{2}\delta(y-x_k-v_kt)\left(S[u, y-ct]+S[u, y+ct]\right), \\ R[u, x_k+v_kt-x_h] &= \int_{-\infty}^{+\infty} dv_h\, g(v_h) S[u, x_k+v_kt-x_h-v_ht]. \end{aligned} \tag{E.10}$$

The second term in the RHS of (E.10) clearly represents the probability that the zeroth particle stays in the zeroth trajectory at time t, while the first term represents the probability that it has been scattered to another trajectory.

Let us first concentrate on evaluating the second term first. Using the definition of $g(v)$, we find that

$$\begin{aligned} \frac{1}{2N}\sum_u e^{-iju}\Bigg[&\delta(y-ct)\left(\frac{1}{L}\int_0^L dx R[u, ct-x]\right)^{N-1} \\ + &\delta(y+ct)\left(\frac{1}{L}\int_0^L dx R[u, -ct-x]\right)^{N-1}\Bigg] \end{aligned} \tag{E.11}$$

Now we go to the thermodynamic limit in which $L\to\infty$ and $N\to\infty$ such that

$$\lim_{N,L\to\infty}\frac{N}{L}=\rho, \quad \lim_{N\to\infty}\frac{1}{N}\sum_u = \int_{-\infty}^{\infty}\frac{du}{2\pi}, \tag{E.12}$$

where ρ is the density of particles. In this limit after some manipulations very well described in Jepsen's paper [64] this expression evaluates to

$$\frac{1}{2}[\delta(y-ct)+\delta(y+ct)]e^{-\rho c|t|}. \tag{E.13}$$

We evaluate the second term in a very similar way. The calculations are tedious but straightforward. We find that this term vanishes outside the light cone and inside the light cone it evaluates to

$$\frac{\rho}{2}e^{-\rho c|t|}\left[I_0(2\rho(c^2t^2-y^2)^{1/2})+\frac{ct}{(c^2t^2-y^2)^{1/2}}I_1(2\rho(c^2t^2-y^2)^{1/2}).\right] \tag{E.14}$$

Putting these two expressions together, we immediately arrive at the result quoted in 3.9.

E.2 Evaluation of the One-particle Distribution Function in a Finite System

Again here the starting point is the expression quoted in equation E.10 The second term can be easily simplified using the definitions given above and in (3.5). It is

$$\begin{aligned}(\delta(y+ct)+\delta(y-ct))P^{(1)}(t) = \\ \delta(y-ct)\frac{1}{2N}\sum_u\left[\frac{1}{2}\left(1+e^{ipu}\left(1+\frac{2ct-pL}{L}(e^{iu}-1)\right)\right)\right]^{N-1} \\ +\delta(y+ct)\frac{1}{2N}\sum_u\left[\frac{1}{2}\left(1+e^{-ipu}\left(1+\frac{2ct-pL}{L}(e^{-iu}-1)\right)\right)\right]^{N-1}\end{aligned} \tag{E.15}$$

Here p is defined so that

$$0<2ct-pL<L. \tag{E.16}$$

$P^{(1)}(t)$ can't be evaluated in a closed analytic form. But we have evaluated it numerically for fixed values of N and L. $P^{(1)}(t)$ has been plotted in Fig 3.2 for $N=50, L=$

$1, c = \pm 1$. As mentioned before, the peaks at times $\mathscr{T}, 2\mathscr{T}, 3\mathscr{T}, \ldots$ are due to the exact recurrence of some configurations. We plot this function again for $N = 50$ and $51, L = 1, c = \pm 1$ in Fig 3.4. Note that the peaks at times $\mathscr{T}, 2\mathscr{T} \ldots$ disappear.

The first term will be handled in a manner similar to above. For simplicity we shall evaluate only the autocorrelation part. To do this, we set $y = nL$ where n is an integer.

$$P^{(2)}(t) = \sum_{k \neq 0} \langle \delta(x_k + v_k t - nL) A_{0k}(t) \rangle. \tag{E.17}$$

Using previous definitions we find that

$$P^{(2)}(t) = \frac{1}{4N} \sum_{u} \frac{N-1}{L} [\theta(nL - ct) - \theta(nL - ct - L) + \theta(nL + ct) - \theta(nL + ct - L)] \times$$
$$(S[u, nL + ct] + S[u, nL - ct]) \left[\int_0^L \frac{dx}{2L} (S[u, nL - x - ct] + S[u, nL - x + ct]) \right]^{N-2} \tag{E.18}$$

Here it will be convenient to define an integer p as before such that

$$0 < ct - pL < L. \tag{E.19}$$

Carrying out the integrals above we get

$$\begin{aligned} P^{(2)}(t) &= \frac{1}{4N} \sum_{u} \frac{N-1}{L} \left(e^{-iu} + e^{2ipu}\right) \frac{1}{2^{N-2}} \\ &\times \left[\frac{L - (ct - pL)}{L} \left(1 + e^{2ipu}\right) + \frac{ct - pL}{L} \left(e^{-iu} + e^{i(2p+1)u}\right) \right]^{N-2} + \text{c.c} \end{aligned} \tag{E.20}$$

The above function $P^{(2)}(t)$ has been plotted in Fig 3.3.

Appendix F

Calculation of Impurity Spin Autocorrelations

In this appendix, we shall outline the details of calculating the autocorrelation functions of the impurity spin.

F.1 Spin Gap Regime

We are interested in the autocorrelation function, which to one loop order is given by

$$\langle S_\alpha(\tau)S_\alpha(0)\rangle = \frac{1}{\mathscr{Z}}[S(S+1) + \frac{\gamma_0^2}{2}\int d\tau_1 d\tau_2 D(\tau_1-\tau_2) \times \langle 0|T_\tau(S_\alpha(\tau)S_\alpha(0)S_\beta(\tau_1)S_\beta(\tau_2))|0\rangle] \quad \text{(F.1)}$$

The state $|0\rangle$ is the spin ground state of the impurity. We assume that $\tau > 0$. We shall also need to expand $\mathscr{Z}$ to order γ_0^2 which is given by

$$\mathscr{Z} = 1 + \frac{\gamma_0^2}{2}\int d\tau_1 d\tau_2 D(\tau_1-\tau_2)\langle 0|T_\tau(S_\beta(\tau_1)S_\beta(\tau_2))|0\rangle \quad \text{(F.2)}$$

Evaluating the time ordered expectation value of the spin operators is straightforward, but tedious. For example

$$\begin{aligned} T_\tau(S_\alpha(\tau)S_\alpha(0)S_\beta(\tau_1)S_\beta(\tau_2)) &= 2S_\alpha S_\alpha S_\beta S_\beta \theta(-\tau_1)\theta(\tau_1-\tau_2) \\ &+ 2S_\alpha S_\beta S_\alpha S_\beta \theta(\tau-\tau_1)\theta(\tau_1)\theta(-\tau_2) \\ &+ 2S_\beta S_\alpha S_\alpha S_\beta \theta(\tau_1-\tau)\theta(-\tau_2) \\ &+ 2S_\alpha S_\beta S_\beta S_\alpha \theta(\tau-\tau_1)\theta(\tau_1-\tau_2)\theta(\tau_2) \\ &+ 2S_\beta S_\alpha S_\beta S_\alpha \theta(\tau_1-\tau)\theta(\tau-\tau_2)\theta(\tau_2) \\ &+ 2S_\beta S_\beta S_\alpha S_\alpha \theta(\tau_1-\tau_2)\theta(\tau_2-\tau) \end{aligned} \tag{F.3}$$

The factors of two in the RHS arise because the time ordered product is symmetric with respect to interchanging $\tau_1 \leftrightarrow \tau_2$. The products of spin operator can be simplified by using the commutation relation for spin operators. For example

$$S_\alpha S_\beta S_\alpha S_\beta = (S_\alpha S_\alpha)^2 - S_\alpha S_\alpha. \tag{F.4}$$

After a little massaging of the above expression for the autocorrelation, we find that

$$\begin{aligned} T_\tau(S_\alpha(\tau)S_\alpha(0)S_\beta(\tau_1)S_\beta(\tau_2)) &= (S_\alpha S_\alpha)^2 \\ &- 2S_\alpha S_\alpha \theta(\tau-\tau_1)\theta(\tau_1)\theta(-\tau_2) \\ &- 2S_\alpha S_\alpha \theta(\tau_1-\tau)\theta(\tau-\tau_2)\theta(\tau_2) \end{aligned} \tag{F.5}$$

Putting this all back in the expression for the autocorrelation we find the previously quoted expression 4.32

$$\begin{aligned} \langle S_\alpha(\tau)S_\alpha(0)\rangle &= S(S+1)\left[1-\gamma_0^2\left(\int_0^\tau d\tau_1 \int_{-\infty}^0 d\tau_2 D(\tau_1-\tau_2)\right.\right. \\ &+ \left.\left.\int_\tau^\infty d\tau_1 \int_0^\tau d\tau_2 D(\tau_1-\tau_2)\right)\right] \\ &= S(S+1)\left[1-2\gamma_0^2\int_0^\tau d\tau_1 \int_{-\infty}^0 d\tau_2 D(\tau_1-\tau_2)\right] \end{aligned} \tag{F.6}$$

In the last line above, we have performed a change of variables and used the fact that $D(\tau) = D(-\tau)$.

Next we need to evaluate this integral in the limit $\tau \to \infty$.

$$\lim_{\tau\to\infty} S^2\langle S_\alpha(\tau)\cdot S_\alpha(0)\rangle = S(S+1)\left[1 - 2\gamma_0^2\int_0^\infty d\tau_1\int_{-\infty}^0 d\tau_2 D(\tau_1-\tau_2)\right] \tag{F.7}$$

Introducing new dimensionless coordinates $y = m(\tau_1 - \tau_2)$, $x = m(\tau_1 + \tau_2)$, we write

$$\lim_{\tau\to\infty}\langle S_\alpha(\tau)\cdot S_\alpha(0)\rangle = S(S+1)\left[1 - \frac{2\gamma_0^2}{m^2}\int_0^\infty dyyD(y/m)\right] \tag{F.8}$$

The relevant integral to be evaluated is (with $\alpha = (d-1)/2$)

$$\begin{aligned}\int_0^\infty dyy\cdot y^{-\alpha}K_\alpha(y) &= \int_0^1 dyy^{1-\alpha}K_\alpha(y) + \int_1^\infty dyy^{1-\alpha}K_\alpha(y)\\ &\approx \int_0^1 dyy^{1-\alpha}\frac{\Gamma(\alpha)}{2}\left(\frac{y}{2}\right)^{-\alpha} + \int_1^\infty dyy^{1-\alpha}\left(\frac{\pi}{2y}\right)^{1/2}e^{-y}\\ &= \frac{2^{\alpha-1}\Gamma(\alpha)}{2-2\alpha} + \left(\frac{\pi}{2}\right)^{1/2}\Gamma(3/2-\alpha,1)\end{aligned} \tag{F.9}$$

In the second line above we have used the asymptotic forms of the function $K_\alpha(y)$ for very small and large values of its argument [73], and $\Gamma(3/2-\alpha,1)$ is the incomplete Gamma function. Now putting it all back together and using the definition of γ from equation 4.24

$$\lim_{\tau\to\infty}\langle S_\alpha(\tau)\cdot S_\alpha(0)\rangle = S(S+1)\left[1 - 2\gamma^2\left(\frac{1}{\epsilon}\left(\frac{\mu}{m}\right)^\epsilon + \left(\frac{\pi}{2}\right)^{1/2}\Gamma(1/2,1)\right)\right], \tag{F.10}$$

which is the result quoted in equation 4.33.

F.2 Ordered Regime

The relevant action is given in equations 4.42 and 4.43. Since there is a field $\gamma_0 v$ in the z direction, it is going to lead to a precession of the S_x and S_y components around the z axis. This field has to be treated exactly since $\gamma_0 v \sim \mathcal{O}(\gamma_0/\sqrt{g_0})$. We can now define the time dependent spin operators in the Heisenberg representation as

$$\begin{aligned}\mathcal{H}_{0S} &= \gamma_0 v S_z\\ S_\pm &= S_x \pm iS_y\\ S_z(\tau) &= e^{\mathcal{H}_{0S}\tau}S_z e^{-\mathcal{H}_{0S}\tau} = S_z\\ S_\pm(\tau) &= e^{\mathcal{H}_{0S}\tau}S_\pm e^{-\mathcal{H}_{0S}\tau} = S_\pm e^{\pm\gamma_0 v\tau}.\end{aligned} \tag{F.11}$$

The ground state of the spin Hamiltonian $\mathscr{H}_{0S}$ is $|S_z = -S\rangle \equiv |0\rangle$. We also construct combinations of fields

$$\phi_{\pm}(x,\tau) = \frac{1}{2}(\phi_x(x,\tau) \pm \phi_y(x,\tau)). \tag{F.12}$$

With these definitions, the impurity part of the action from equation 4.43 becomes

$$\mathscr{S}_{\rm imp} = \gamma_0 \int d\tau \left[\phi_z(\tau)S_z(\tau) + \phi_+(\tau)S_-(\tau) + \phi_-(\tau)S_+(\tau)\right] \tag{F.13}$$

For notational convenience we have replaced the $\tilde{\phi}_z$ by ϕ_z. Also we have only kept the $\phi_\alpha(x=0,\tau)$ modes in the action. The free part of the action for the background field is now given by

$$\begin{aligned}\mathscr{S}_{\rm bg} &= \int d\tau_1 d\tau_2 \frac{1}{2}\Big[\phi_z(\tau_1)D'^{-1}(\tau_1-\tau_2)\phi_z(\tau_2) + 2\phi_+(\tau_1)D_0^{-1}(\tau_1-\tau_2)\phi_-(\tau_2) \\ &+ 2\phi_-(\tau_1)D_0^{-1}(\tau_1-\tau_2)\phi_+(\tau_2)\Big].\end{aligned} \tag{F.14}$$

We have dropped all interaction terms because to one loop order, they will not contribute anything. $D'(\tau)$ is nothing but $D(\tau)$ with a mass $\sqrt{2}m$. The object of interest is to calculate $\langle S_z\rangle$ which to one loop is given by

$$\begin{aligned}\langle S_z(0)\rangle &= \frac{1}{\mathscr{Z}}\Big[-S + \frac{\gamma_0^2}{2}\int d\tau_1 d\tau_2 \langle T_\tau(S_z(0)S_z(\tau_1)S_z(\tau_2))\rangle D'(\tau_1-\tau_2) \\ &+ \langle T_\tau(S_z(0)S_+(\tau_1)S_-(\tau_2))\rangle D_0(\tau_1-\tau_2) \\ &+ \langle T_\tau(S_z(0)S_-(\tau_1)S_+(\tau_2))\rangle D_0(\tau_1-\tau_2)\Big].\end{aligned} \tag{F.15}$$

The denominator for the partition function evaluates to

$$\begin{aligned}\mathscr{Z} = 1 &+ \frac{\gamma_0^2}{2}\int d\tau_1 d\tau_2 \Big[\langle T_\tau(S_z(\tau_1)S_z(\tau_2))\rangle D'(\tau_1-\tau_2) \\ &+ \frac{1}{2}\langle T_\tau(S_+(\tau_1)S_-(\tau_2))\rangle D_0(\tau_1-\tau_2) \\ &+ \frac{1}{2}\langle T_\tau(S_-(\tau_1)S_+(\tau_2))\rangle D_0(\tau_1-\tau_2)\Big]\end{aligned} \tag{F.16}$$

Useful relations for evaluating these spin correlations are

$$\begin{aligned}\langle S_+S_-\rangle &= \langle S^2 - S_z^2 + S_z\rangle = 0 \\ \langle S_-S_+\rangle &= \langle S^2 - S_z^2 - S_z\rangle = 2S.\end{aligned} \tag{F.17}$$

As before we can evaluate the time ordered spin operators as follows:

$$\begin{aligned}
\langle T_\tau[S_z(0)S_z(\tau_1)S_z(\tau_2)]\rangle &= -S^3 \\
\langle T_\tau[S_z(0)S_+(\tau_1)S_-(\tau_2)]\rangle &= 2S[-S\theta(\tau_2-\tau_1)+\theta(\tau_2)\theta(-\tau_1)]e^{\gamma_0 v(\tau_1-\tau_2)} \\
\langle T_\tau[S_z(0)S_-(\tau_1)S_+(\tau_2)]\rangle &= 2S[-S\theta(\tau_1-\tau_2)+\theta(\tau_1)\theta(-\tau_2)]e^{-\gamma_0 v(\tau_1-\tau_2)}
\end{aligned} \tag{F.18}$$

Using all this, we arrive at

$$\begin{aligned}
\langle S_z\rangle &= -S\left[1-\gamma_0^2\int d\tau_1 d\tau_2\theta(\tau_1)\theta(-\tau_2)e^{-\gamma_0 v(\tau_1-\tau_2)}\frac{\tilde{S}_{d+1}}{|\tau_1-\tau_2|^{d-1}}\right] \\
&= -S\left[1-\gamma_0^2\frac{\tilde{S}_{d+1}\Gamma(\epsilon)}{(\gamma_0 v)^\epsilon}\right]
\end{aligned} \tag{F.19}$$

As usual, the integral is ultraviolet divergent and we have regulated by evaluating in $d = 3-\epsilon$ dimensions. Using the definitions of the wavefunction renormalization from 4.34 and the definitions of γ and g from 4.24, we find

$$\langle S_z\rangle_R = -S\left[1+\gamma^2\left(\ln(m/\mu)+\gamma_E+\frac{1}{2}\ln(3\gamma^2/g)\right)\right]. \tag{F.20}$$

This is the result quoted in equation 4.44.

Bibliography

[1] M. Takigawa, T. Asano, Y. Ajiro, and M. Mekata. *Physical Review B*, 52:R13087, 1995.

[2] M.-H. Julien, T. Fehrer, M. Horavatic, C. Berthier, O. N. Bakharev, P. Segransan, G. Collin, and J.-F. Marucco. *Phys. Rev. Lett.*, 84:3422, 2000.

[3] B. Frischmuth, S. Haas, G. Sierra, and T. M. Rice. *Physical Review B*, 55:R3340. 1997.

[4] H. Bethe. *Z. Phys*, 71:205, 1931.

[5] H. Mutka et. al. *Physical Review Letters*, 67:497, 1991.

[6] R. A. Cowley. In A. Skjeltorp and D. Sherrington, editors, *Dynamical Properties of Unconventional Magnetic Systems*, Norwell, MA, 1998. Kluwer Academic.

[7] C. Broholm. In A. Skjeltorp and D. Sherrington, editors, *Dynamical Properties of Unconventional Magnetic Systems*, Norwell, MA, 1998. Kluwer Academic.

[8] H. Schulz. *Physical Review B*, 34:6372, 1986.

[9] M. Takigawa, O. Starykh, A. Sandvik, and R. R. P. Singh. *Physical Review B*, 56:13681, 1997.

[10] E. H. Lieb, T. Shultz, and D. J. Mattis. *Ann. Phys. (N.Y.)*, 16:407, 1961.

[11] I. Affleck and E. H. Lieb. *Lett. Math. Phys.*, 12:57, 1986.

[12] I .Affleck. In E. Brezin and J. Zinn-Justin, editors, *Fields, Strings and Critical Phenomena*. Elsevier Science Publishers B.V, 1989.

[13] A. Luther and I. Peschel. *Physical Review B*, 9:2911, 1974.

[14] R. Shankar. In J. Pati, Q. Shafi, and Yu Lu, editors, *Current Topics in Condensed Matter and Particle Physics*. World Scientific, 1993.

[15] F. D. M. Haldane. *Physical Review Letters*, 50:1153, 1983.

[16] F. D. M. Haldane. *Phys. Lett. A*, 93:464, 1983.

[17] R. Shankar. *Principles of Quantum Mechanics*. Plenum Press, New York, 2nd edition, 1994.

[18] J. W. Negele and H. Orland. *Quantum Many Particle Systems*. Addison Wesley, Redwood City, CA, 1988.

[19] S. Sachdev. *Quantum Phase Transitions*. Cambridge University Press, 2000.

[20] E. Brezin. *J. de Phyique*, 43:15, 1982.

[21] A. d'Adda, M. Luscher, and P. Di Vecchia. *Nuclear Physics B*, 146:63, 1978.

[22] A. M. Polyakov. *Gauge Fields and Strings*. Harwood, New York, 1987.

[23] R. Shankar and N. Read. *Nucl. Phys. B*, 336:457, 1990.

[24] R. S. Eccleston, T. Barnes, J. Brody, and J. W. Johnson. *Physical Review Letters*, 73:2626, 1994.

[25] M. Azuma, Z. Hiroi, M. Takano, K. Ishida, and Y. Kitaoka. *Physical Review Letters*, 73:3463, 1994.

[26] E. Dagotto and T. M. Rice. *Science*, 271:618, 1996.

[27] P. Hasenfratz and F. Niedermeyer. *Phys. Lett. B*, 245:529, 1990.

[28] S. Eggert, I. Affleck, and M. Takahashi. *Physical Review Letters*, 73:332, 1994.

[29] C. Buragohain and S. Sachdev. *Physical Review B*, 59:9285, 1999.

[30] K. Damle and S. Sachdev. *Physical Review B*, 57:8307, 1998.

[31] O. Starykh, R. R. P. Singh, and A. W. Sandvik. *Physical Review Letters*, 78:539, 1997.

[32] M. Luscher. *Phys. Lett. B*, 118:391, 1982.

[33] X. Zotos. *Physical Review Letters*, 82:1764, 1999.

[34] B. N. Narozhny, A. J. Millis, and N. Andrei. *Physical Review B*, 58:R2921, 1998.

[35] K. Fabricius and B. M. McCoy. *Physical Review B*, 57:8340, 1998.

[36] A. Chubukov and Th. Jolicoeur. *Physical Review B*, 46:11137, 1992.

[37] I. Affleck, T. Kennedy, E. H. Lieb, and H. Tasaki. *Physical Review Letters*, 59:799, 1987.

[38] David Huse and Veit Elser. *Physical Review Letters*, 60:2531, 1988.

[39] J. D. Reger and A. P. Young. *Physical Review B*, 37:5978, 1988.

[40] N. Katoh and M. Imada. *Journal of the Phys. Soc. of Japan*, 63:4529, 1994.

[41] S. Sachdev and M. Vojta. *cond-mat/9908008.*

[42] J. A. Hertz. *Physical Review B*, 14:1165, 1976.

[43] S. L. Sondhi, S. M. Girvin, J. P. Carini, and D. Shahar. *Rev. Mod. Phys.*, 69:315, 1997.

[44] K. G. Wilson. *wilson's original article in RG.*

[45] H. Alloul, P. Mendels, H. Casalta, J. F. Marucco, and J. Arabski. *Physical Review Letters*, 67:3140, 1991.

[46] H. F. Fong, P. Bourges, Y. Sidis, L. P. Regnault, J. Bossy, A. Ivanov, D. L. Milius, I. A. Aksay, and B. Keimer. *Physical Review Letters*, 82:1939, 1999.

[47] S. H. Pan, E. W. Haudson, K. M. Lang, H. Eisaki, S. Uchida, and J. C. Davis. *Nature*, 403:746, 2000.

[48] T. Masuda, A. Fujioka, Y. Uchiyama, I. Tsukuda, and K. Uchinokura. *Physical Review Letters*, 80:4566, 1998.

[49] Y. Uchiyama, Y Sasago, I Tsukuda, K. Uchinokura, A. Zheludev, T. Hayashi, N. Miura, and P. Boni. *Physical Review Letters*, 83:632, 1999.

[50] A. M. Finkelstein, V. E. Kataev, E. F. Kukovitskii, and G. B. Teitel'baum. *Physica C*, 168:370, 1990.

[51] N. Read and S. Sachdev. *Physical Review Letters*, 62:1694, 1989.

[52] S. Sachdev, C. Buragohain, and M. Vojta. *Science*, 286:2479, 1999.

[53] M. Hase, I. Terasaki, and K. Uchinokura. *Physical Review Letters*, 70:3651, 1993.

[54] N. Elstner, A. Sokol, R.R.P. Singh, M. Greven, and R.J. Birgeneau. *Physical Review Letters*, 75:938, 1995.

[55] G. S. Joyce. *Phys. Rev.*, 155:478, 1967.

[56] S. Chakravarty. *Physical Review Letters*, 77:4446, 1996.

[57] A. M. Tsvelik. *Sov. Phys. JETP*, 66:221, 1985.

[58] O. Starykh, A. W. Sandvik, and R. R. P. Singh. *Physical Review B*, 55:14953, 1997.

[59] Y. J. Kim, M. Greven, U.-J. Wiese, and R.J. Birgeneau. *Eur. Phys. Journal B*, 4:291, 1998.

[60] G. Reiter and A. Sjölander. *J. Phys. C*, 13:3027, 1980.

[61] U. Wolff. *Physical Review Letters*, 62:361, 1989.

[62] A. V. Chubukov, S. Sachdev, and J. Ye. *Physical Review B*, 49:11919, 1994.

[63] Th. Jolicoeur and O. Golinelli. *Physical Review B*, 50:9265, 1994.

[64] D. W. Jepsen. *Journal of Math. Phys.*, 6:405, 1965.

[65] J. L. Lebowitz and J. K. Percus. *Phys. Rev.*, 155:122, 1967.

[66] S. Sachdev. *cond-mat/0011233.*

[67] M. Vojta, C. Buragohain, and S. Sachdev. *Physical Review B*, 61:15152, 2000.

[68] E. Brezin, J. C. Le Guillou, and J. Zinn-Justin. Phase transition and critical phenomena vol 6. London, 1976. Academic Press.

[69] E. Brezin and J. Zinn-Justin. *Physical Review B*, 14:3110, 1976.

[70] A. Fateev, E. Onofri, and Al. B. Zamolodchikov. *Nucl. Phys. B*, 406:521, 1993.

[71] S. Lukyanov. *Nucl. Phys. B*, 522:533, 1998.

[72] P. Hasenfratz, M. Maggiore, and F. Niedermeyer. *Phys. Lett. B*, 245:522, 1990.

[73] M. Abramowitz and I. Stegun. *Handbook of Mathematical Functions.* Dover, New York, 1965.